STM Study of Unconventional Superconductivity

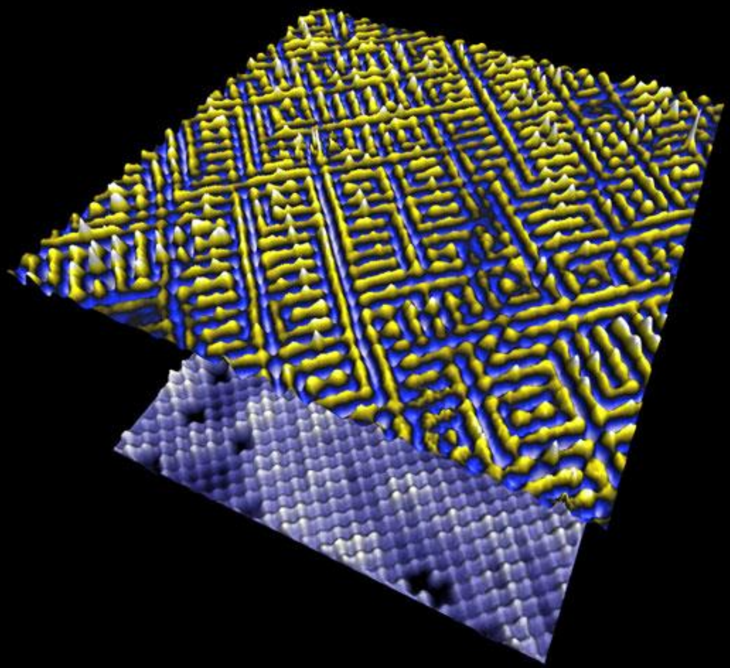

1. Introduction to conventional superconductivity
2. Introduction to scanning tunneling microscopy (STM)
3. High Tc Superconductor : Cuprates
4. High T_c Superconductor : Fe-based Compounds

FeSC Family

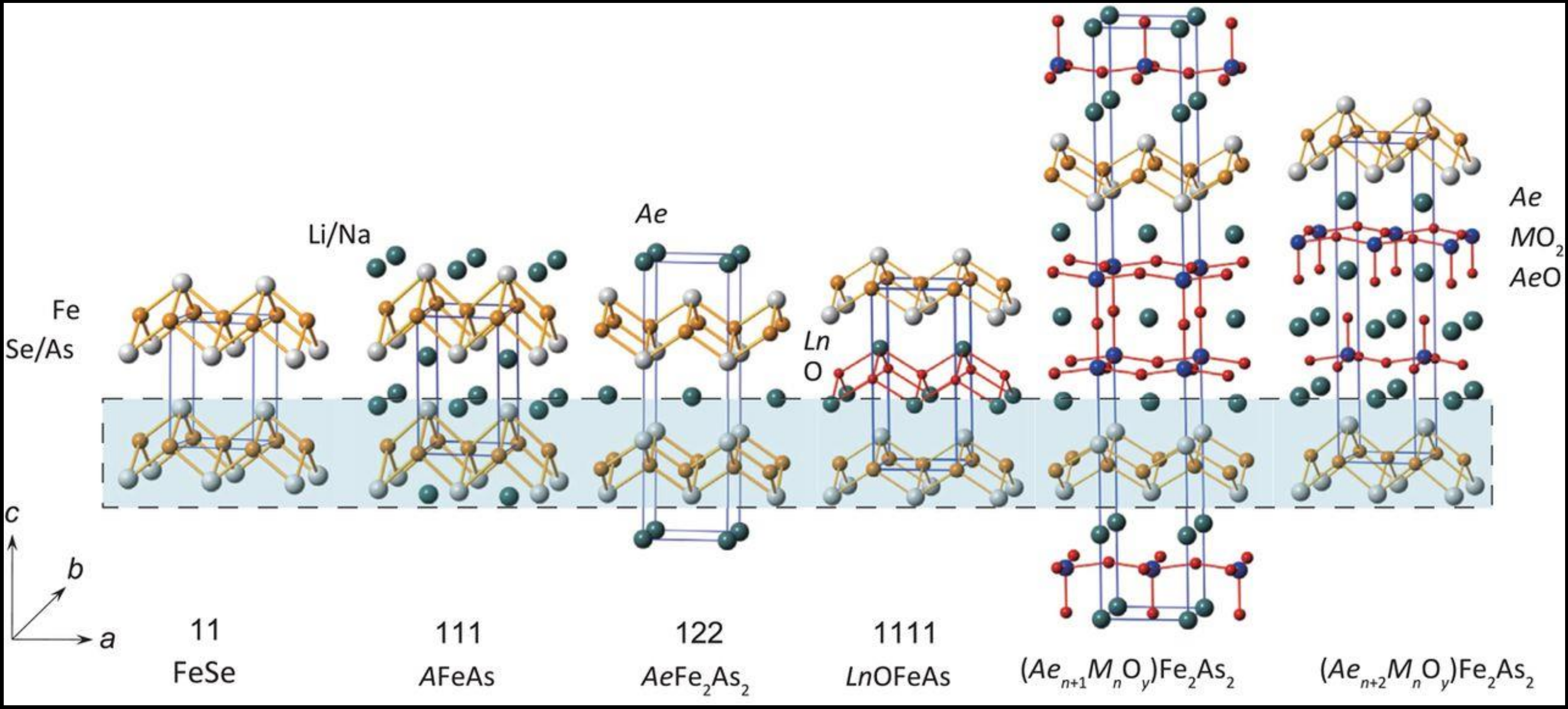

X.H. Chen *et al.*, National Science Review 1: 371–395 (2014)

FeSC Family

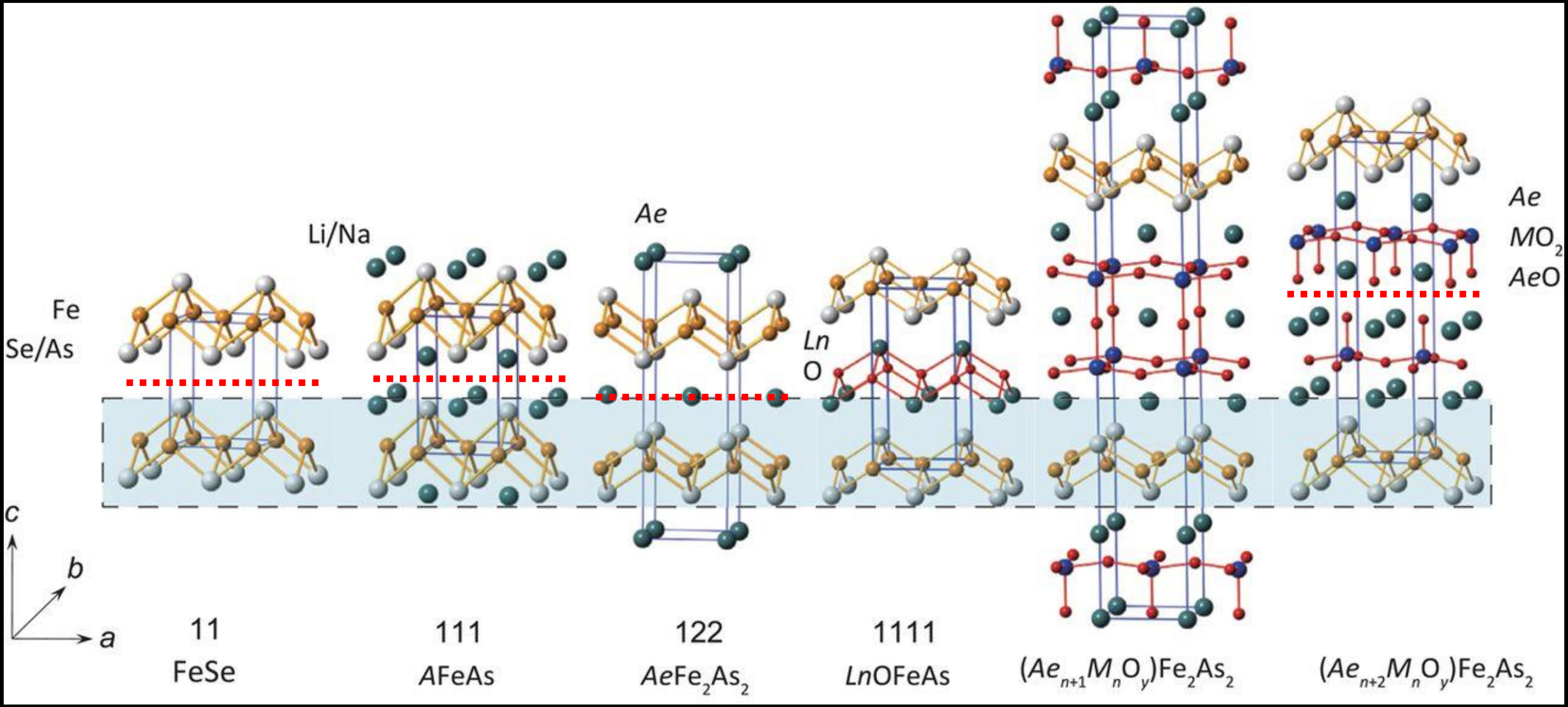

☺ ☺ 😐 😐

Glide plane : Good for STM/ARPES measurements

X.H. Chen *et al.*, National Science Review 1: 371–395 (2014)

FeSC : Complex Band Structure

SC layer with SDW ground state

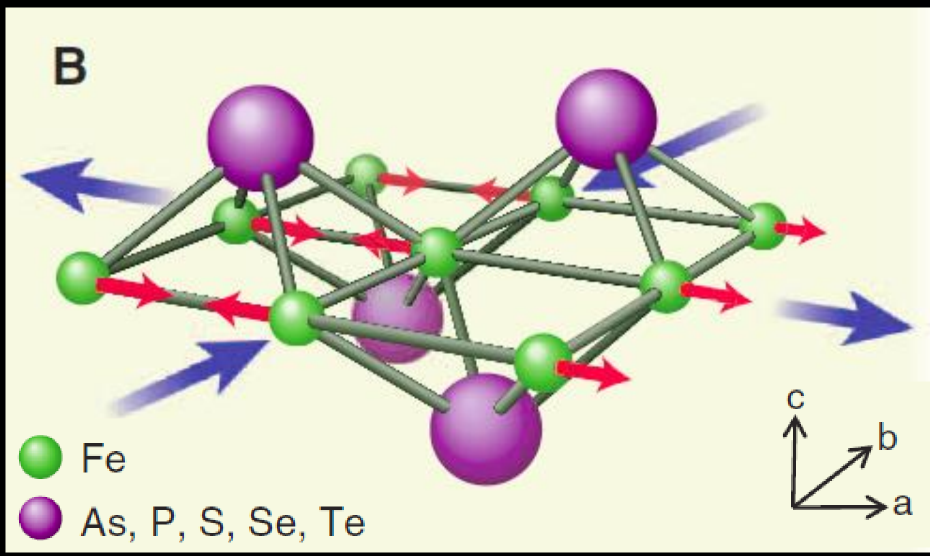

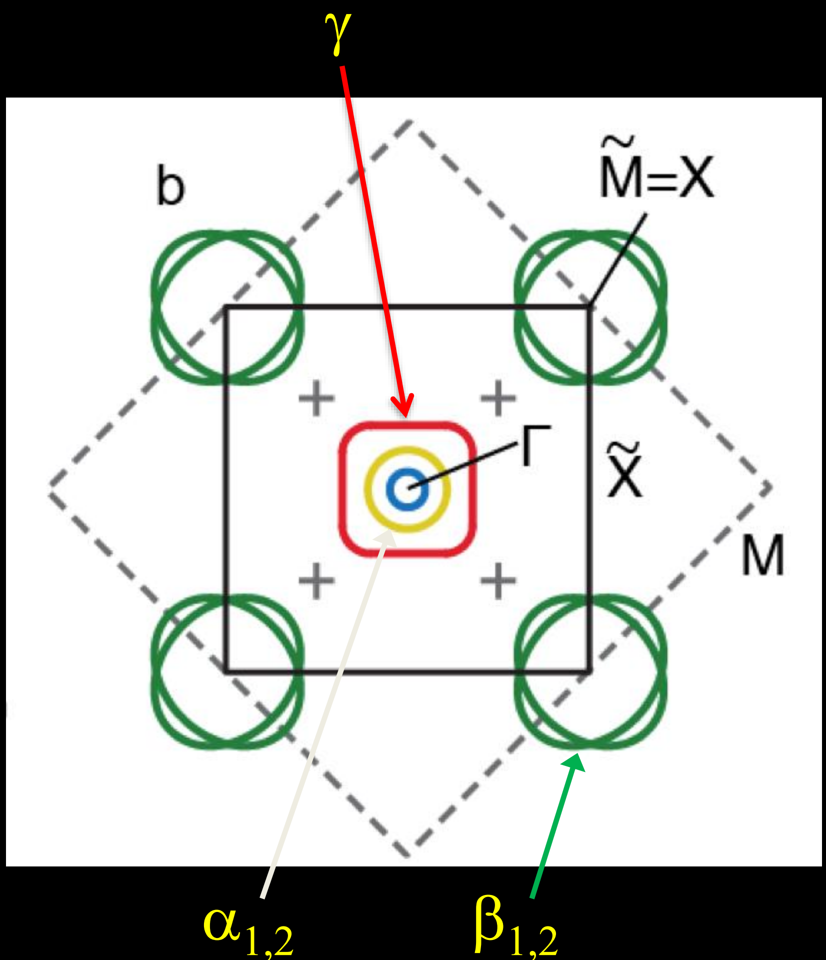

F. Wang *et al.*, Science 332, 200 (2011)
P. J. Hirschfeld e*t al.*, Rep.Prog.Phys.**74**,124508 (2011)

FeSC Phase Diagram

FeSC

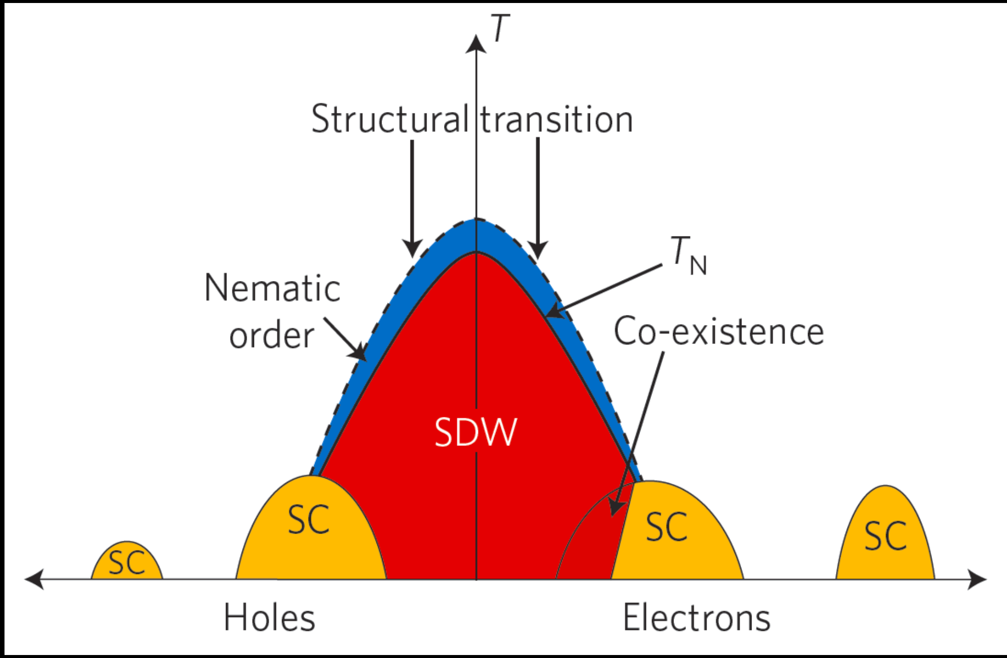

D.N. Basov *et al.*, NPhys **7**, 272 (2011)

FeSC vs Cuprates : Phase Diagram

Many common electronic characteristics!
Both have antiferromagnetic 'parent' states.

Cuprates

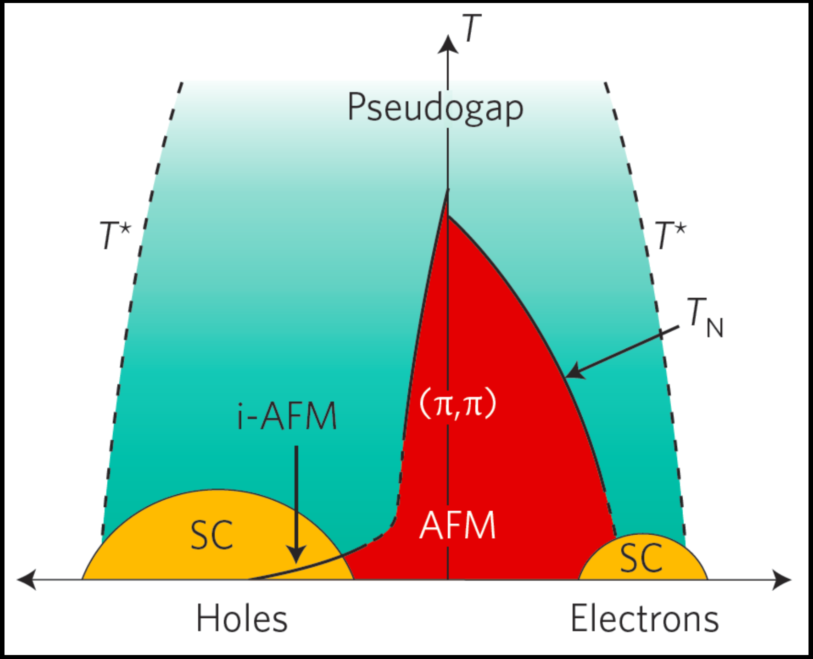

FeSC

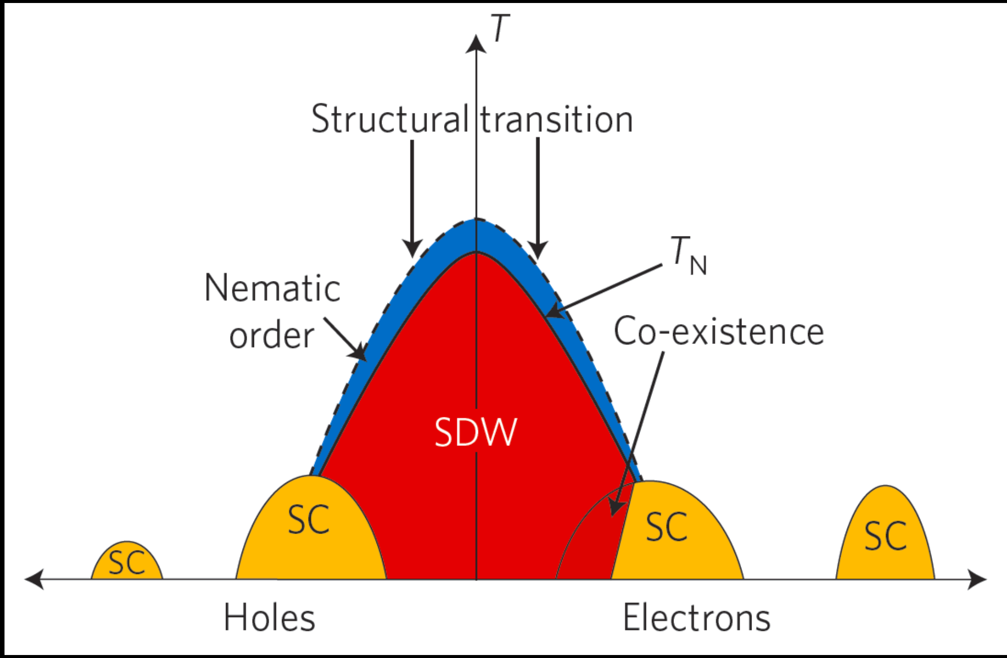

D.N. Basov *et al.*, NPhys **7**, 272 (2011)

FeSC Phase Diagram

FeSC

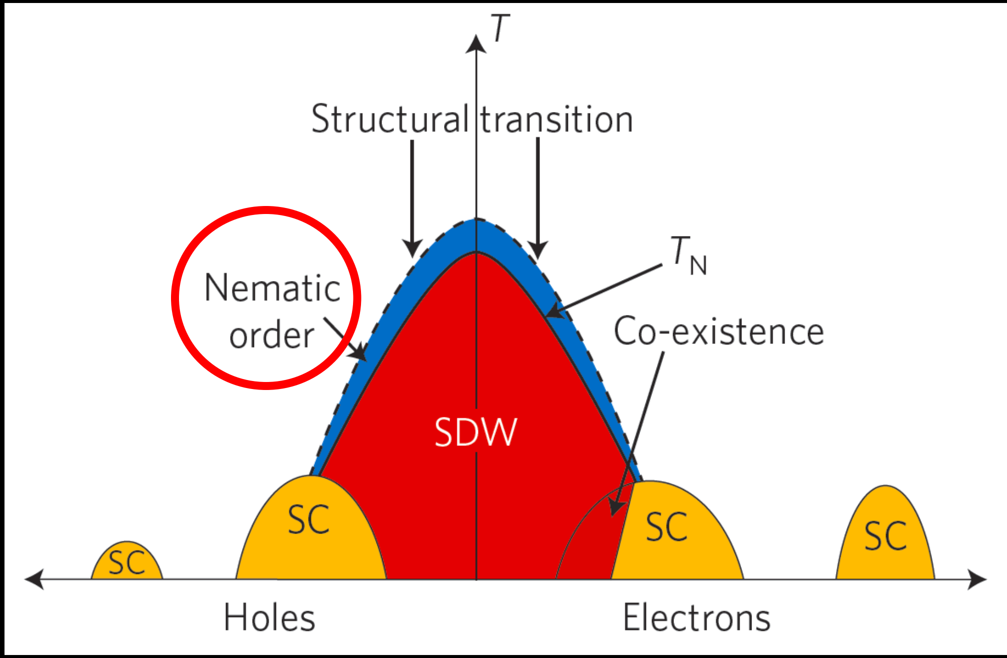

D.N. Basov *et al.*, NPhys **7**, 272 (2011)

Liquid Crystal Phases

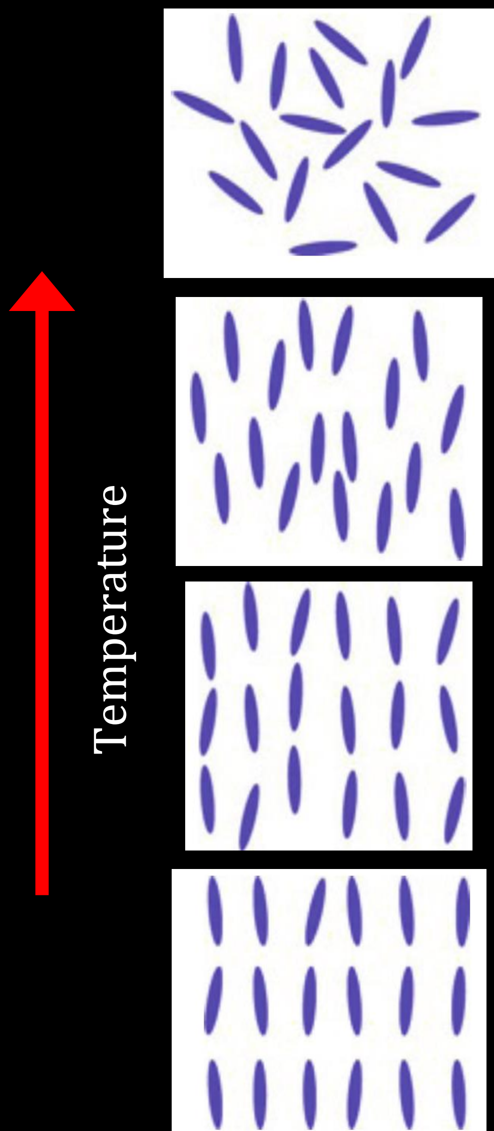

Liquid
(Isotropic)

Nematic

Smectic

Crystal

Liquid crystal

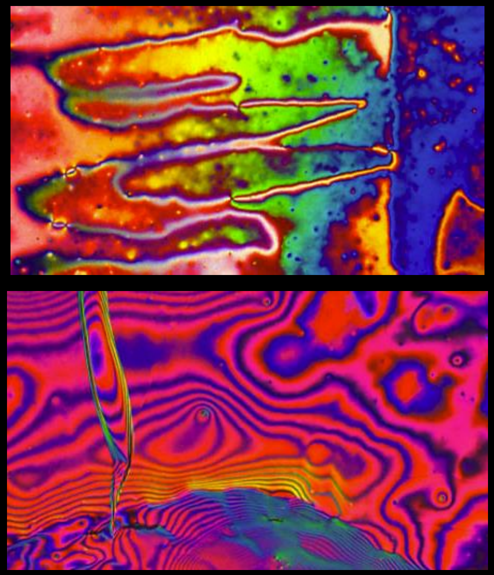

© M. W. Davidson, FSU.

F. Reinitzer, doi:10.1007/BF01516710 (1888)

Liquid Crystal Phases : Nematic Vs. Smectic

Nematic LC
breaks rotational
symmetry only

Smectic LC
breaks rotational & translational
symmetry

Strong Electron Correlation : Electronic Liquid Crystal Phases

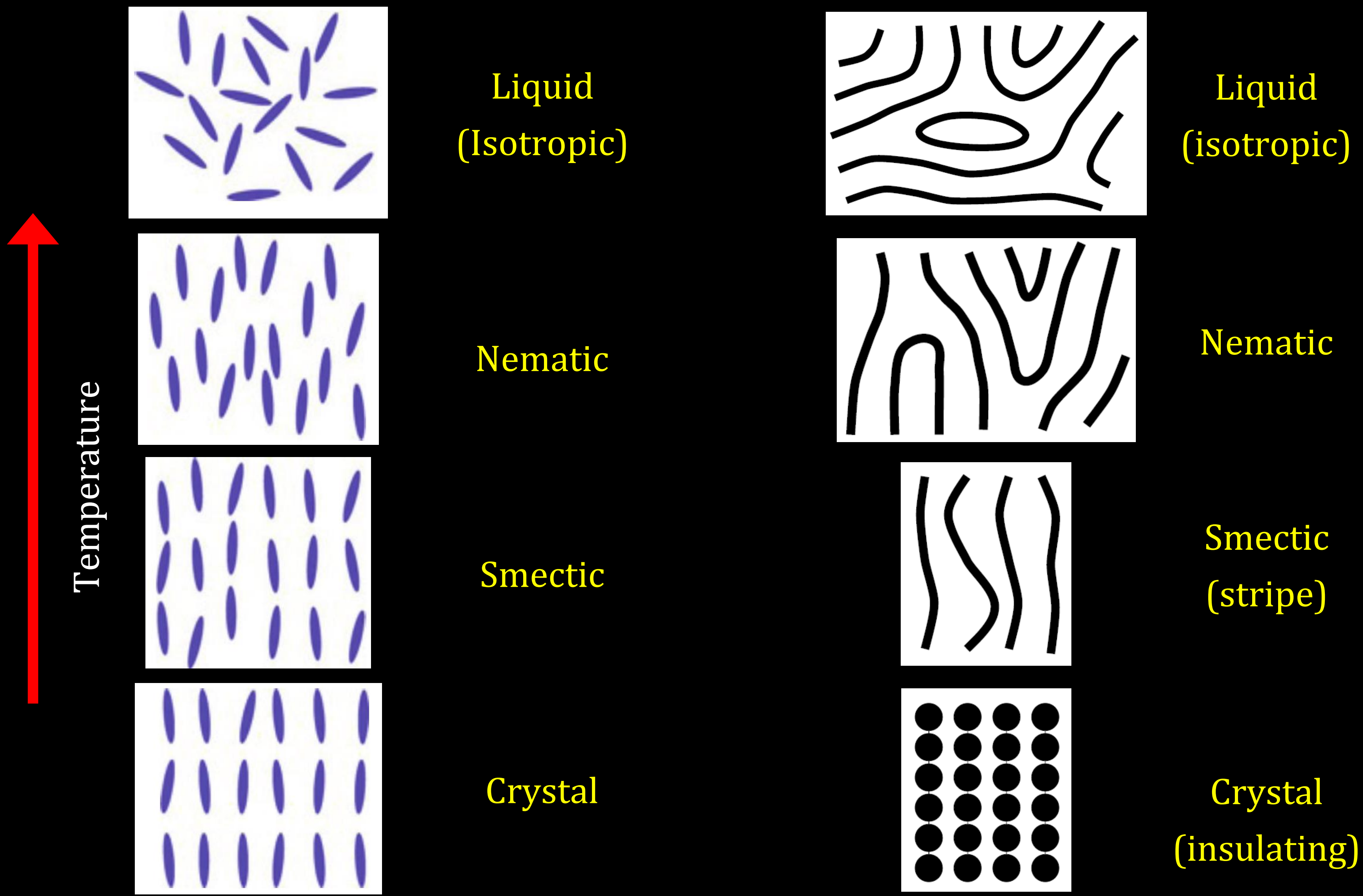

F. Reinitzer, doi:10.1007/BF01516710 (1888)

S. A. Kivelson *et al.*, Nature **393**, 550 (1998)

Electronic Liquid Crystal Phases in Cuprates

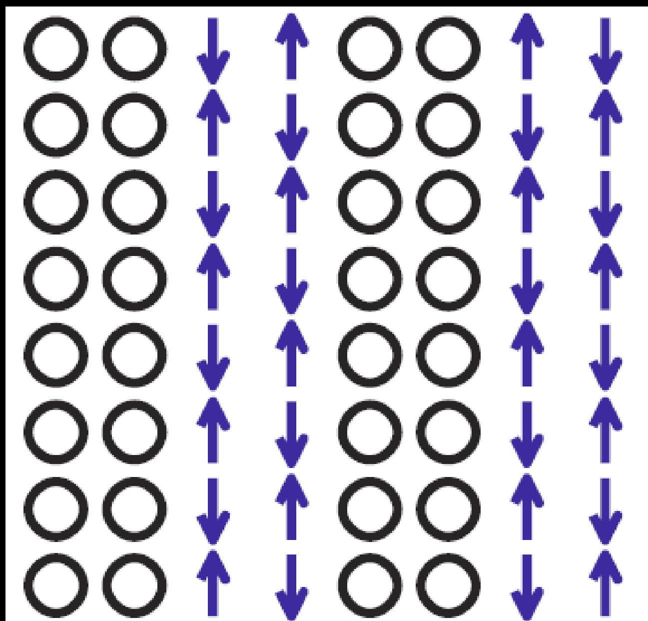

J. Zaanen *et al.*,PRB **40**, 7391 (1989).
S. A. Kivelson *et al.*, Nature **393**, 550 (1998).
V. J. Emery *et al.*, PNAS **96**, 8814 (1999).
S. R. White *et al.*, PRL **91**, 136403 (2003).
S. Sachdev, RMP **75**, 913 (2003).
J. M Tranquada *et al.*, Nature **429**, 534 (2004)

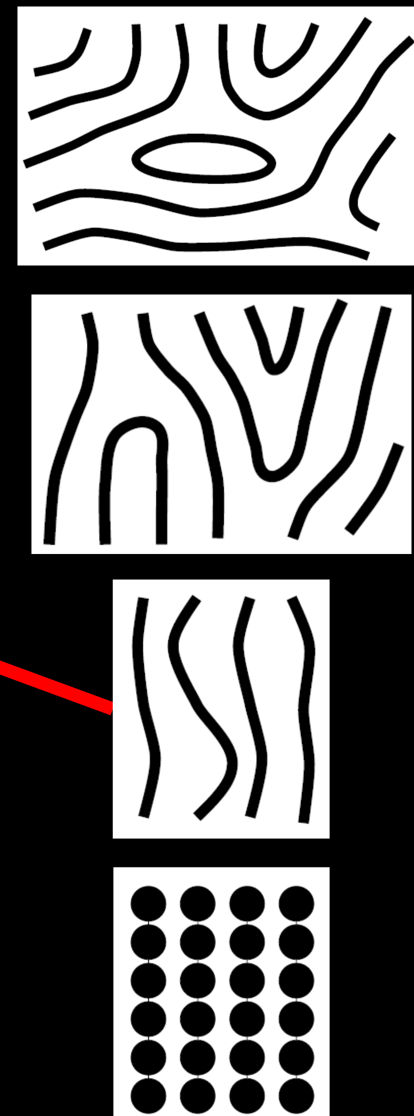

Liquid (isotropic)

Nematic

Smectic (stripe)

Crystal (insulating)

S. A. Kivelson *et al.*, Nature **393**, 550 (1998)

Electronic Nematicity in Underdoped $Ca(Fe_{0.97}Co_{0.03})_2As_2$

Tien-Ming Chuang

Milan Allan

Topograph

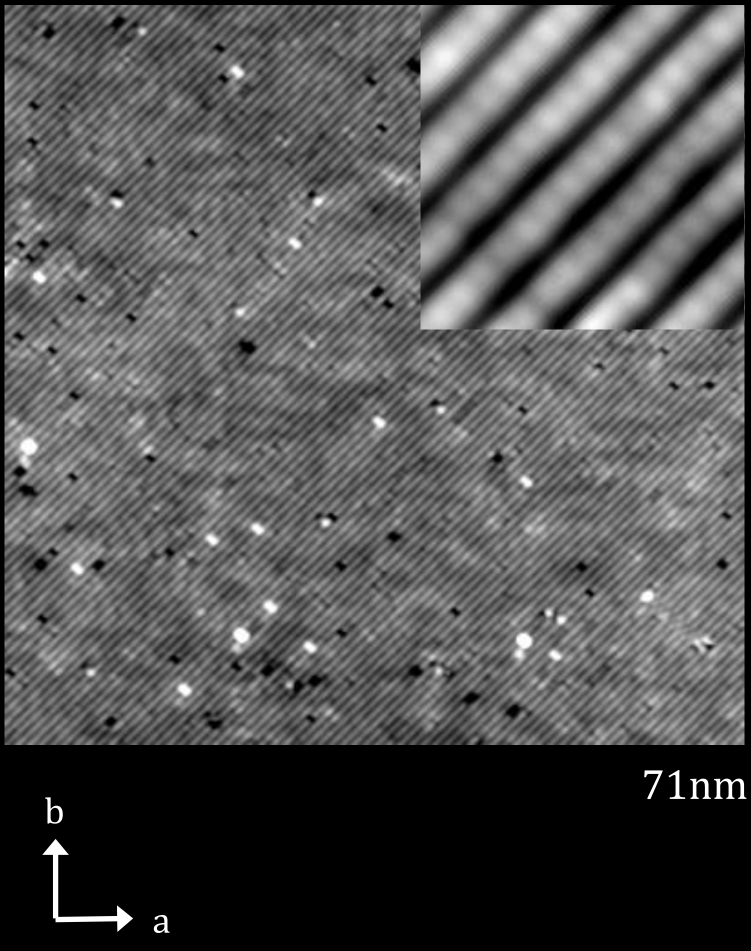

1x2 reconstruction

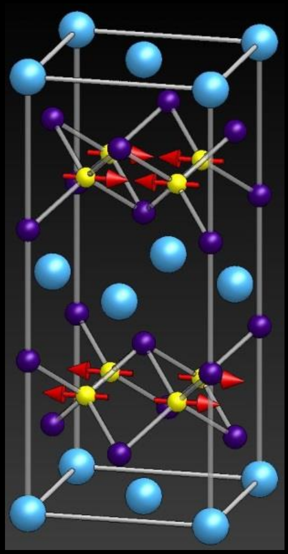

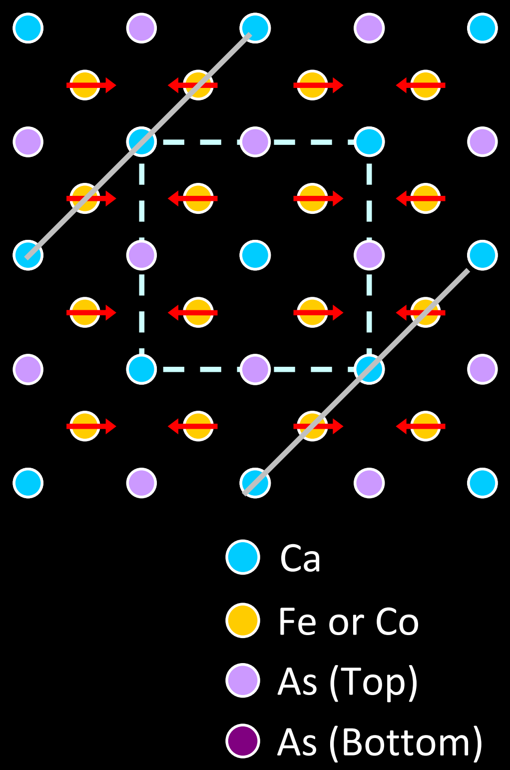

T.-M. Chuang *et al.*, Science **327**, 181 (2010)

Electronic Nematicity in Underdoped $Ca(Fe_{0.97}Co_{0.03})_2As_2$

Static $I(\vec{r}, E{=}50\text{meV})$

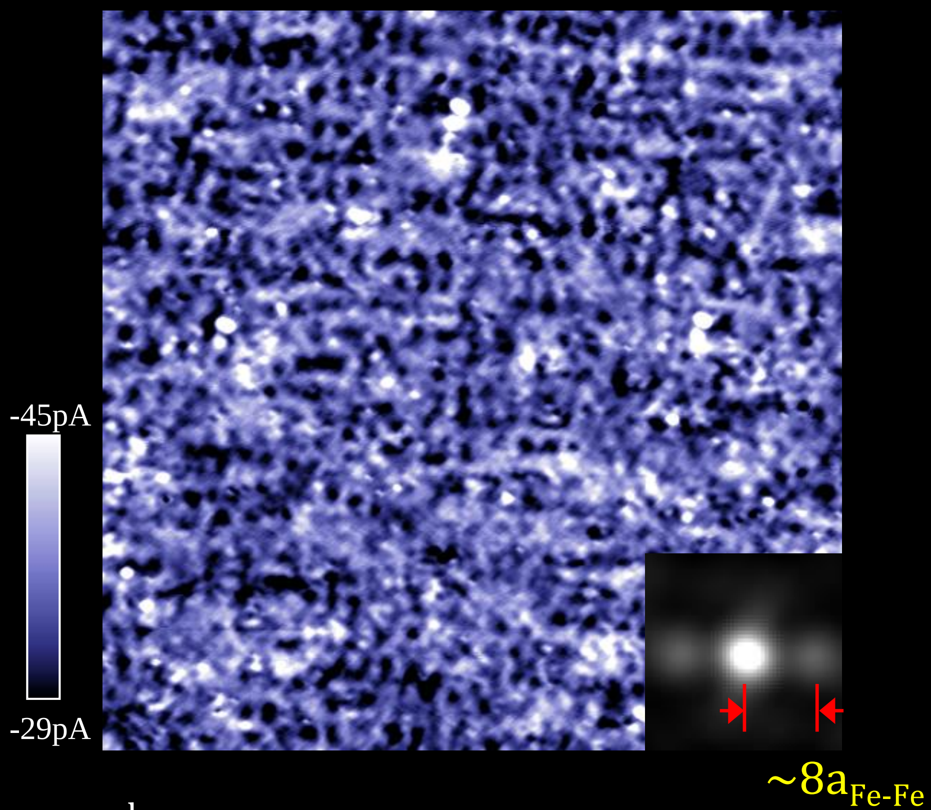

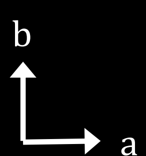

No long range order!

Delocalized State, $LDOS(\vec{q}, E)$

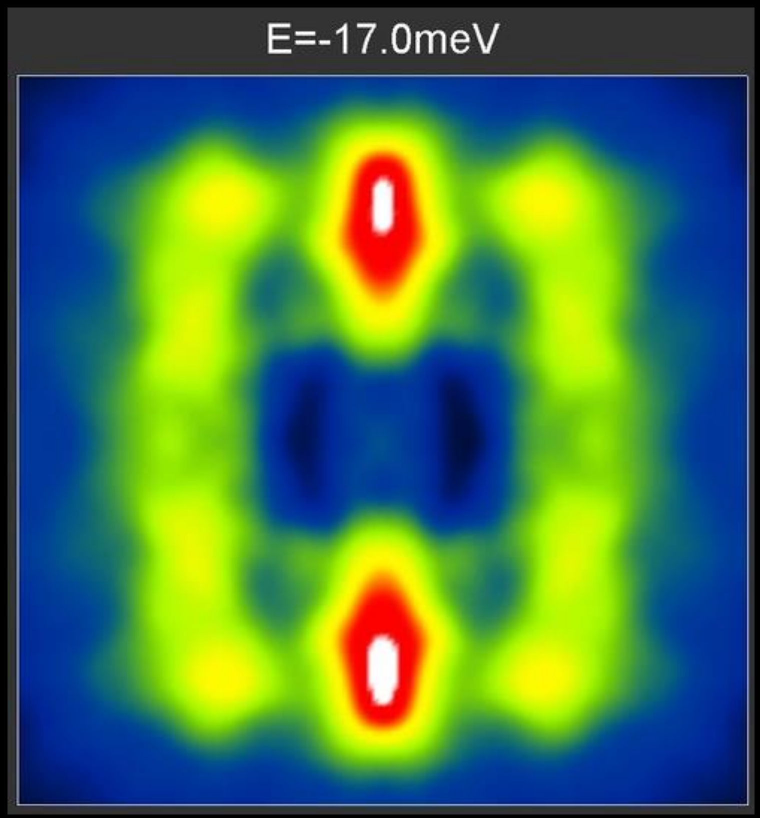

T.-M. Chuang *et al.*, Science **327**, 181 (2010)

Electronic Nematicity in Underdoped $Ca(Fe_{0.97}Co_{0.03})_2As_2$

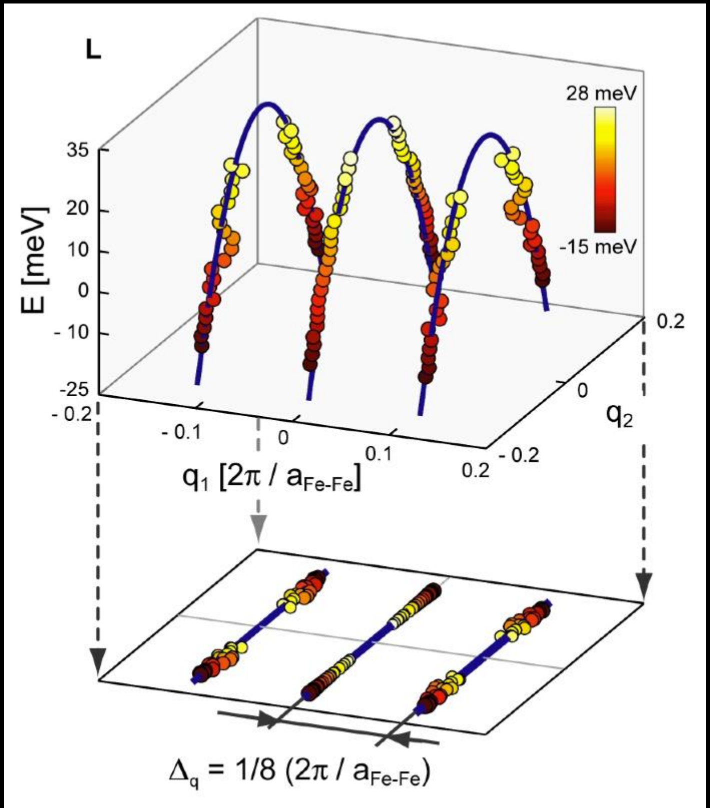

Delocalized State, $LDOS(\vec{q}, E)$

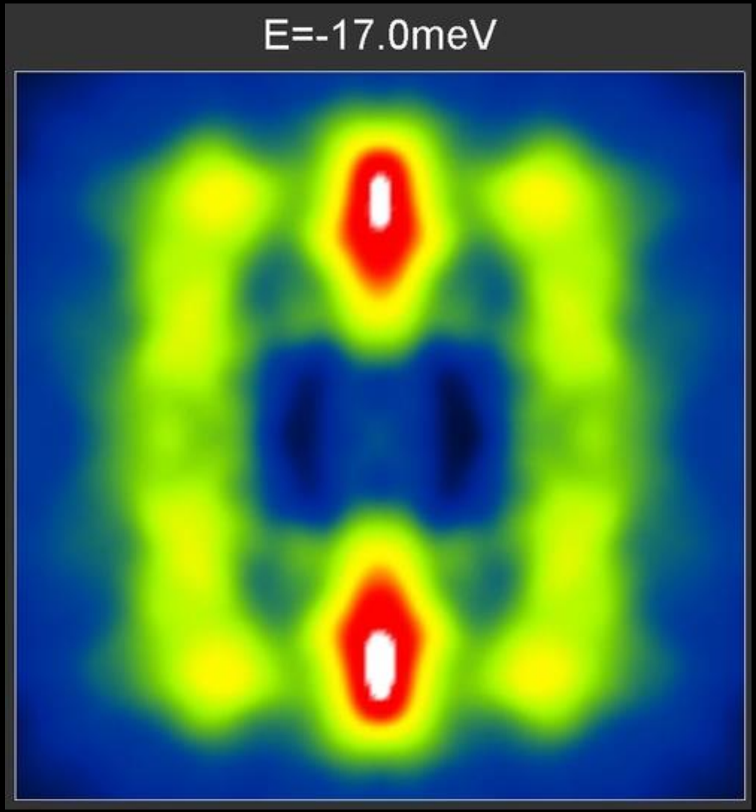

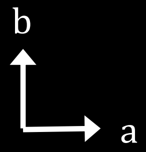

T.-M. Chuang *et al.*, Science **327**, 181 (2010)

Nematic Electronic Structure at Twin Domain Boundary

Surface reconstruction doesn’t affect the nematic electronic structure.
Nematic electronic structure correlates to the crystal symmetry.

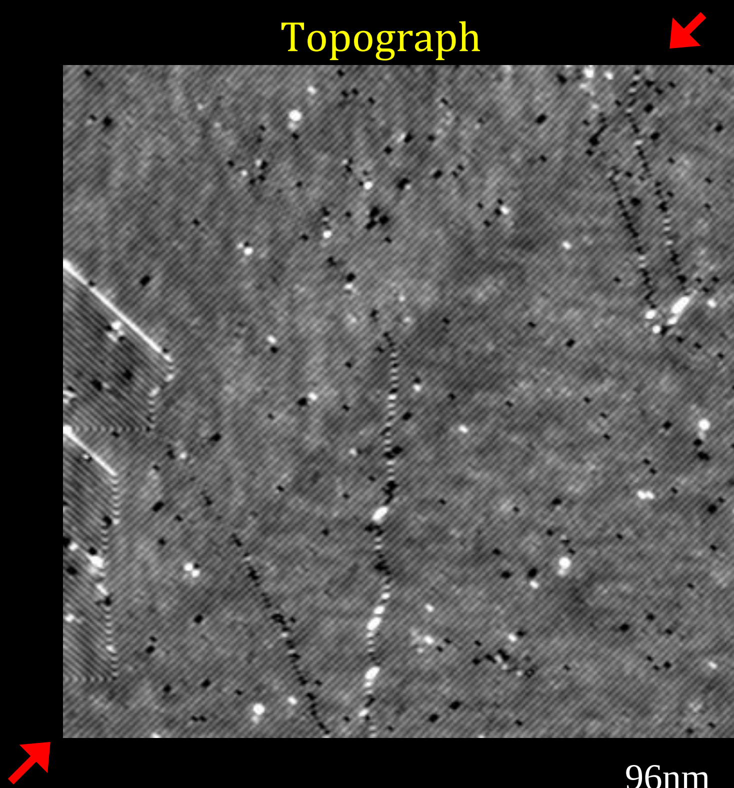

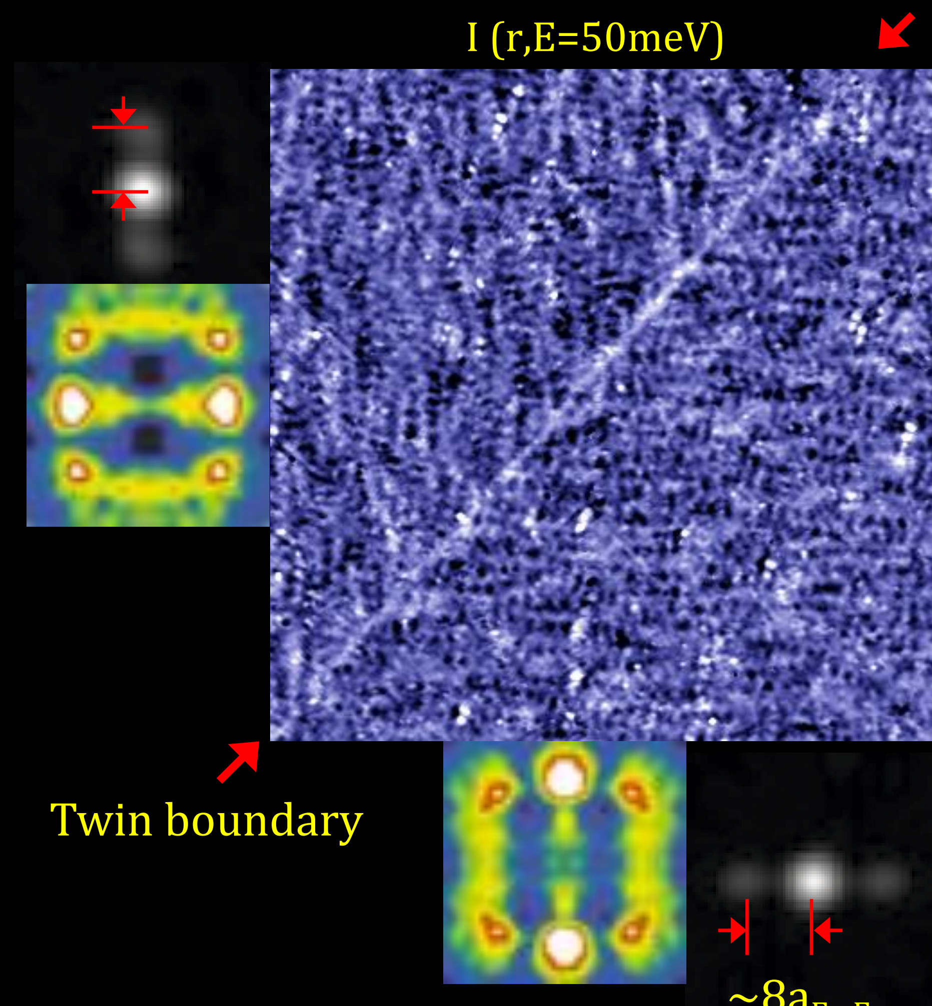

T.-M. Chuang *et al.*, Science **327**, 181 (2010)

Electronic Nematicity in Detwinned $Ba(Fe_{1-x}Co_x)_2As_2$

$\rho_a < \rho_b$

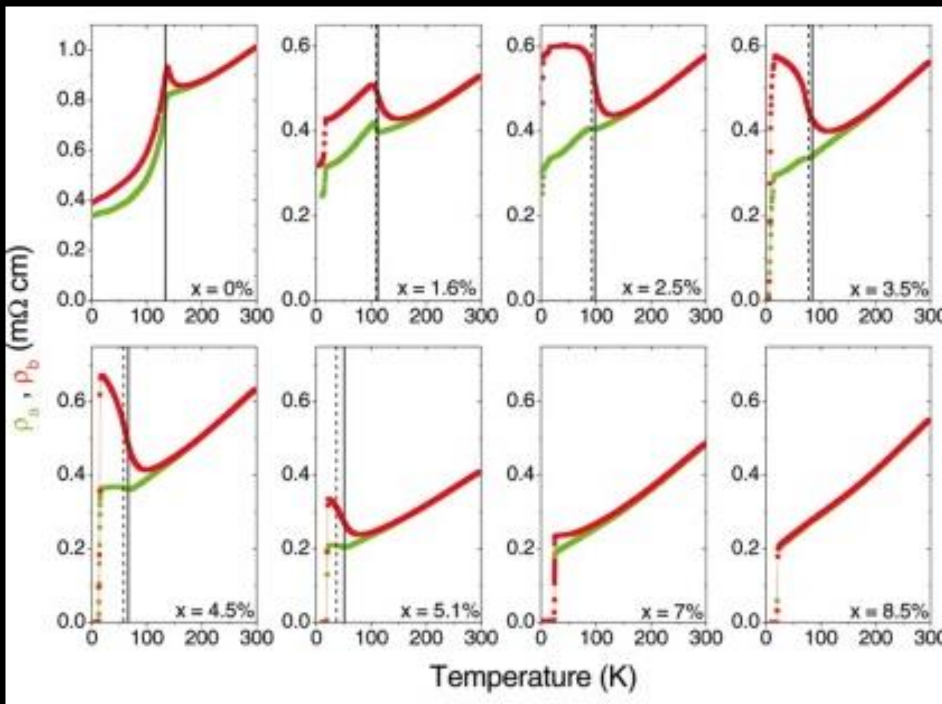

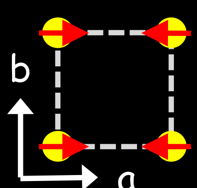

DC electric transport:

J.H. Chu *et al.* Science **329**, 824-826 (2010).
M.A. Tanatar *et al.* PRB **81**, 184508 (2010).
S. Ishida *et al.* PRB **84**, 184514 (2010).
E.C. Blomberg *et al.* PRB **83**, 134505 (2011).
H.H. Kuo *et al.* PRB **84**, 054540 (2011).
J.J. Ying *et al.* PRL **107**, 067001 (2011).
J.H. Chu *et al.* Science **337**, 710 (2012).
A.F. Wang *et al.* New J. Phys. 15 043048(2013).

AC electric transport:

A. Dusza *et al.* EPL **93,** 37002 (2011).
M. Nakajima *et al.* PNAS **108**, 12238 (2011).
M. Nakajima *et al.* PRL **109**, 217003 (2012)

ARPES:

Q. Wang, *et al.* arXiv:1009.0271 (2010).
M. Yi *et al.*, PNAS **108**, 6878 (2011).
I.R. Fisher *et al.*, Rep. Prog. Phys. 74 124506 (2011)

Magnetic torque:

S. Kasahara *et al.* Nature **486**, 382 (2012).

STM:

C.L. Song *et al.*, Science **332**, 1410 (2011).
X. Zhou *et al.* PRL. **106**, 087001 (2011).

In-plane Resistivity Anisotropy in Detwinned $Ba(Fe_{1-x}Co_x)_2As_2$

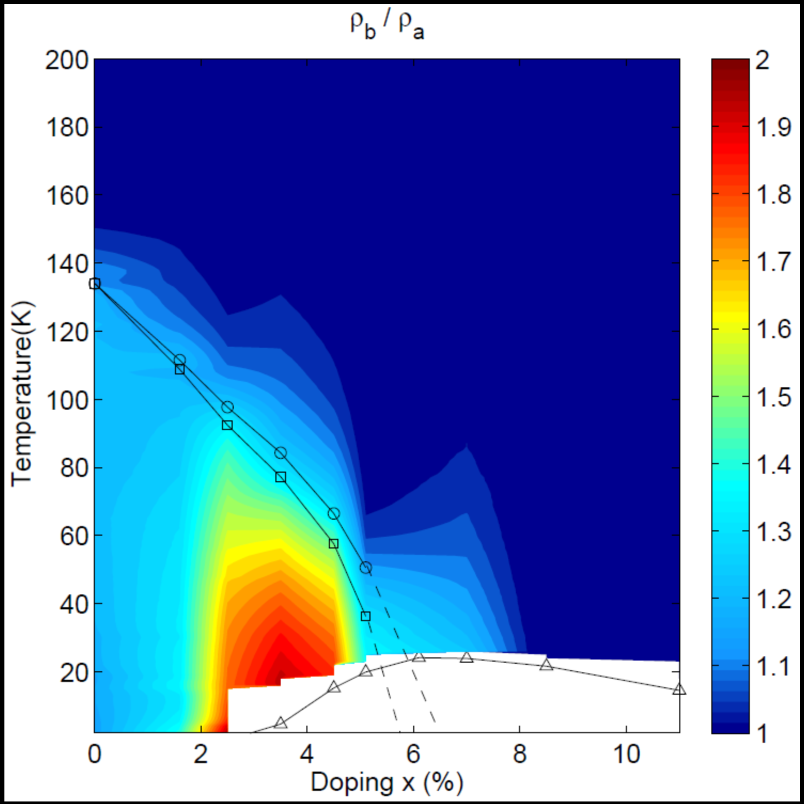

Crystalline anisotropy monotonically decreases with doping but nematicity does not !

J.-H. Chu *et al.*, Science **329**, 824 (2010)
M. A. Tanatar *et al.*, PRB **81**,184508 (2010)

Doping Dependence of Transport Anisotropy?

Proposal by I.R. Fisher:

High mobility isotropic pocket "short-circuits" the aniostropic section of FS

H.-H. Kuo *et al.*, PRB 84, 054540 (2011)

Dirac pocket at Λ=(0.75π,0)

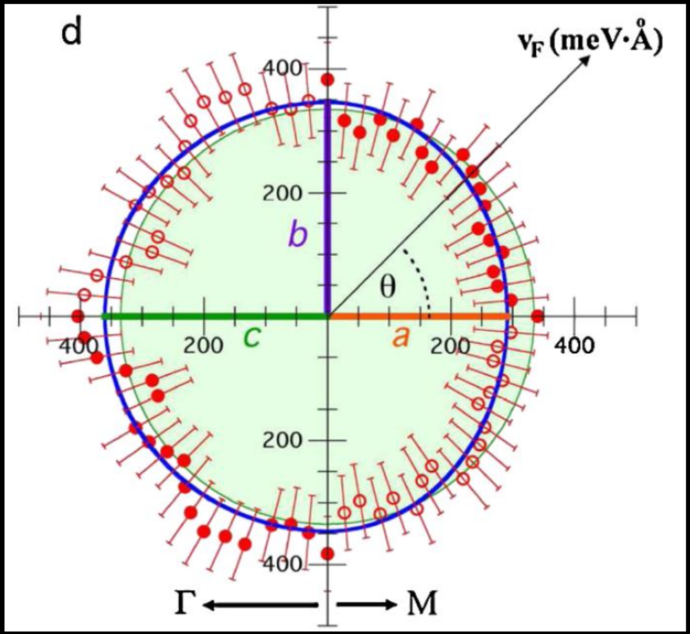

P. Richard *et al.*, PRL104, 137001 (2010)

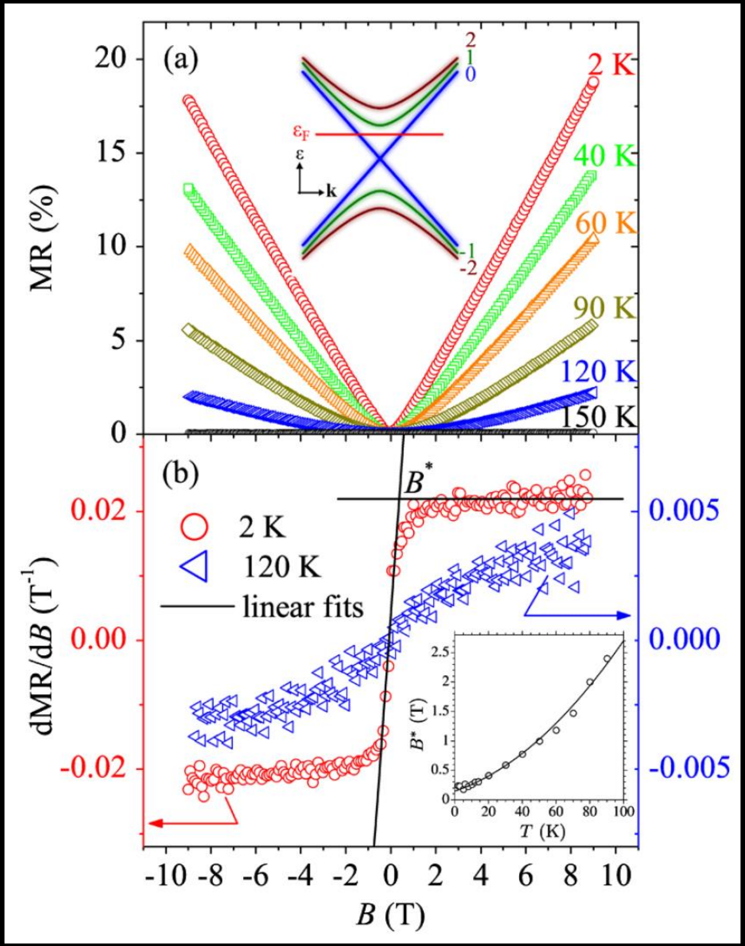

K.K. Huynh *et al.*, PRL106, 217004 (2011)

Alternative?

Theorectical Proposal : Impurity States

Impurity-induced nematic state from orbital fluctuation:
Y. Inoue *et al.*, PRB 85, 224506 (2012)

Ising nematic state from the scattering interference between impurities and spin fluctuation.
R.M. Fernandes et al., PRL 107, 217002 (2011)

Impurity states determined by reconstructed nesting wavevector.
Jian Kang & Zlatko Tesanovic, PRB85, 220507(2012)

Diminishing Resistivity Anisotropy by Annealing

Defects and impurities play any role in transport anisotropy?

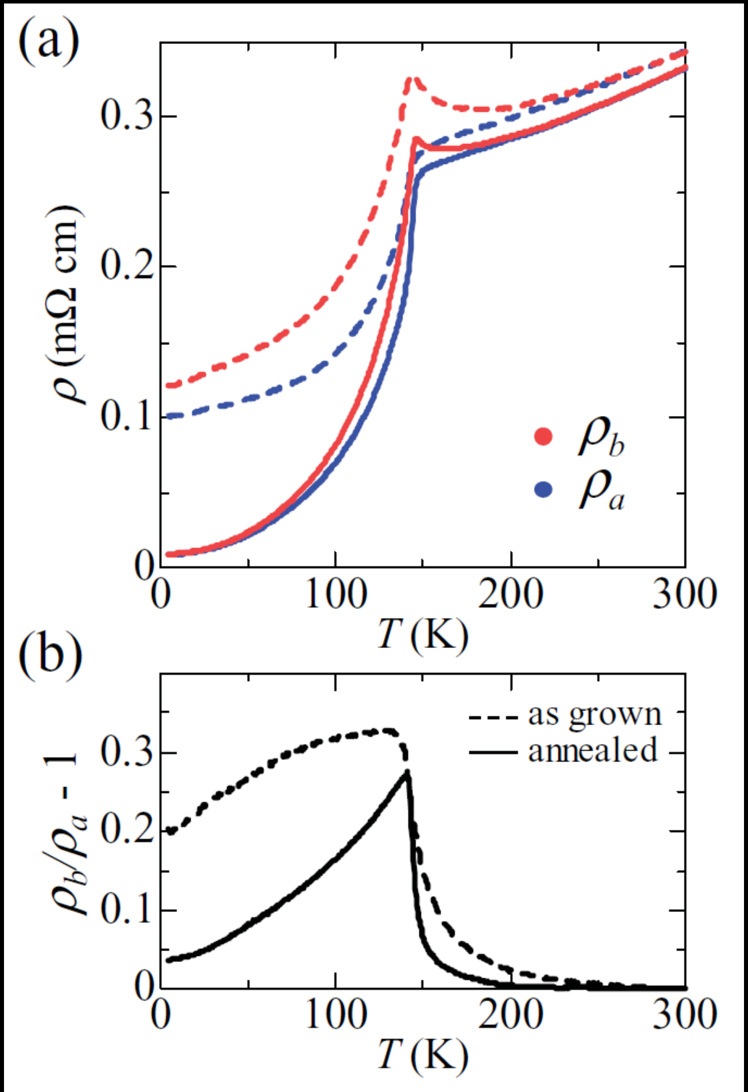

RRR improved a factor of 10.

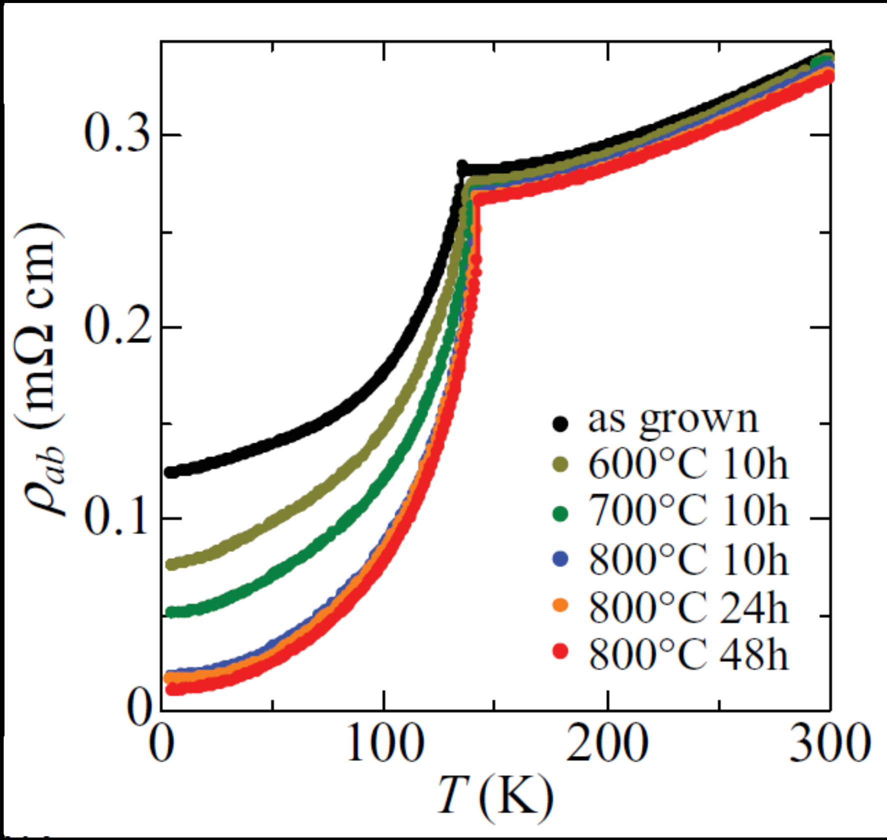

M. Nakajima *et al*. PNAS **108**, 12238 (2011)
M. Nakajima *et al*. PRL **109**, 217003 (2012)

Doping Dependence of Electronic Structure in $Ca(Fe_{1-x}Co_x)_2As_2$

Co atoms induce nanoscale C_2-symmetric electronic structure.

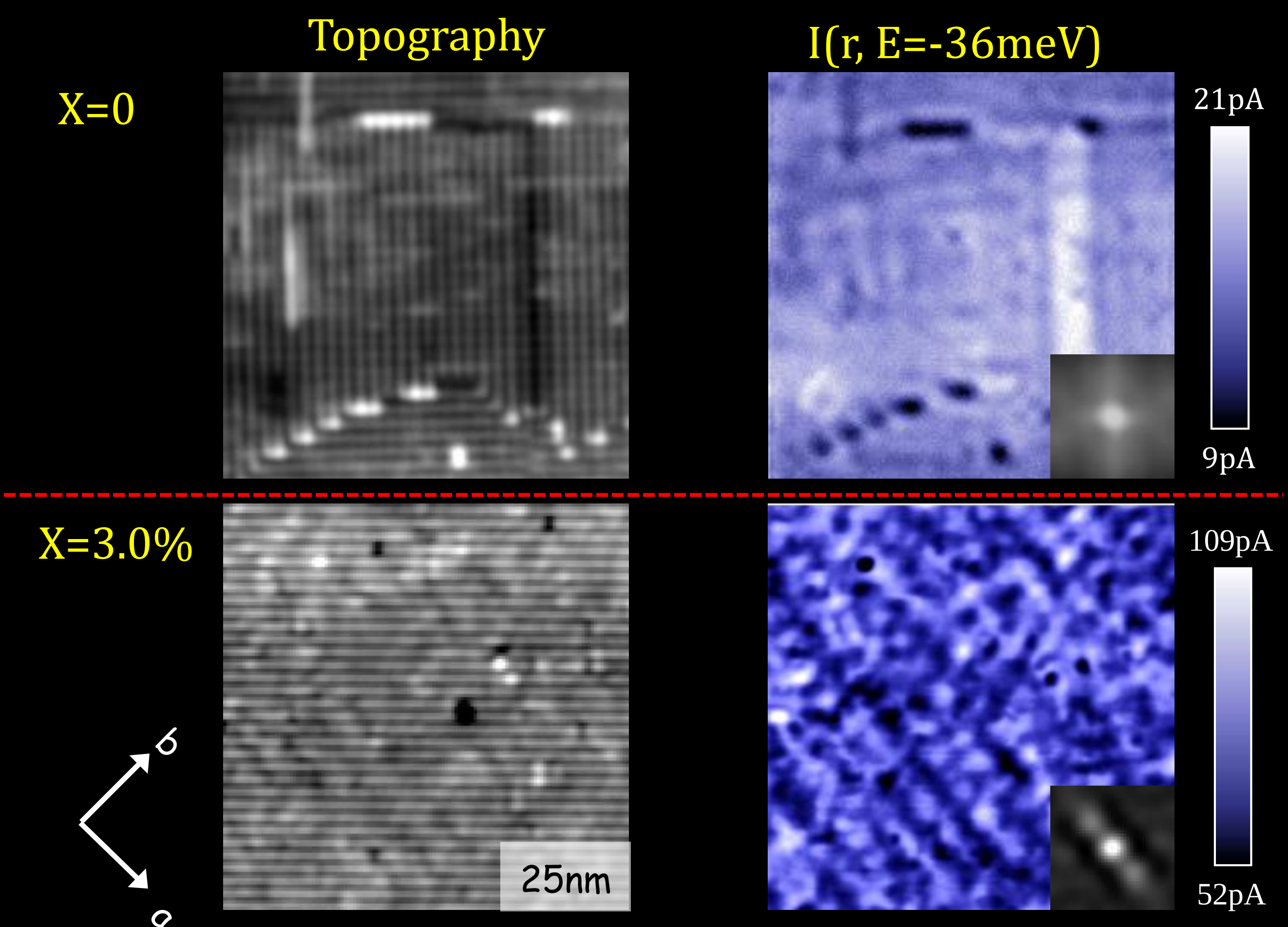

T.-M. Chuang *et al.*, Science **327**, 181 (2010)
M.P. Allan *et al.*, Nature Phys. 9, 220 (2013)

Our Proposal : Anisotropic Impurity State

- Anisotropic electronic impurity state
- Separated by $8a_{Fe\text{-}Fe}$, aligned with AFM a-axis
- Distributed randomly

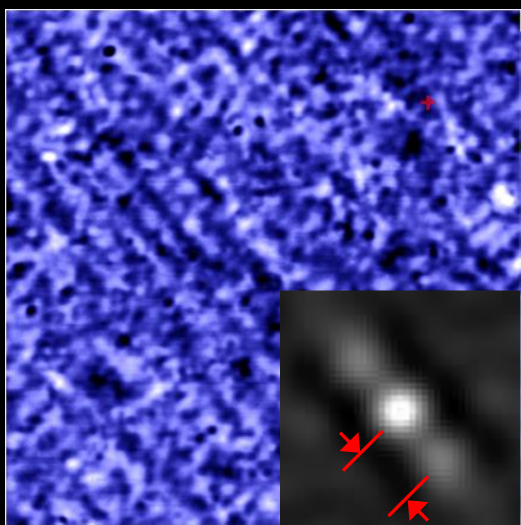

$\sim 8a_{Fe\text{-}Fe}$

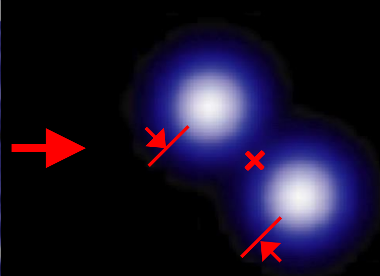

$\sim 8a_{Fe\text{-}Fe}$

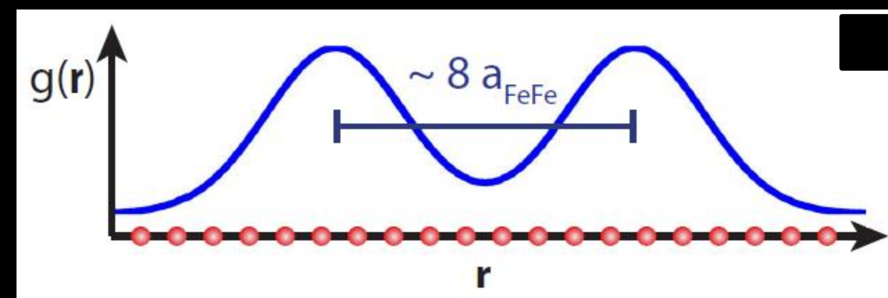

$$g(\mathbf{r}) = \sum_{\mathbf{R_j} \in \mathscr{R}} \mathcal{N}(\mathbf{r} - \mathbf{R_j}),$$

$$\mathcal{N}(\mathbf{r}) = \mathcal{G}_\sigma(\mathbf{r}) + \mathcal{G}_\sigma(\mathbf{r} + \mathbf{d}),$$

$$\mathcal{G}_\sigma(\mathbf{r}) = \left[a \cdot e^{-\frac{|\mathbf{r}|^2}{\sigma^2}} \right] \mathrm{mS},$$

M.P. Allan *et al.*, Nature Phys. 9, 220 (2013)

Static Nematic Electronic Structure vs Simulation

Data, g(***r***, E=-37meV)

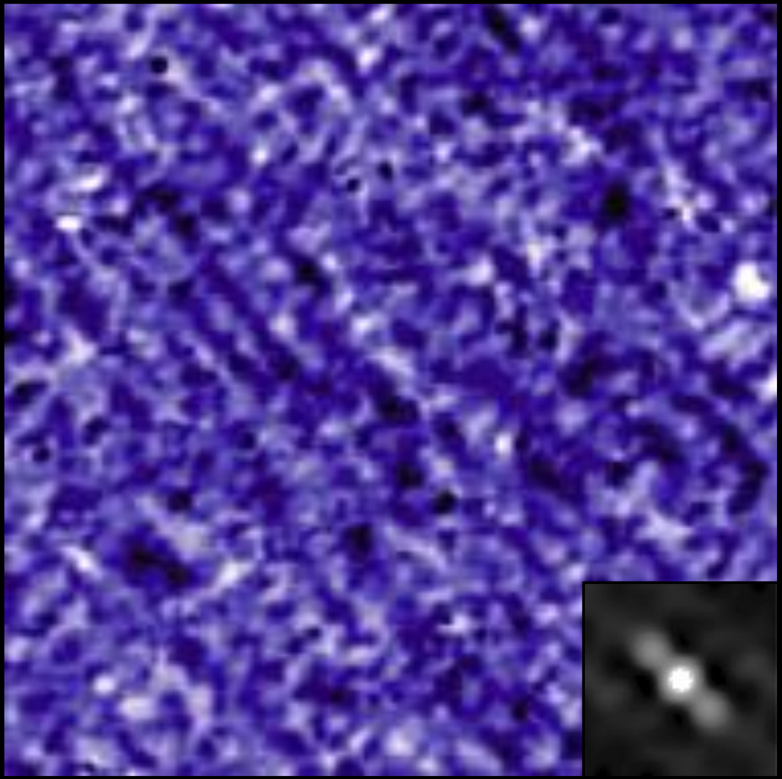

Simulation, 1000 impurities ~ 3% doping

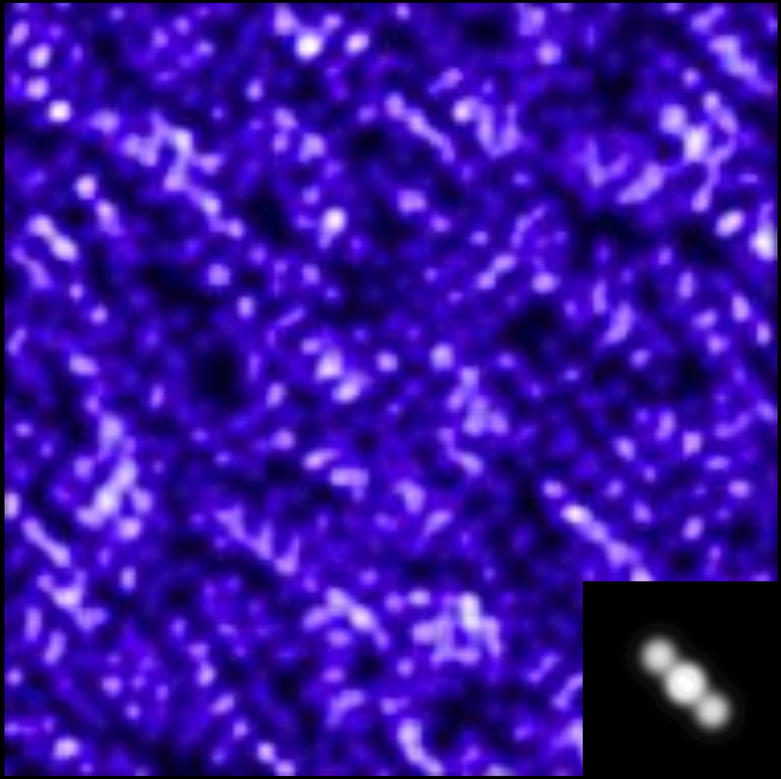

48nm

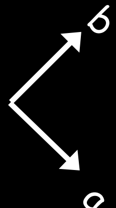

Consistent with real-space electronic structure.

M.P. Allan *et al.*, Nature Phys. 9, 220 (2013)

Where Are Cobalt Dopant Atoms?

What Role Do They Play?

Atom-projected DOS for Co Dopants

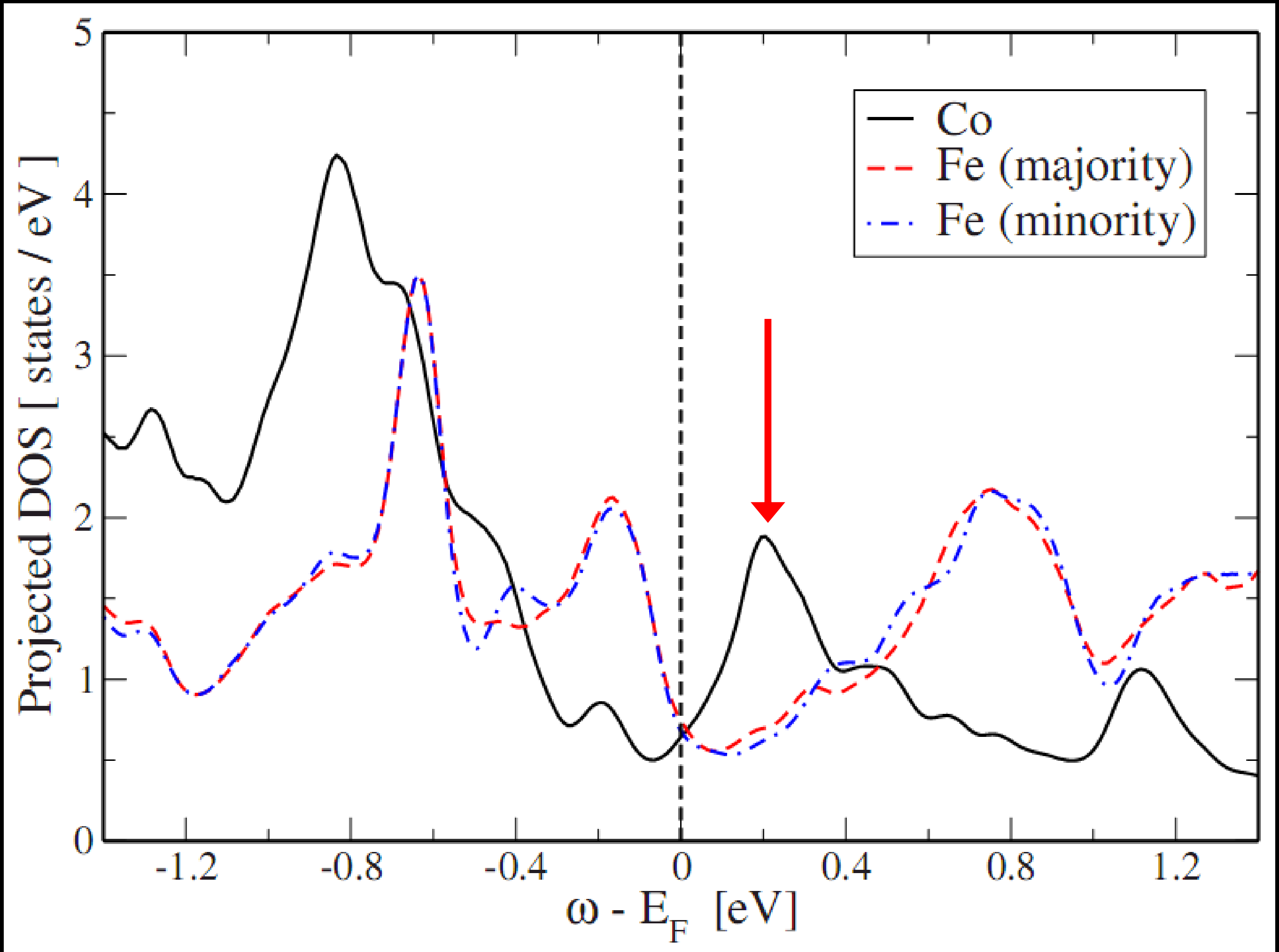

A. F. Kemper *et al.*, PRB **80**, 104511 (2009)

Possible Identification of Co Dopants

$g(\vec{r}, +150mV)$

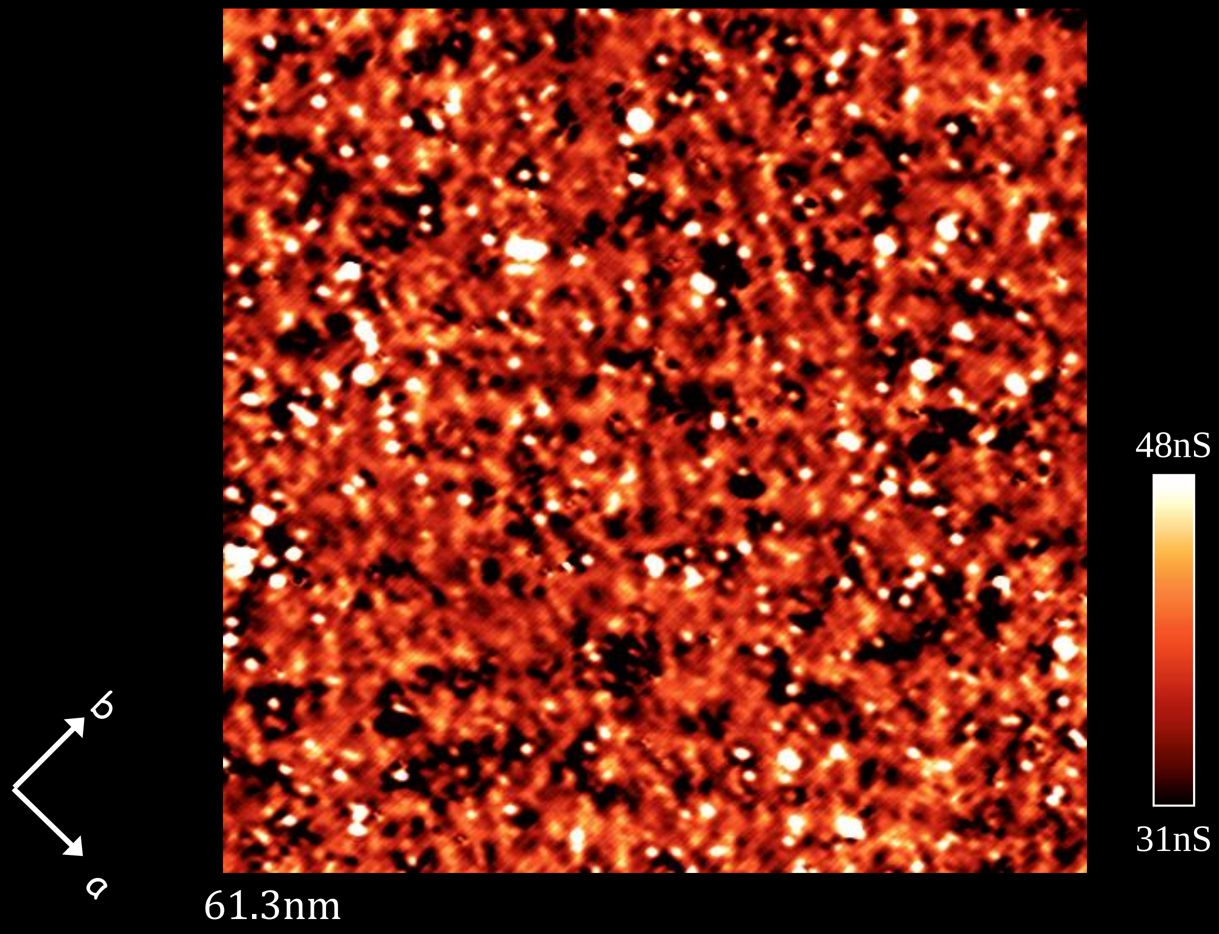

T.-M. Chuang *et al.*, Science **327**, 181 (2010)
M.P. Allan *et al.*, Nature Phys. 9, 220 (2013)

Correlation between Co and Static Electronic Structure

$I(\vec{r}, +50mV)$+ Co Dopants

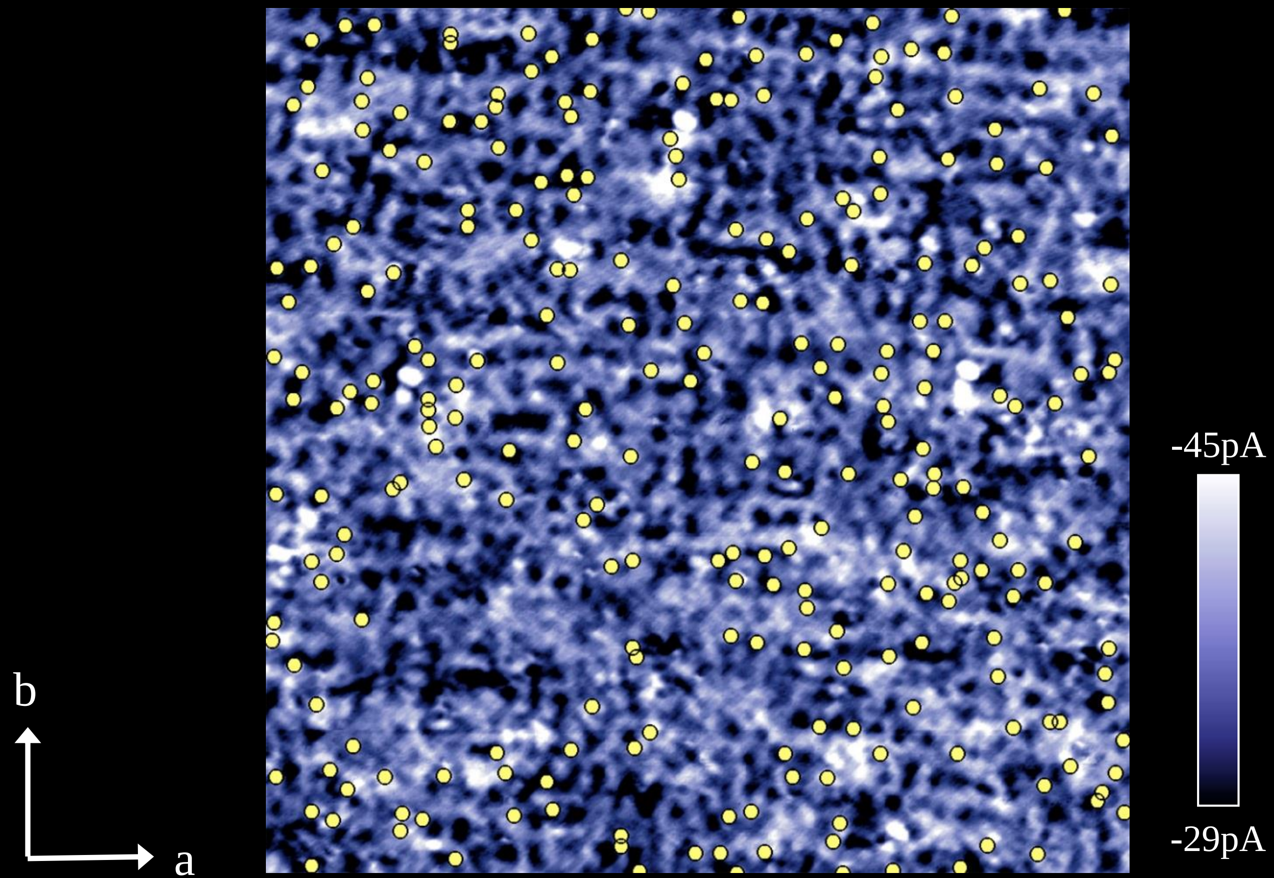

Normalized cross-correlation=0.22

T.-M. Chuang *et al.*, Science **327**, 181 (2010)
M.P. Allan *et al.*, Nature Phys. 9, 220 (2013)

Anisotropic Impurity States Induced or Pinned by Co Atoms

Autocorrelation
of I-map

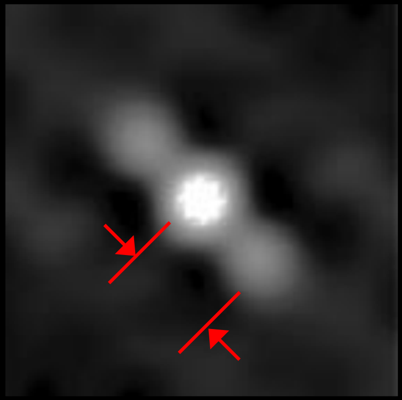

~8$a_{Fe\text{-}Fe}$

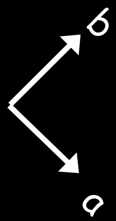

Averaged I-map
around Co

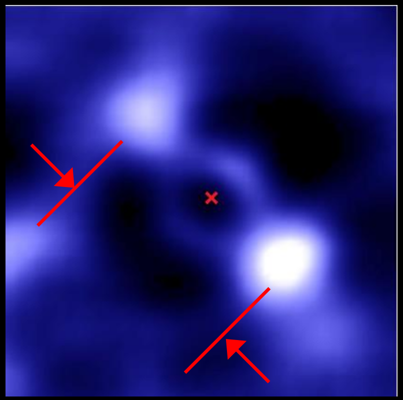

~8$a_{Fe\text{-}Fe}$

Averaged I-map
away from Co

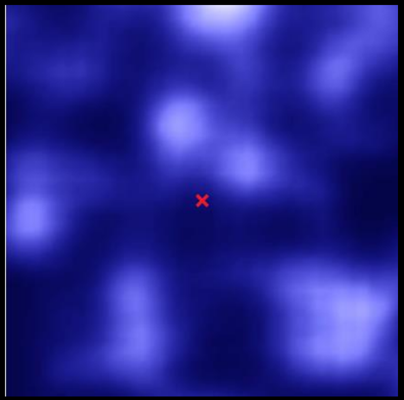

M.P. Allan *et al.*, Nature Phys. 9, 220 (2013)

Reconcile QPI and ARPES

QPI from α2 band at Γ ⟷ Additional symmetry breaking?

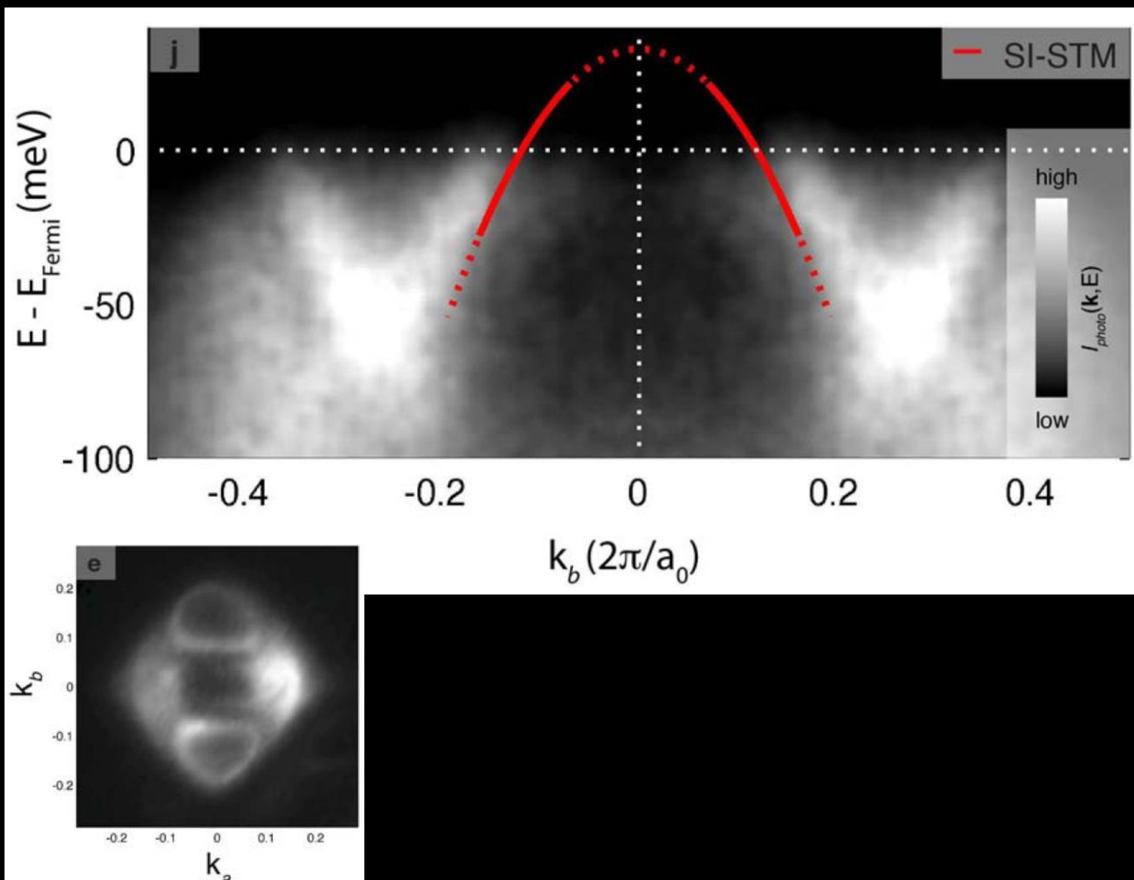

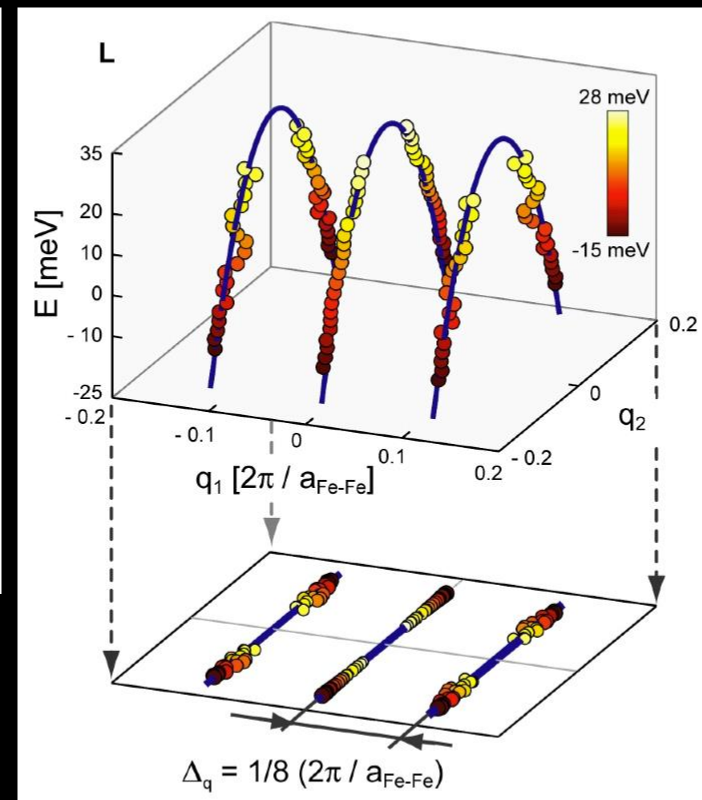

M.P. Allan *et al.*, Nature Phys. 9, 220 (2013)

Impact of Anisotropic Impurity State on QPI

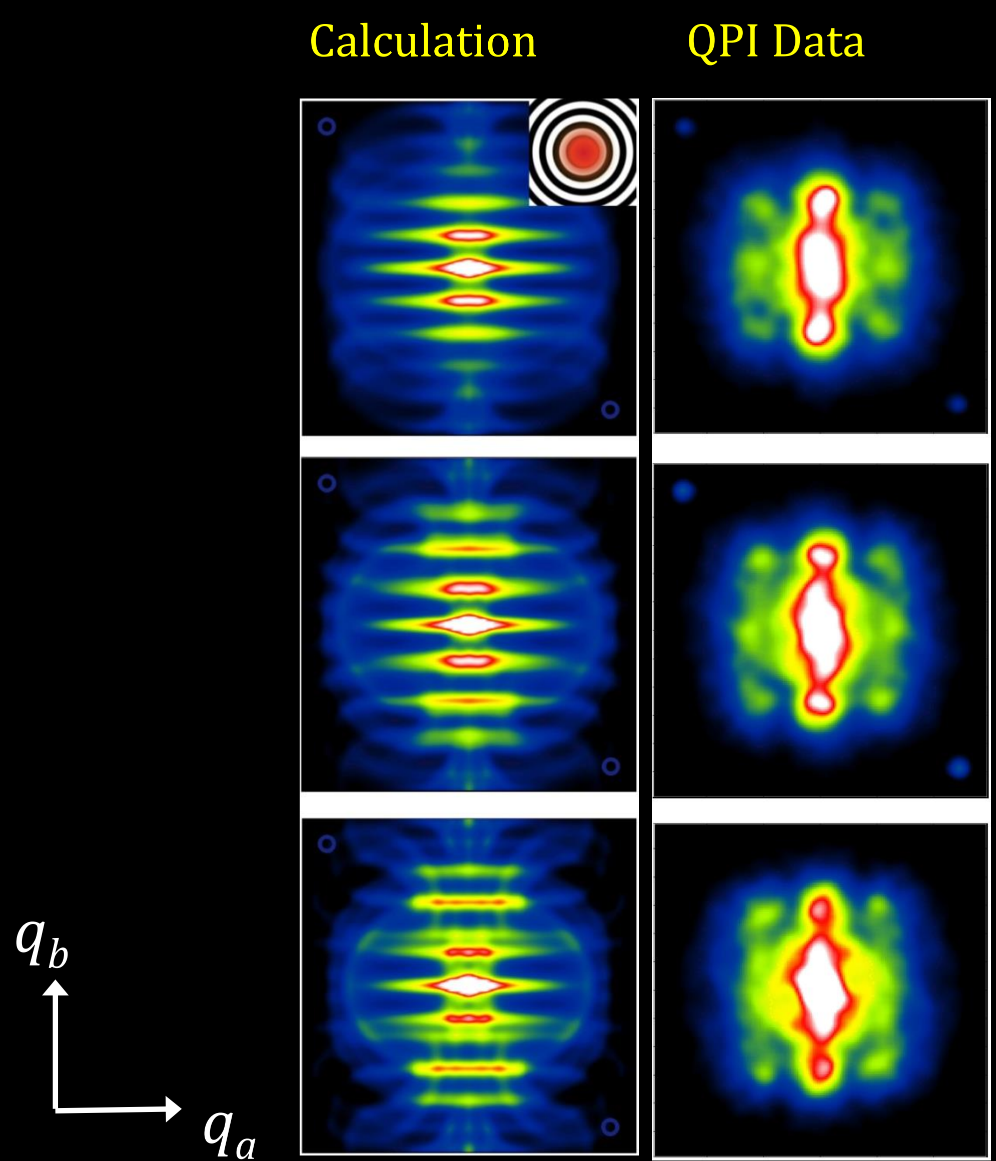

M.P. Allan *et al.*, Nature Phys. 9, 220 (2013)

Power spectral density in differential conductance modulation

$$P(q,\omega) = \frac{1}{N}\left|\frac{1}{\pi}\mathrm{Im}\,\Lambda(q,\omega)\right|^2 |\delta\epsilon(q)|^2$$

Bare QPI

Structure Factor :
FFT of r-space scattering potential

Capriotti *et al.*, PRB 68, 014508 (2003)

Impact of Anisotropic Impurity State on QPI

Calculation | QPI Data

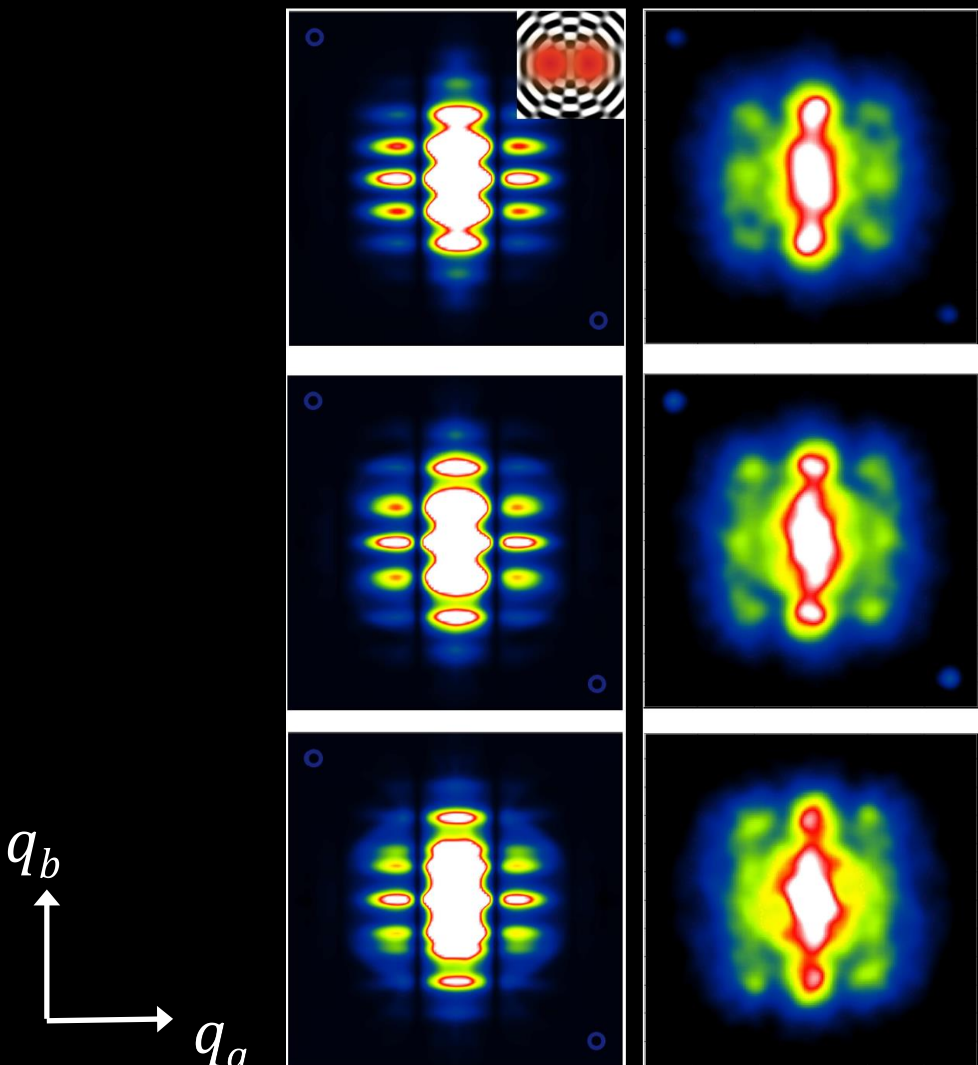

M.P. Allan *et al.*, Nature Phys. 9, 220 (2013)

Power spectral density in differential conductance modulation

$$P(q,\omega) = \frac{1}{N}\left|\frac{1}{\pi}\operatorname{Im}\Lambda(q,\omega)\right|^2 |\delta\epsilon(q)|^2$$

Bare QPI

Structure Factor :
FFT of r-space scattering potential

Capriotti *et al.*, PRB 68, 014508 (2003)

Reconcile with Transport Anisotropy?

Scattering Rate in Born Approximation

Boltzman transport equation :

$$-\mathbf{v}_{\mathbf{k}} \cdot e \frac{\partial f^0_{\mathbf{k}}}{\partial E(\mathbf{k})} \mathbf{E} = \int \mathrm{d}\mathbf{k}' \, P(\mathbf{k}-\mathbf{k}') \Big\{ (f_{\mathbf{k}} - f^0_{\mathbf{k}}) - (f_{\mathbf{k}'} - f^0_{\mathbf{k}'}) \Big\}$$

Band structure

Scattering

Scattering probability

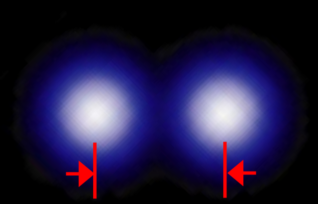

$\sim 8a_{\text{Fe-Fe}}$

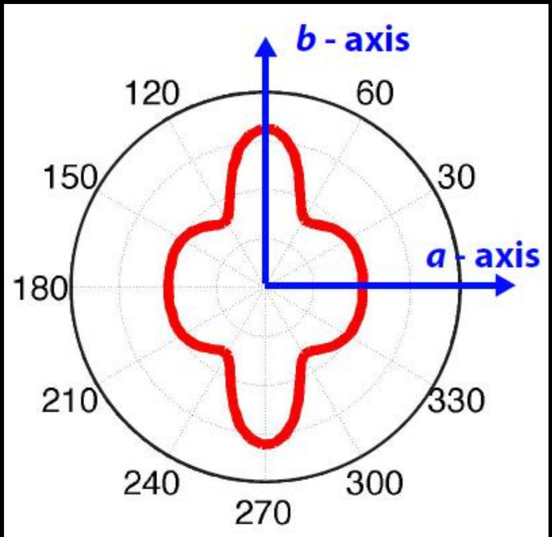

Scattering is anisotropic and q-dependent

$\rightarrow$ possible strong influence on transport.

Effective scattering rates also depend on the Fermi surface

M.P. Allan *et al.*, Nature Phys. 9, 220 (2013)

Consistent with Recent Transport Measurements

ρ_a and ρ_b show similar T dependence in the AFO phase.
→ T-dependent component of resistivity is nearly isotropic.

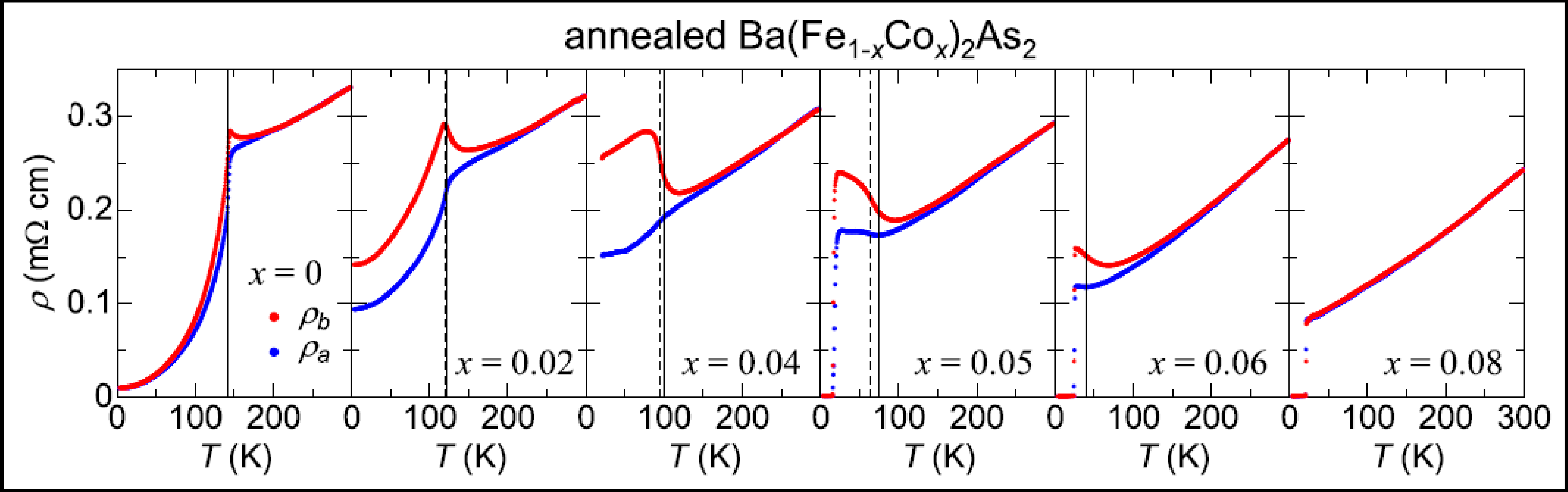

S. Ishida *et al*. PRL **110**, 207001 (2013)

Consistent with Recent Transport Measurements

The anisotropy in resistivity in AFO arises from the anisotropy in the residual component which increases in proportion to the Co concentration x.

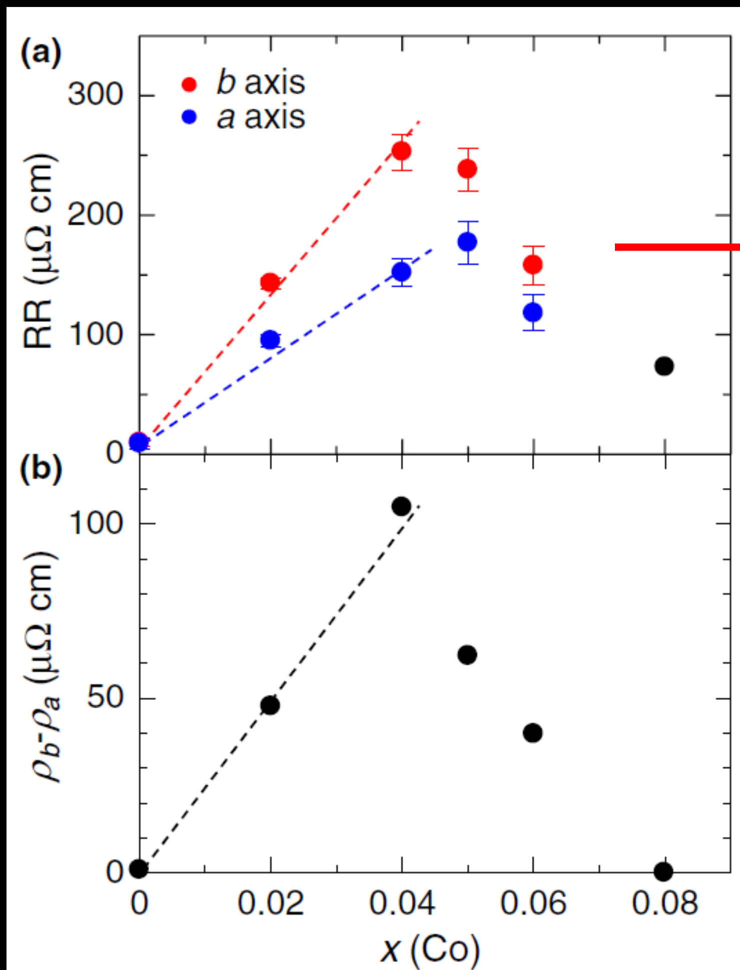

S. Ishida *et al*. PRL **110**, 207001 (2013)

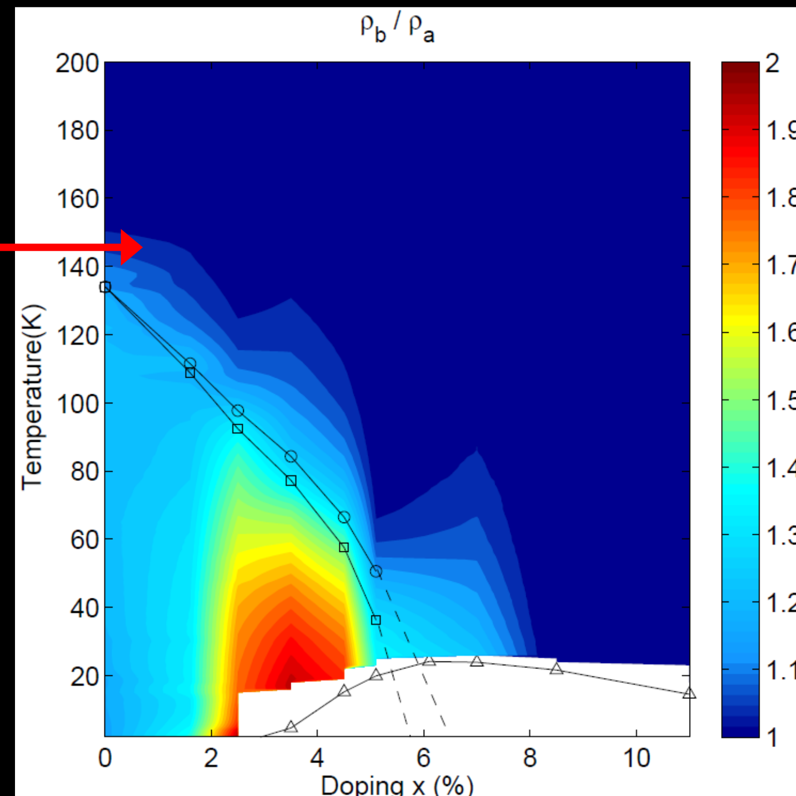

J.-H. Chu *et al.*, Science **329**, 824 (2010)

Nematicity above T_s and T_c

$BaFe_2(As_{1-x}P_x)_2$

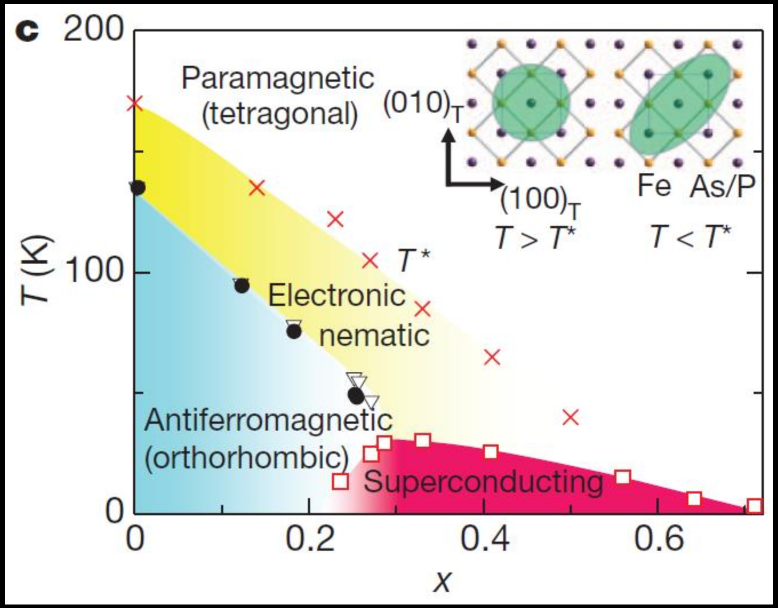

S. Kasahara *et al.*, Nature **486**, 382 (2012)

NaFeAs : T_s=52K, T_N=41K

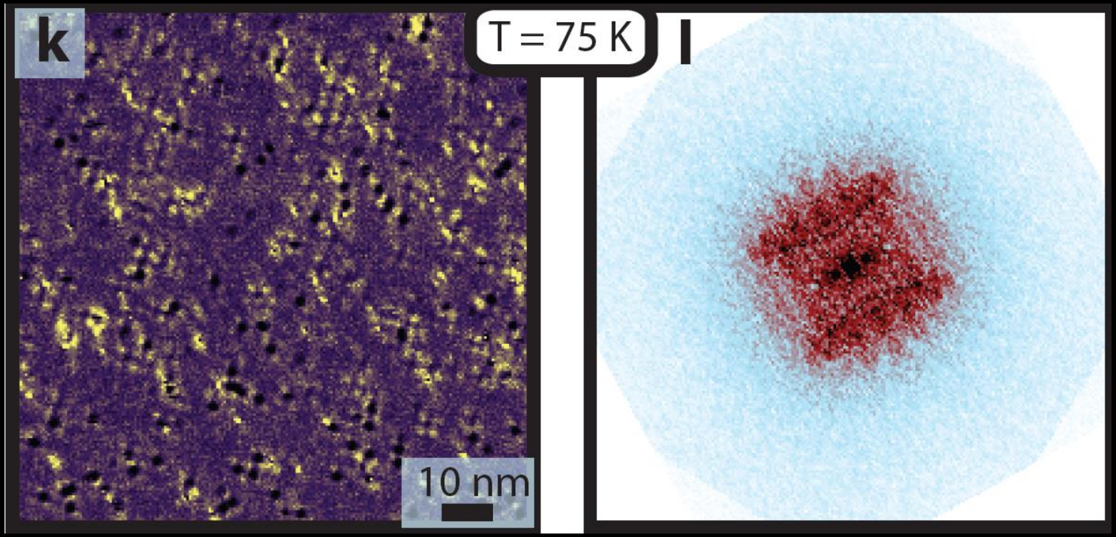

E. P. Rosenthal *et al.*, NatPhys 10, 225 (2014)

What drives the large nematic susceptibility?

Nematicity Relevant to High Tc FeSC?

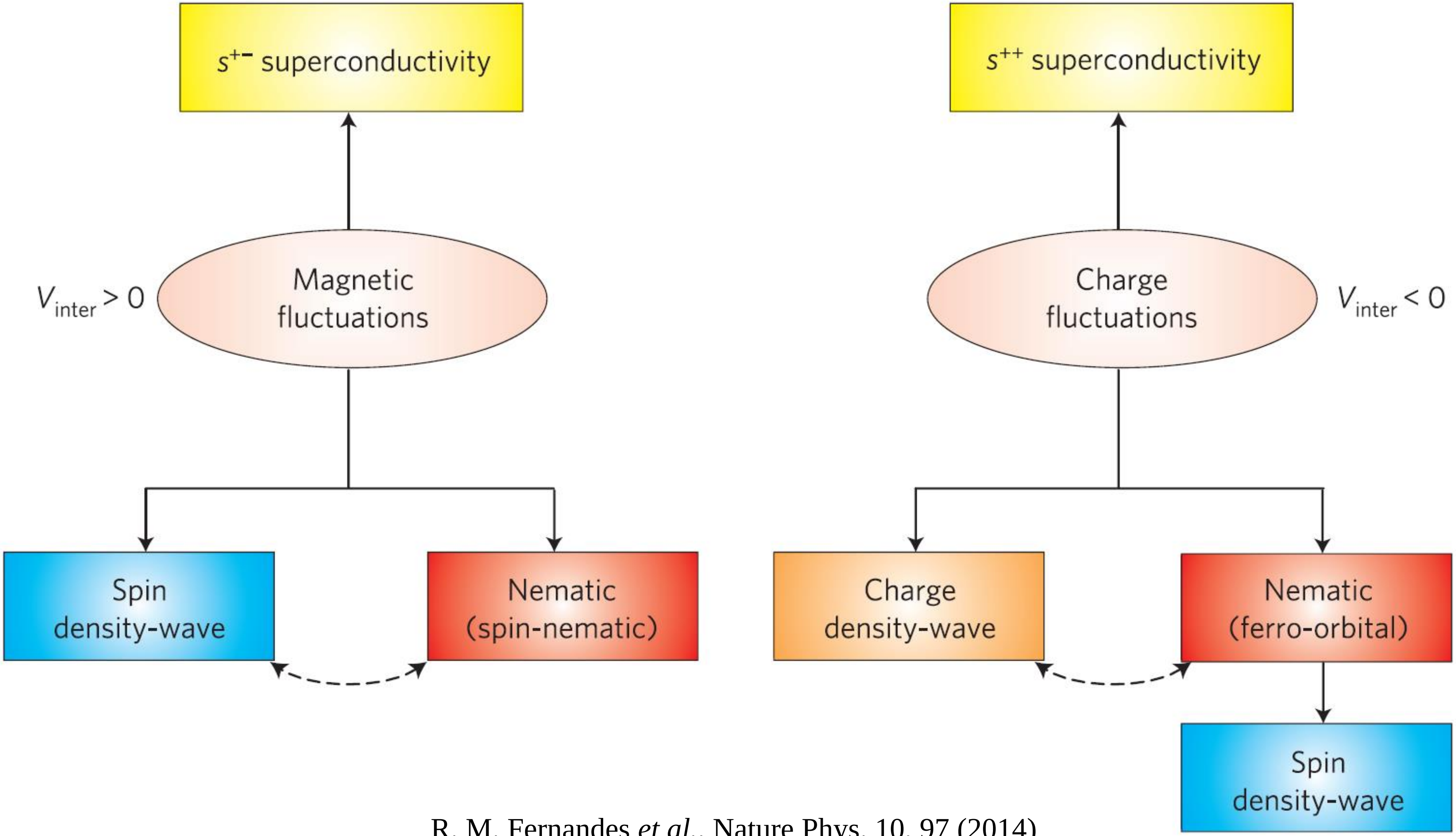

R. M. Fernandes *et al.*, Nature Phys. 10, 97 (2014)

Nematicity Relevant to High T_c Superconductivity?

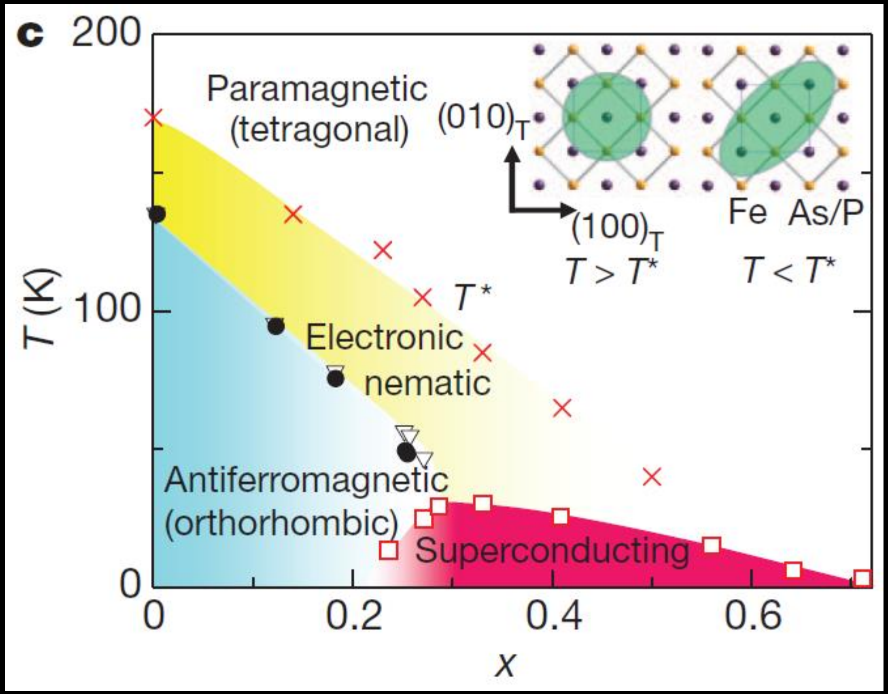

S. Kasahara *et al.*, Nature 486, 382 (2012)

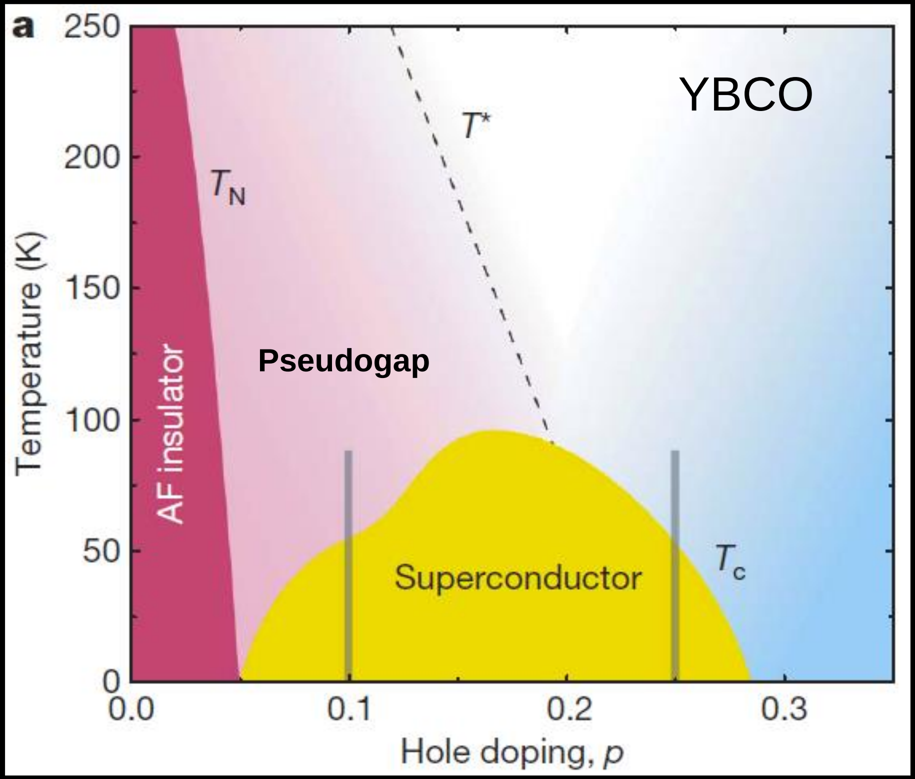

N. Doiron-Leyraud *et. al.*, Nature 447, 565 (2007)

FeSC vs Cuprates : Superconducting Layer

Both have antiferromagnetic 'parent' states.

Cooper pairing mediated by AF ?

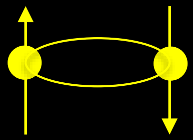

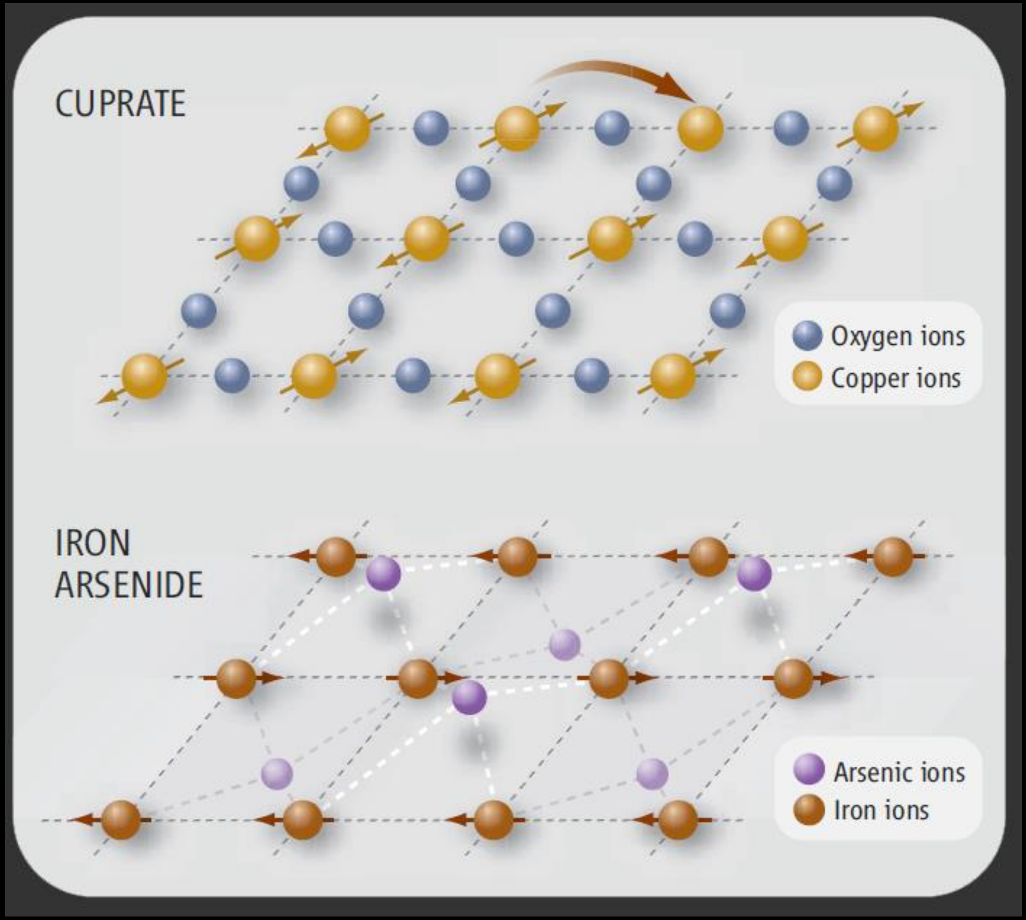

$d_{x^2-y^2}$

5 d-orbitals

A. Cho, Science **320**, 870 (2008)

FeSC: Unconventional Superconductivity

1. The electron-phonon coupling is too weak to account for such high T_C.

L. Boeri *et al.*, PRL 101, 026403 (2008)

2. Isotope effect on some materials shown to be negligible.

P.M. Shirage *et al.*, PRL 105, 037004 (2010)

3. Everything seems to work – doping / pressure / different structures

Possible pairing symmetries

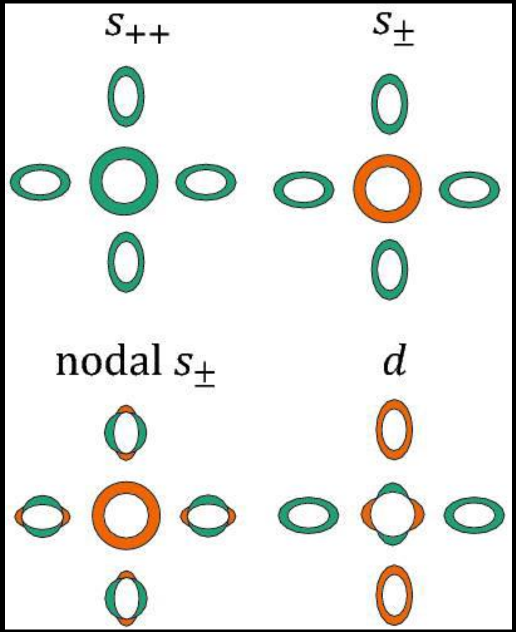

FeSC: Candidates for Pairing Mechanism

SDW suppression leads to SC
→ AF Spin Fluctuation Exchange.
→ S± OP symmetry

I. I. Mazin *et al.*, PRL 101, 057003 (2008)
K. Kuroki *et al.*, PRL 101, 087004 (2008)
K. Seo *et al.*, PRL 101, 206404 (2008).

Orbital Fluctuation → S++ OP symmetry

H. Kontani *et al.*, PRL **104**, 157001 (2010)

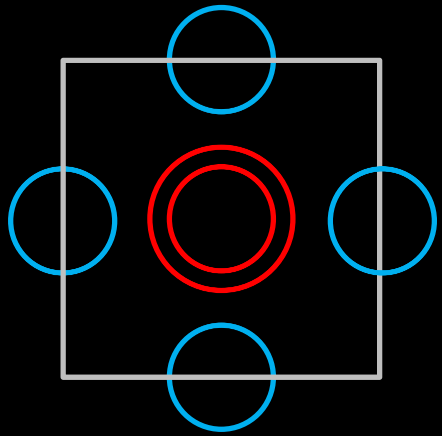

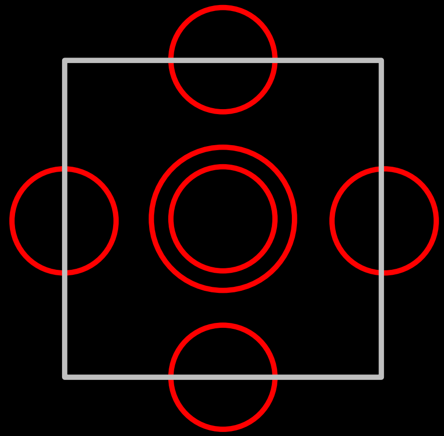

Gap symmetry?
Phase sensitive measurements required!

STM on an iron chalcogenide

Fe (Se,Te) T_c = 13~14.5 K

T ~ 1.5 K

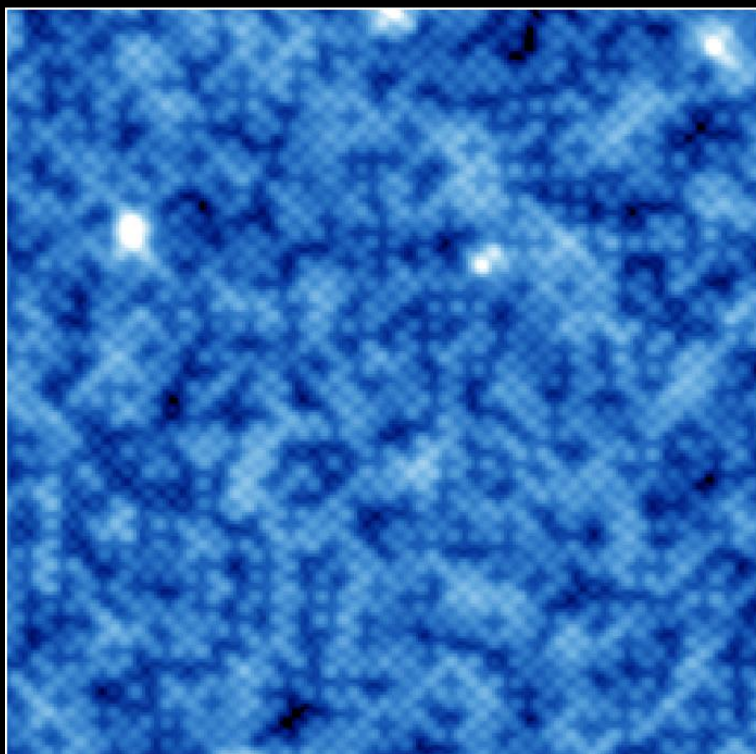

19 nm × 19 nm, -20 mV/0.1 nA

$2\Delta/T_c$ ~ 3.5

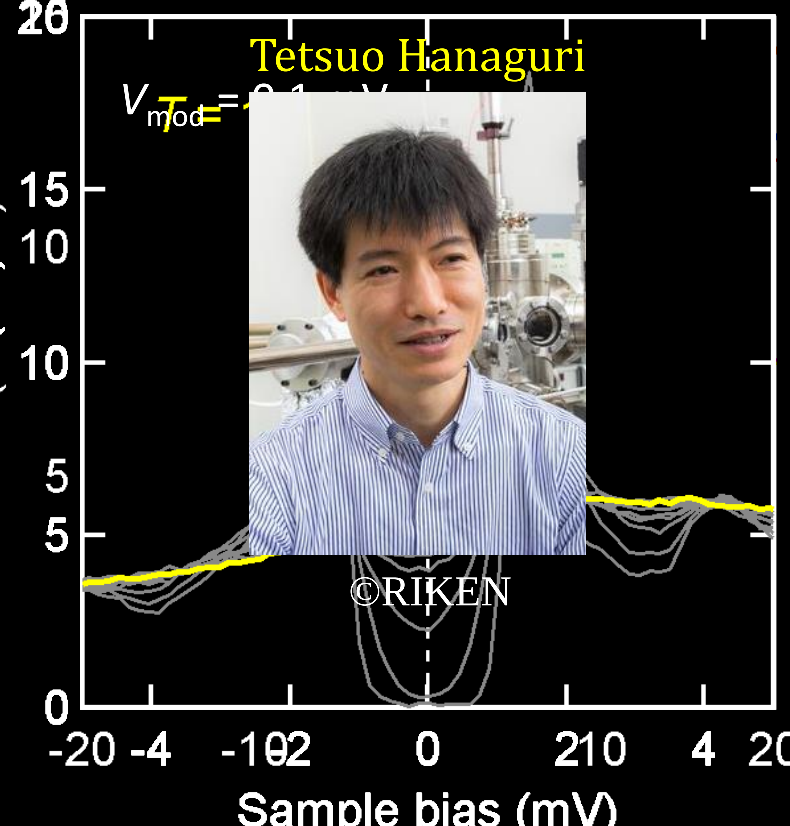

Tetsuo Hanaguri

©RIKEN

SC gap FULLY opens all over the FS pockets.

cf. F. Massee *et al.*, PRB 80, 140507(R) (2009), T. Kato *et al.*, PRB 80, 180507(R) (2009).

How will it work in iron-based SC?

Disconnected pockets

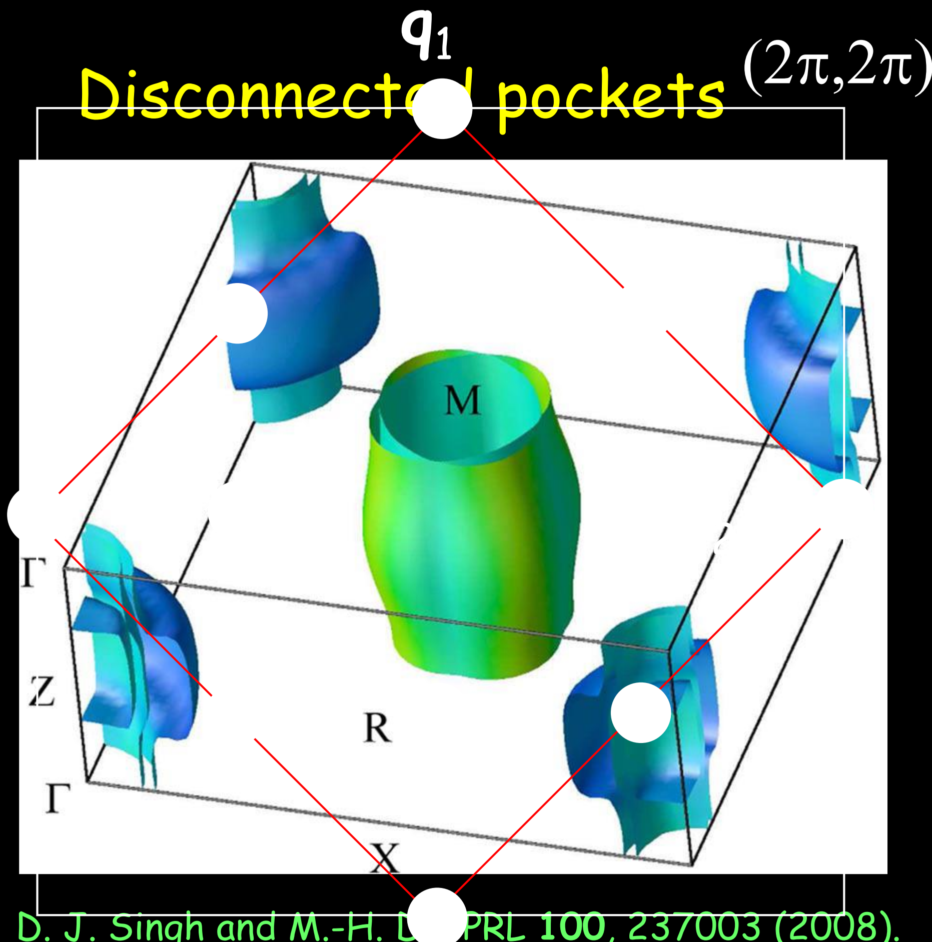

D. J. Singh and M.-H. D[illegible] PRL 100, 237003 (2008).

q space

$E \sim \Delta$

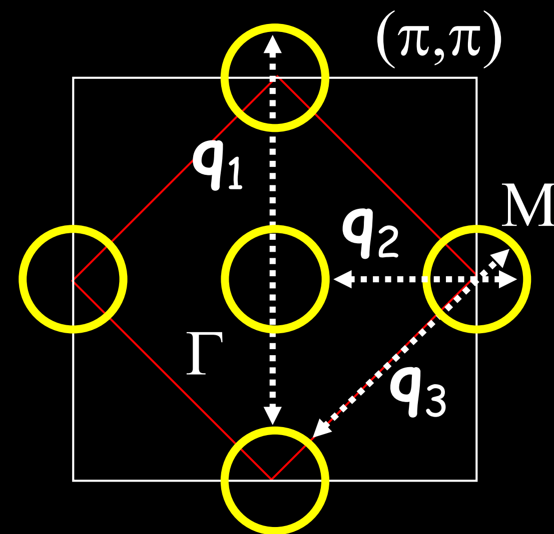

k space

Inter-pocket scattering ⟷ Relationship between the pockets

QPI in an iron chalcogenide

T. Hanaguri *et al.*, Science **328**, 474 (2010).

Fe(Se,Te) $T_c \sim 13$ K

$T \sim 1.5$ K

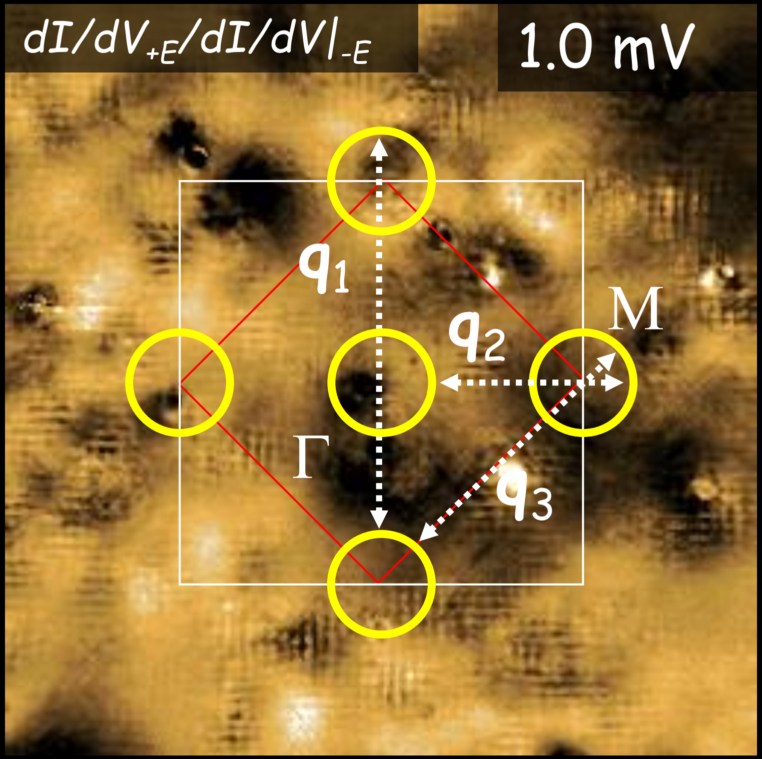

34 nm × 34 nm, -20 mV/0.1 nA

FT-*Z* map 1.0 meV

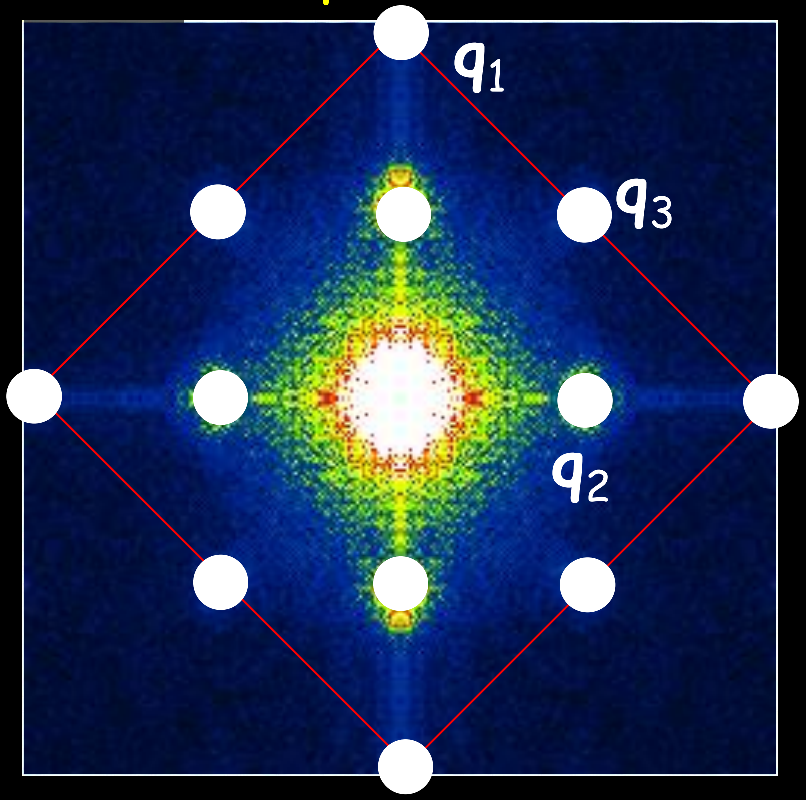

Inter-pocket scatterings are detected.

How to determine the phase?

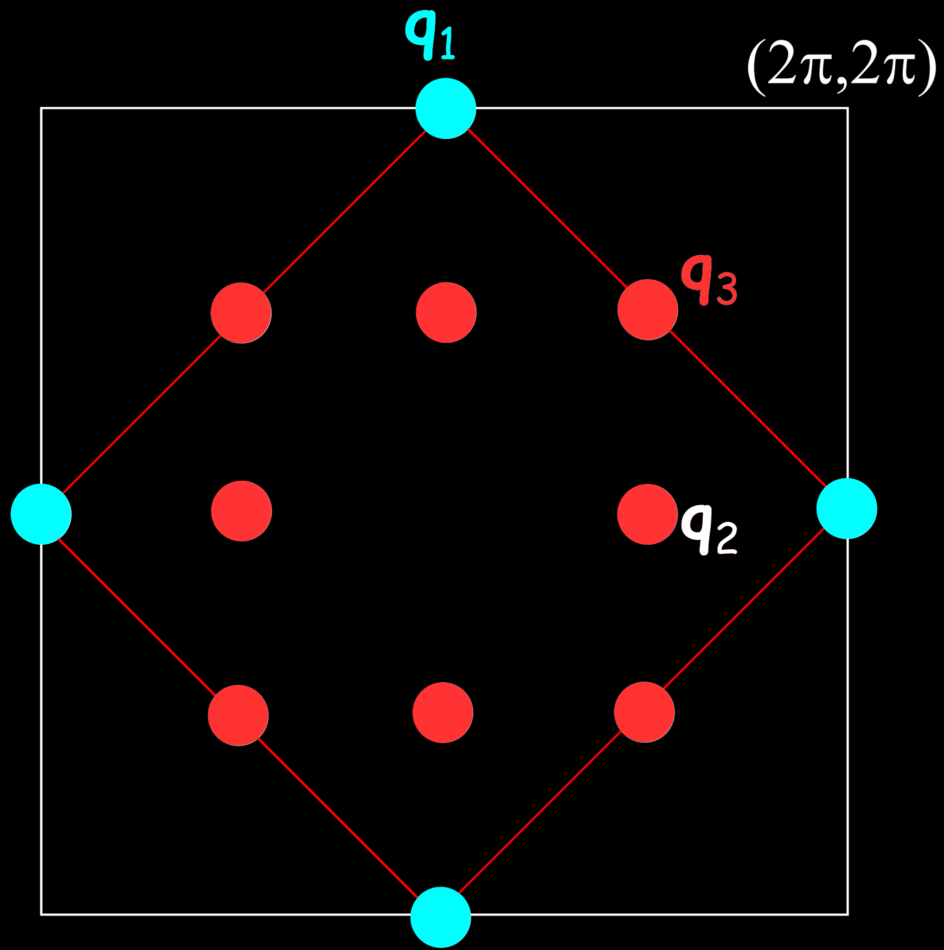

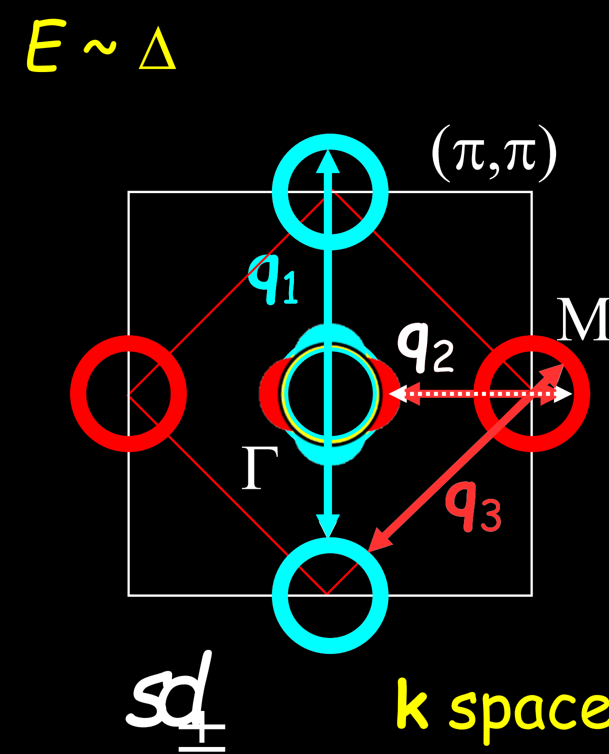

- Sign-preserving scattering
- Sign-reversing scattering

I. I. Mazin *et al.*, PRL **101**, 057003 (2008).
K. Kuroki *et al.*, PRL **101**, 087004 (2008).

cf.
F. Wang, H. Zhai and D. -H. Lee, EPL **85**, 37005 (2009).
Yan-Yang Zhang *et al.*, PRB **80**, 094528 (2009).
E. Plamadeala, T. Pereg-Barnea, and G. Refael PRB **81**, 134513 (2010).

Phase-sensitive STM on an iron chalcogenide

T. Hanaguri *et al.*, Science **328**, 474 (2010).

$Fe_{1+x}(Se,Te)$ $T_c \sim 13$ K

$T \sim 1.5$ K

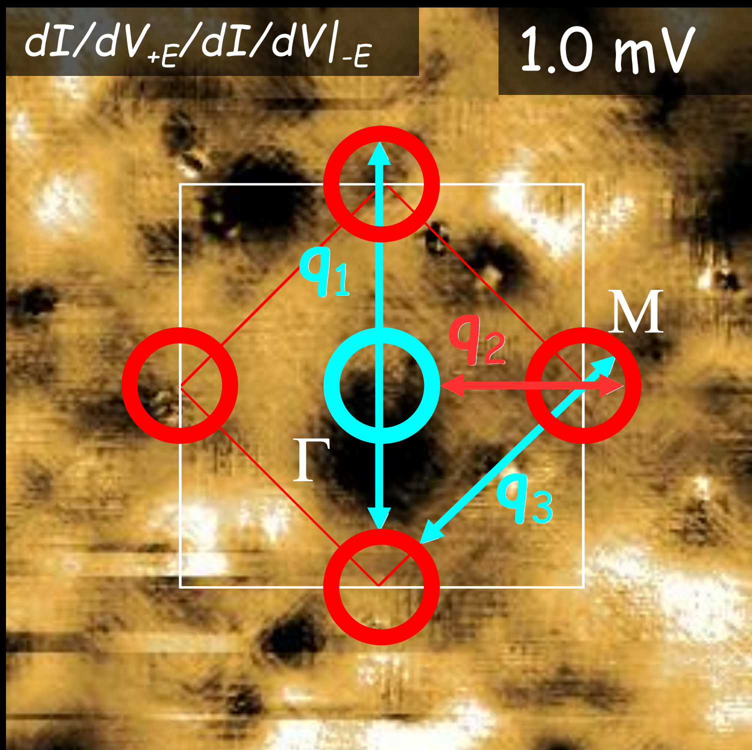

34 nm × 34 nm, -20 mV/0.1 nA

$B = 10$ T

FT-*Z* map 1.0 meV

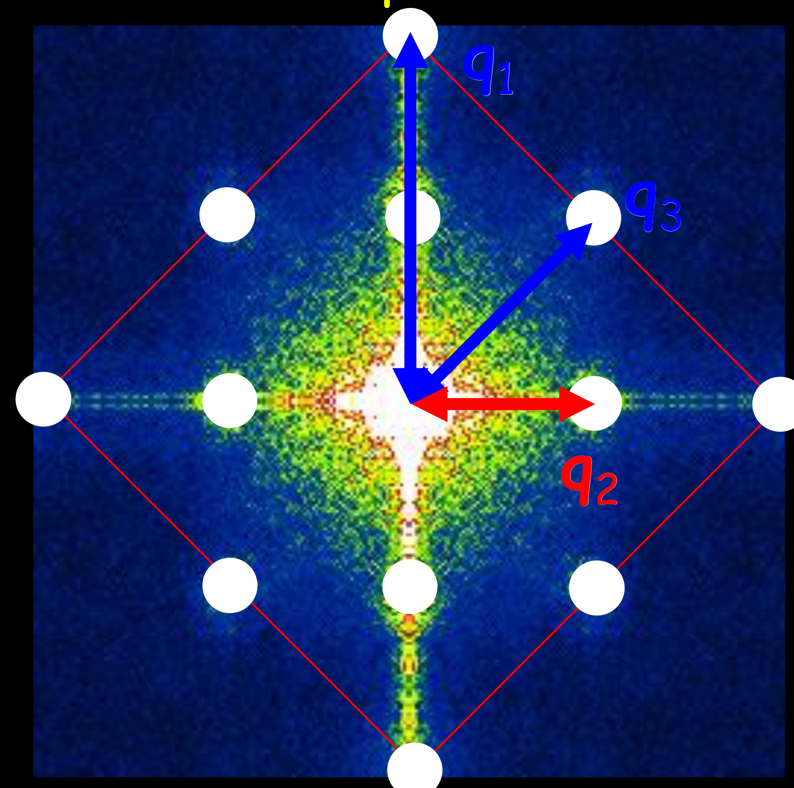

Vortices as magnetic scatterers

Evidence of s±-wave symmetry!

Interpocket scatterings are detected.

Spin fluctuation plausible.

Summary of gap structure of iron-based SC

STM suggests $s_{\pm}$-wave gap in an FeSC!

- Tunneling spectrum suggests that the superconducting gap fully opens over the Fermi surface.
- Inter-Fermi-pocket scatterings are identified in quasi-particle interference patterns, providing momentum-resolved information of the superconducting gap.
- Magnetic-field dependence of the quasi-particle interference pattern contains information on the phase of the superconducting gap function. The result on Fe(Se,Te) suggests $s_{\pm}$-wave superconductivity where the gap changes its sign between hole and electron pockets.

FeSC: SC Energy Gap Functions

Spin Fluctuation → S± OP symmetry

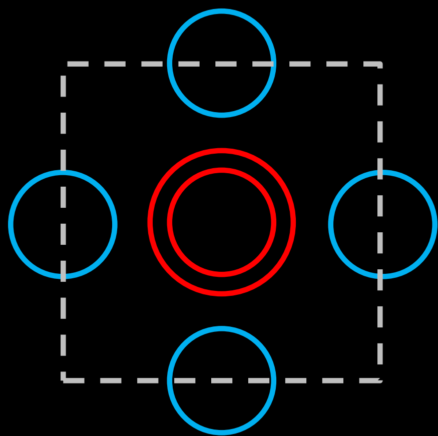

Orbital Fluctuation → S++ OP symmetry

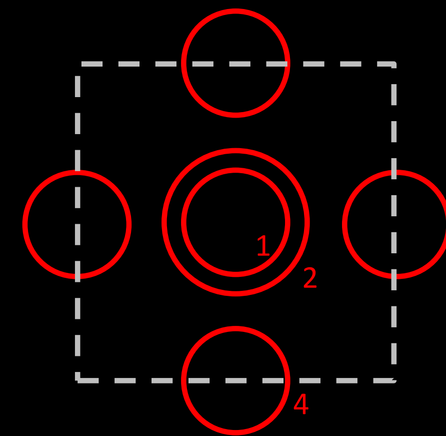

Gaps show different anisotropy at different pockets!

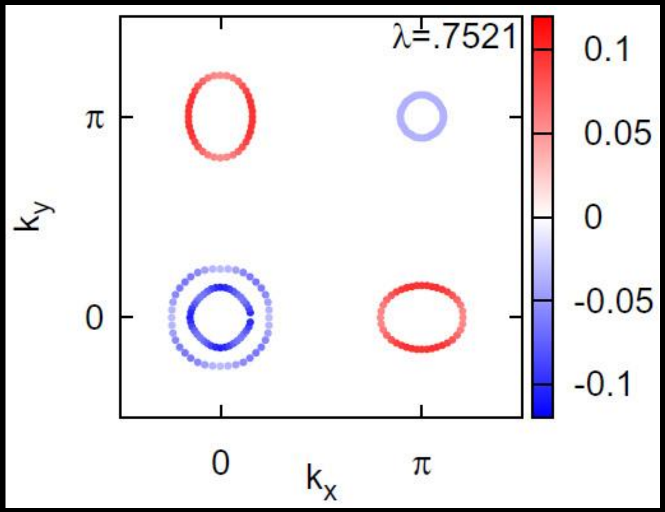

P. J. Hirschfeld et *al*., Rep.Prog.Phys.**74**,124508 (2011)

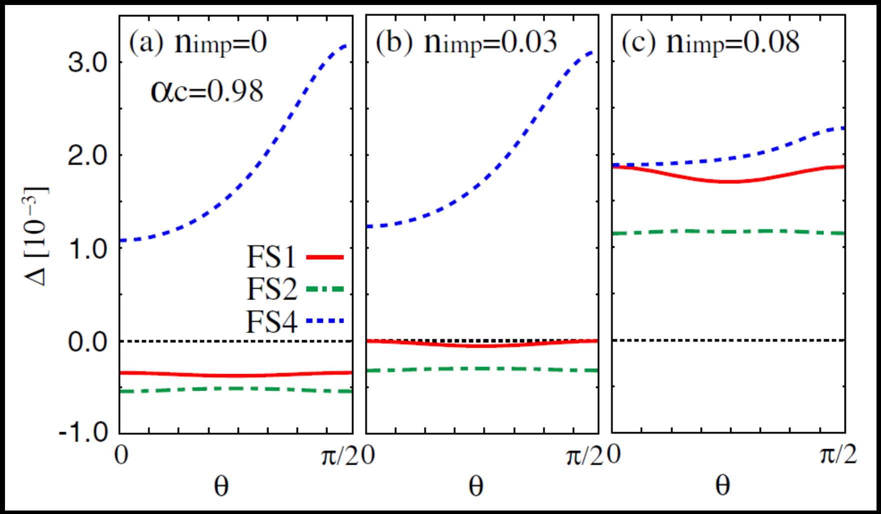

H. Kontani *et al*., PRL **104**, 157001 (2010)

Our Samples : LiFeAs

Charge neutral cleaved surface :No surface states.
Ideal for STM / ARPES !
Large field of view necessary for intra-band QPI measurements!

Milan Allan

Andreas Rost

Tien-Ming Chuang

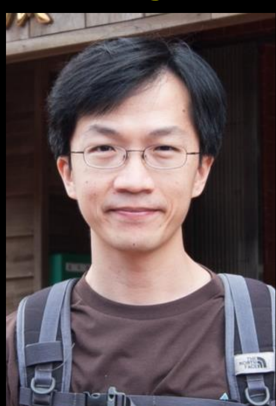

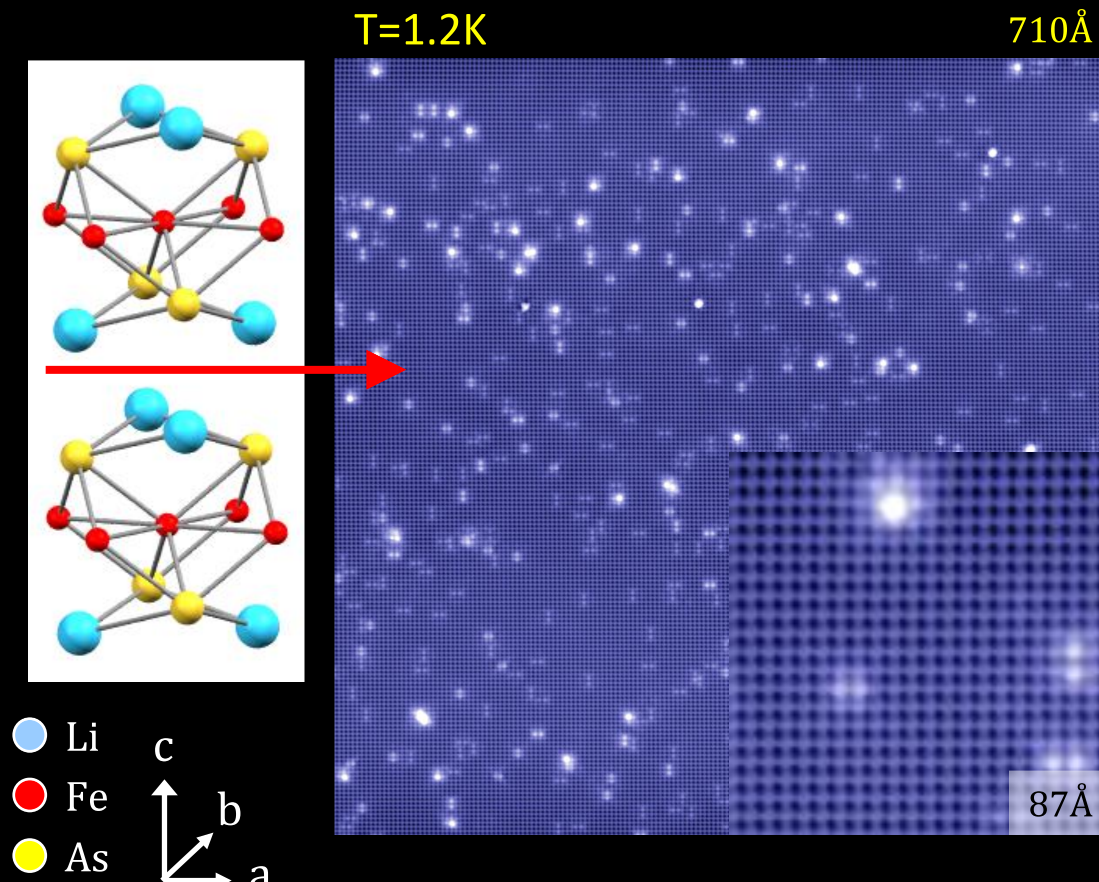

M. P. Allan & A.W. Rost *et al.*, Science **336**, 563 (2012)

Spectroscopic Imaging, LDOS(r,E)

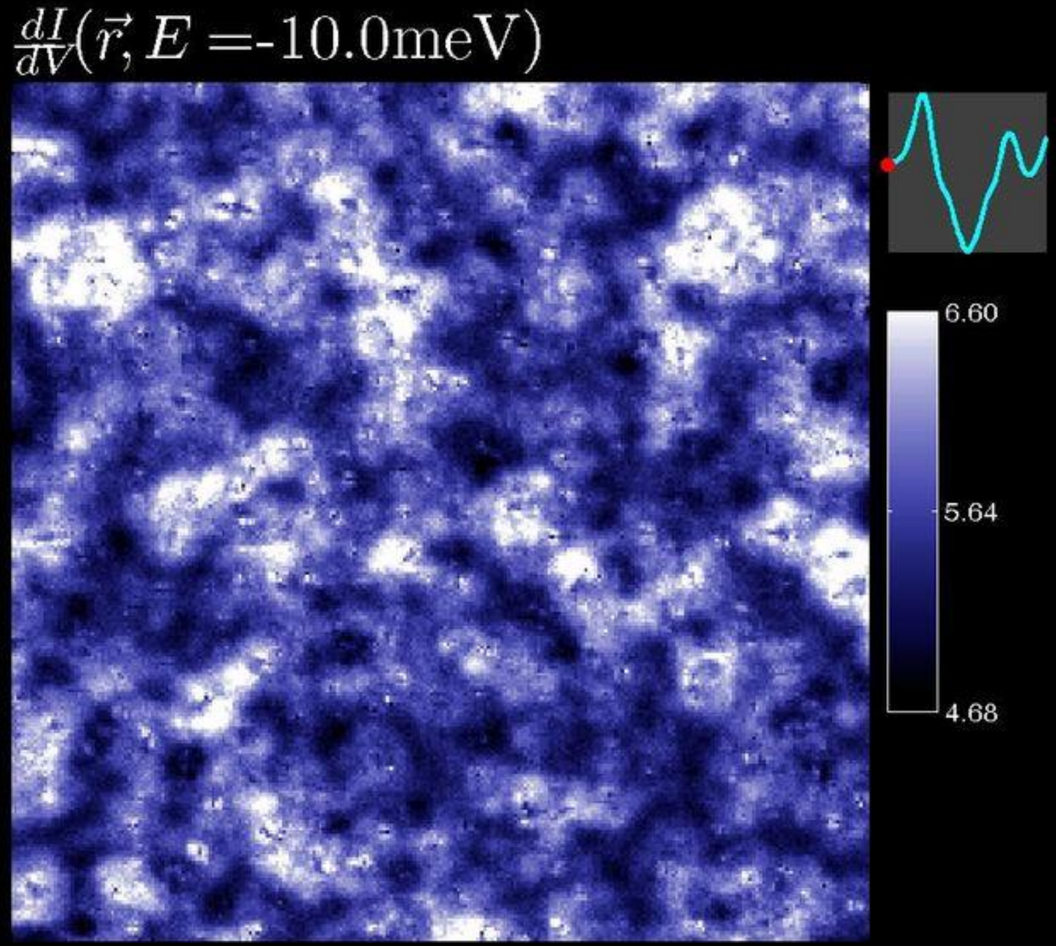

T= 1.2K 880Å

M. P. Allan & A.W. Rost *et al.*, Science **336**, 563 (2012)

Quasiparticle Interference, LDOS(q,E)

Fourier Transform of LDOS(r,E) → LDOS(q, E)

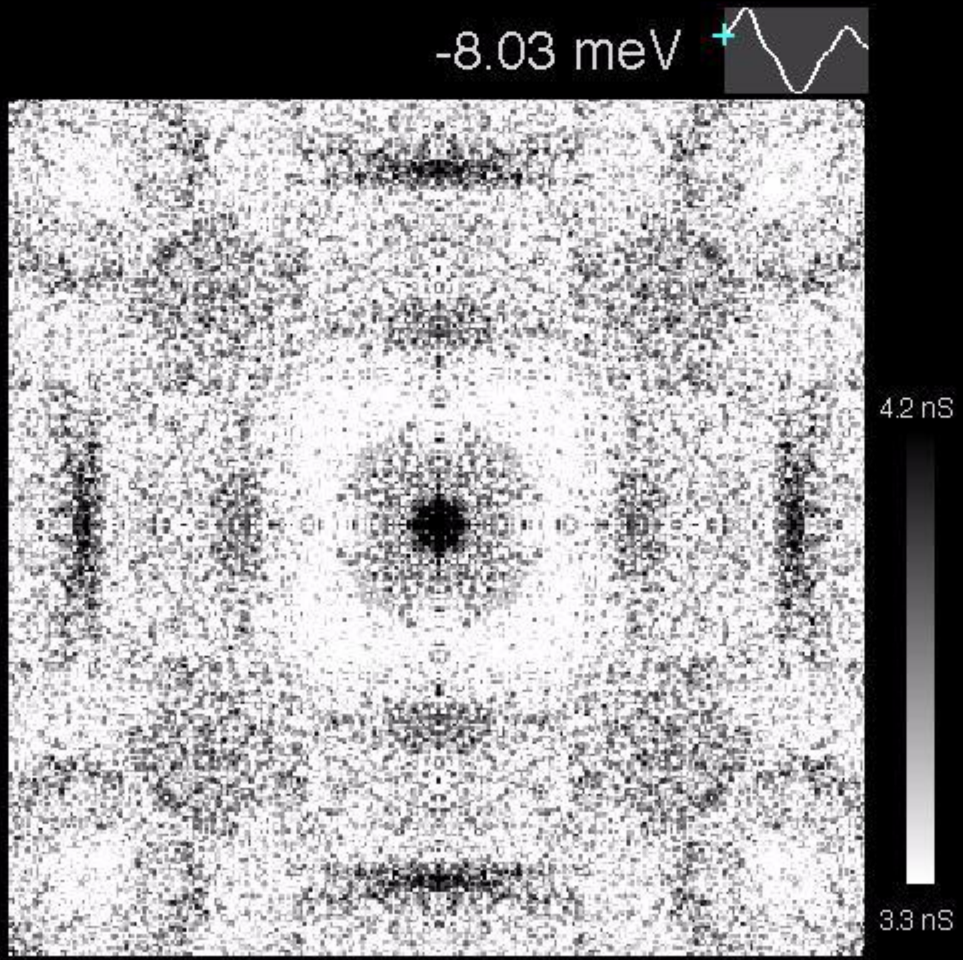

T= 1.2K 880Å

M. P. Allan & A.W. Rost *et al.*, Science **336**, 563 (2012)

Band Identification by QPI above SC gap

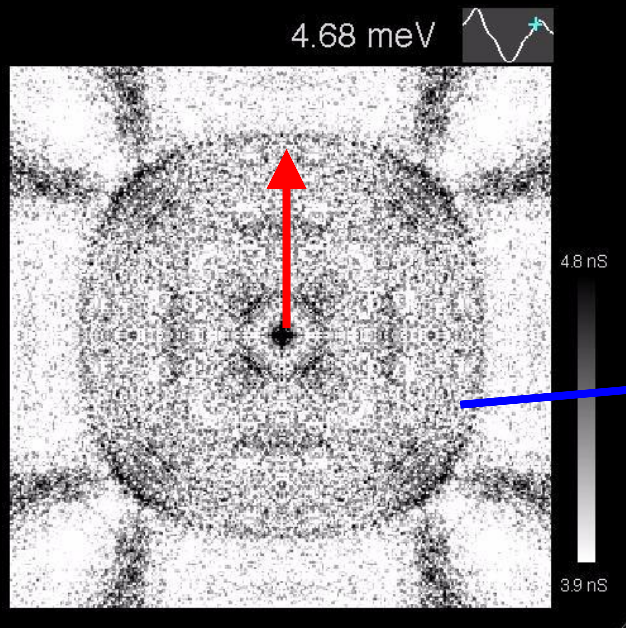

γ band

Identification based on comparison with ARPES and LDA results.

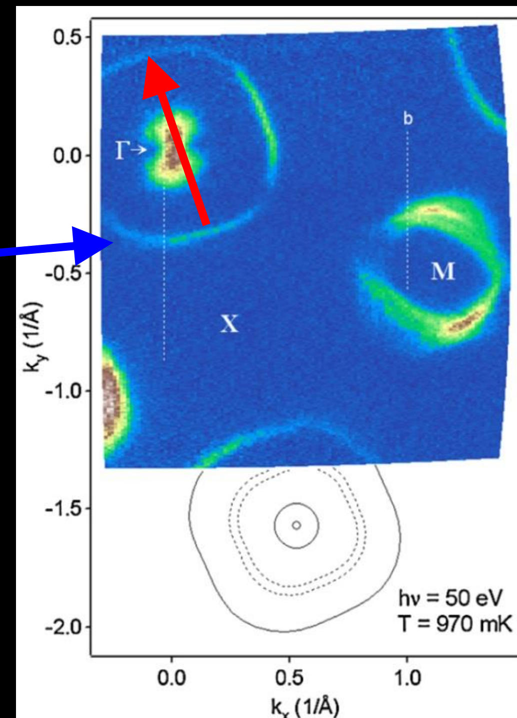

I.R. Shein *et al.*, Solid State Comm.150, 152 (2010)
S.V. Borisenko *et al.*, PRL 105, 067002 (2010)

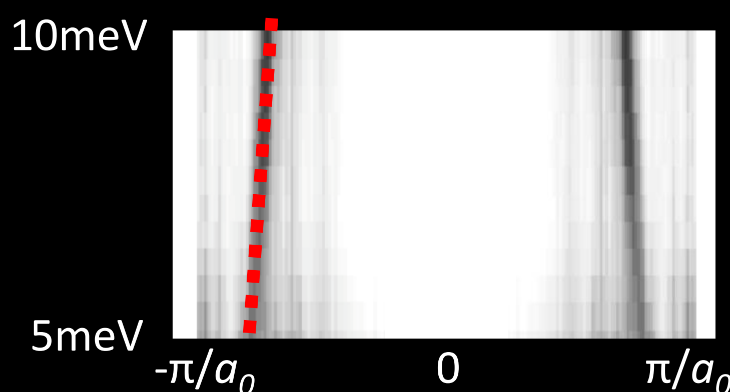

M. P. Allan & A.W. Rost *et al.*, Science **336**, 563 (2012)

Three hole-like bands: γ, α_2, α_1

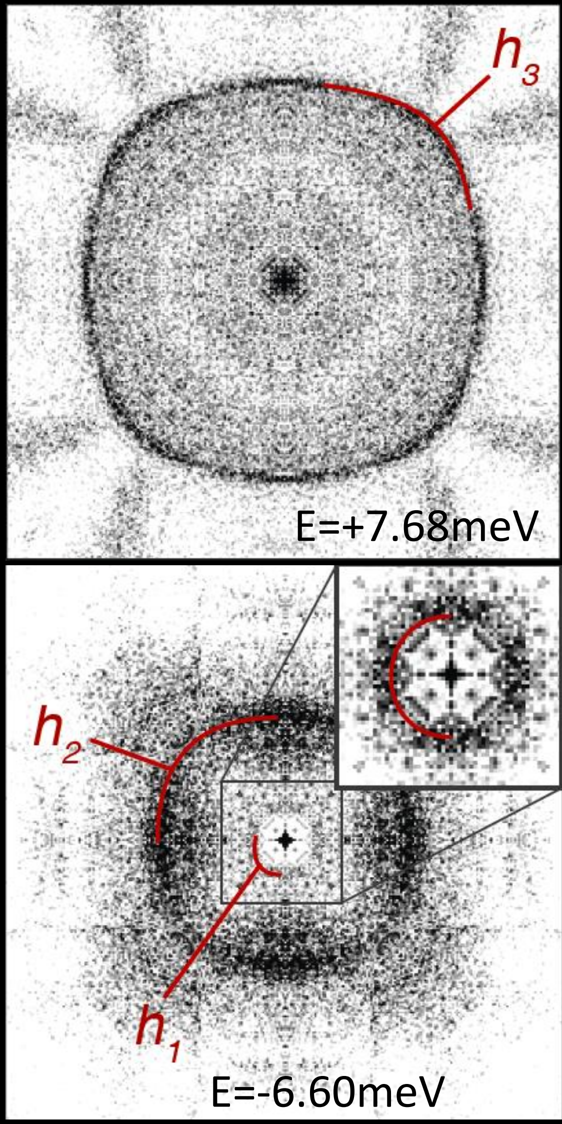

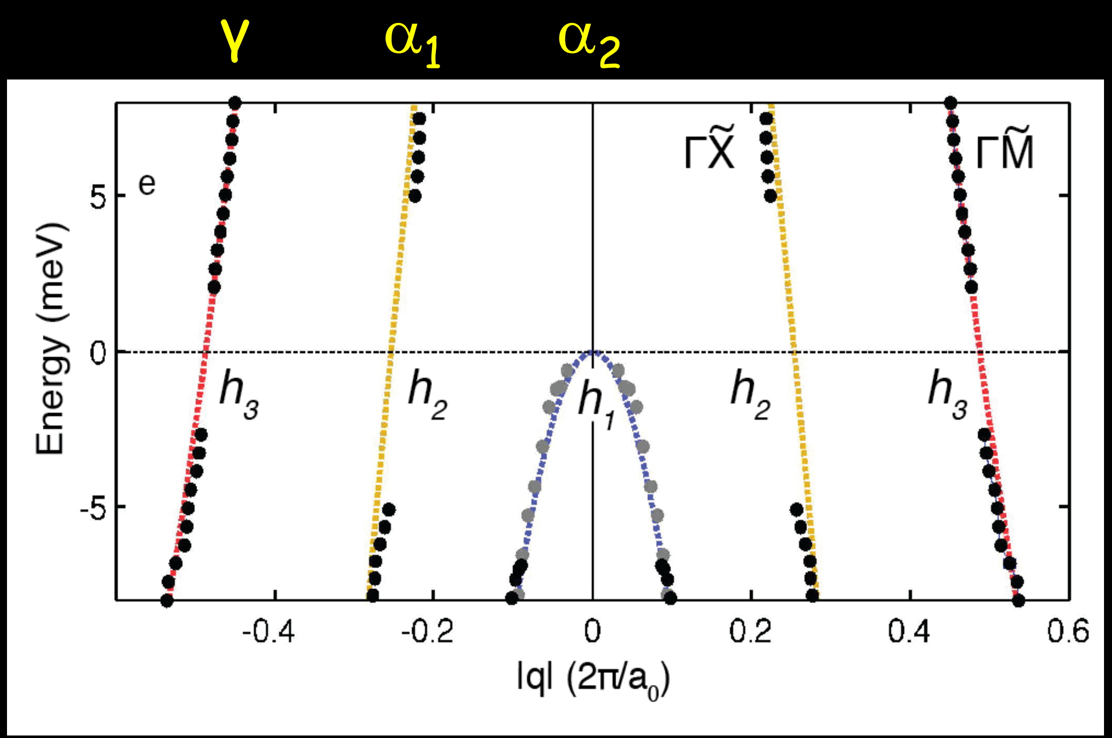

M. P. Allan & A.W. Rost *et al.*, Science **336**, 563 (2012)

Quasiparticle Interference, g(q,E) around SC Gap

Some QPI signals are suppressed.

The SC gap at this Fermi sheet is anisotropic!

+2.00meV

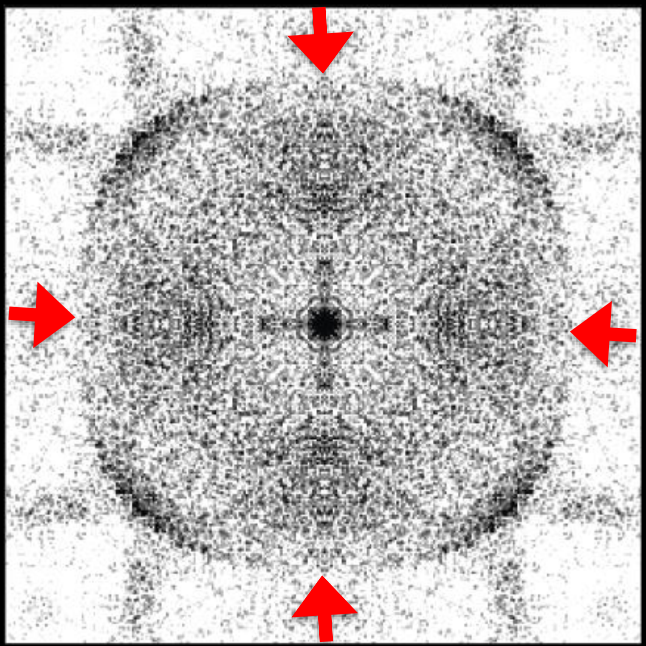

T= 1.2K

+7.68meV

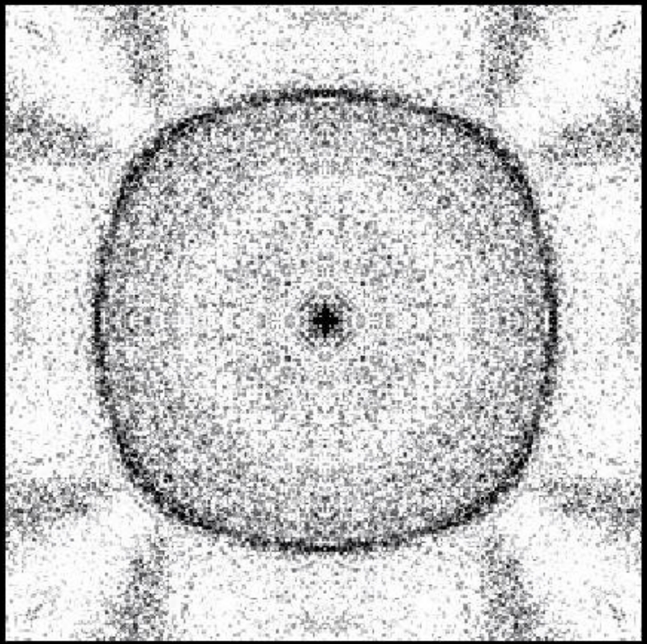

T= 1.2K

M. P. Allan & A.W. Rost *et al.*, Science **336**, 563 (2012)

Determination of Superconducting Energy-Gap Structure

How to obtain $\Delta_i(\boldsymbol{k})$?

q-space

+2.00meV

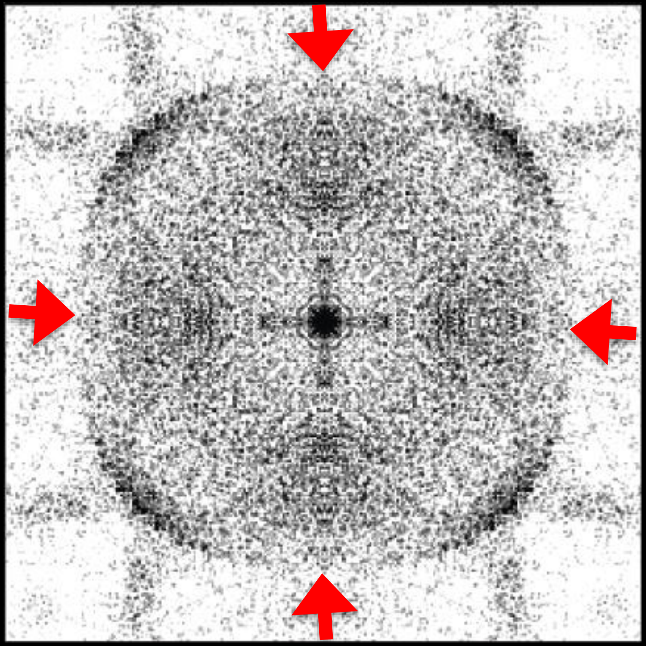

k-space

γ band + anisotropic gap

M. P. Allan & A.W. Rost *et al.*, Science **336**, 563 (2012)

Anisotropic Superconducting Energy-Gap Structure

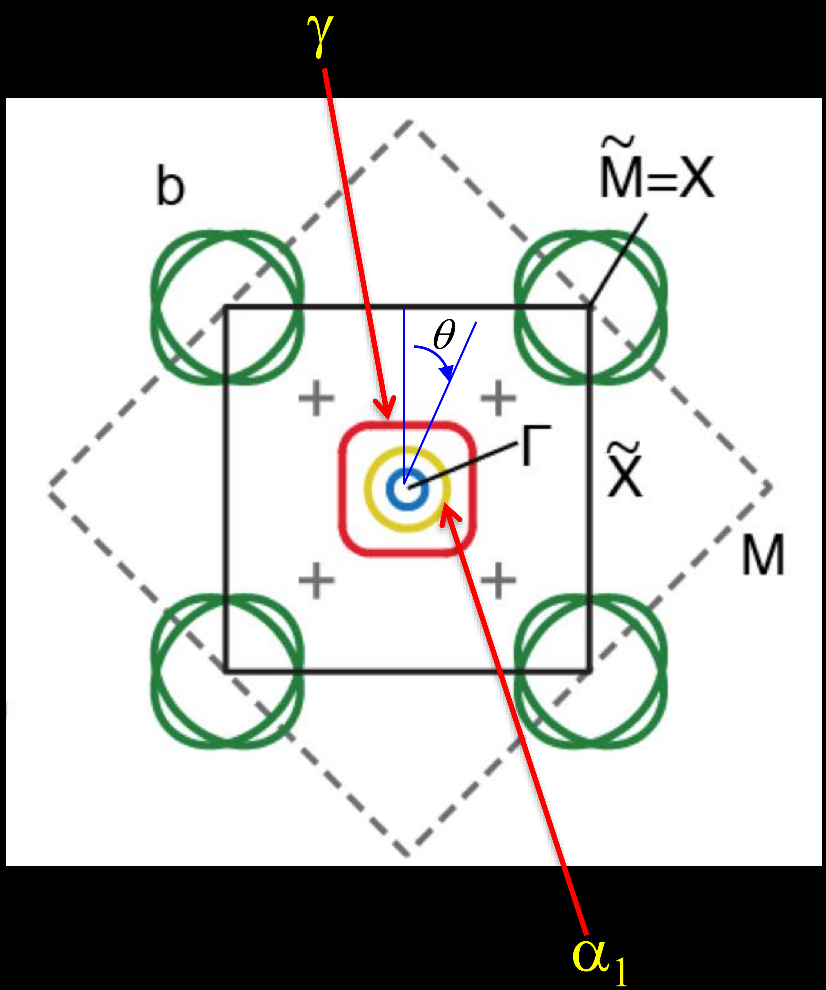

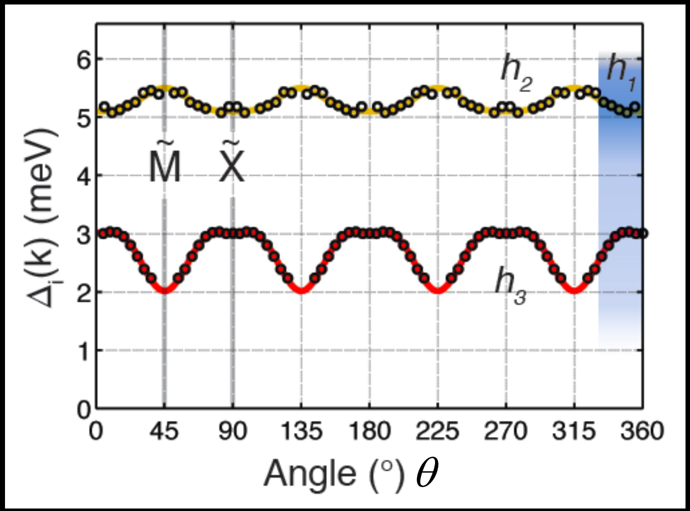

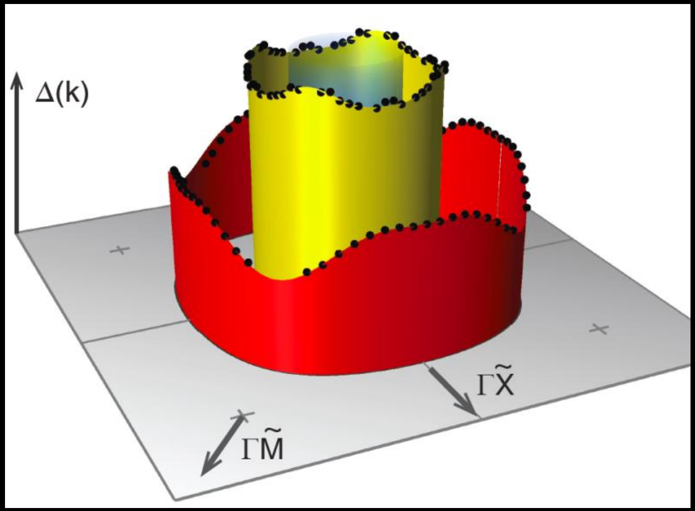

M. P. Allan & A.W. Rost *et al.*, Science **336**, 563 (2012)

Two ARPES Groups Confirm Our Results

STM and ARPES are consistent around Γ.

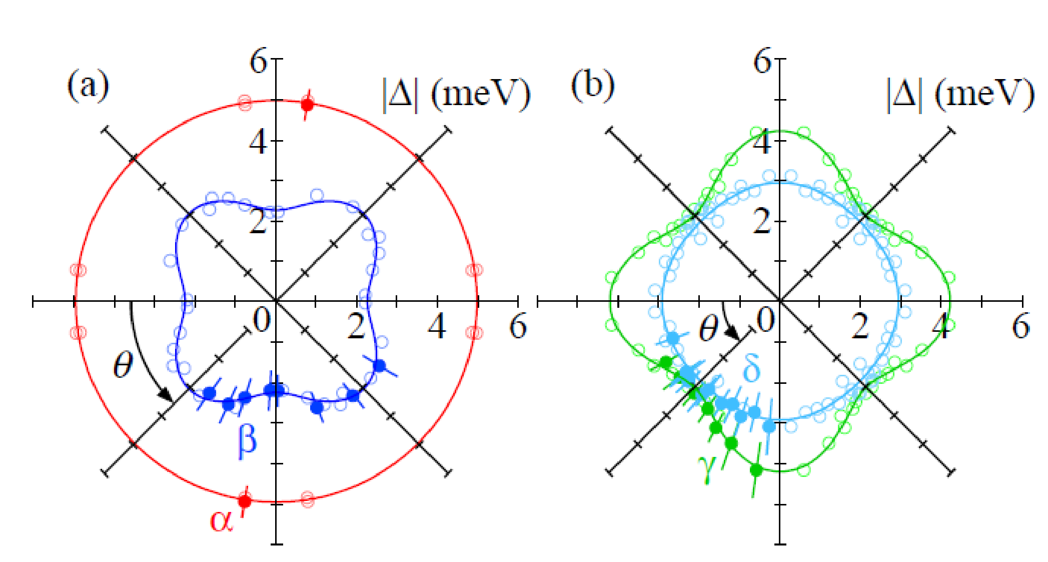

S.V. Borisenko *et al.*, Symmetry 4, 251 (2012)
K. Umezawa *et al.* PRL 108, 037002 (2012)

Consistent with AFSF theory.

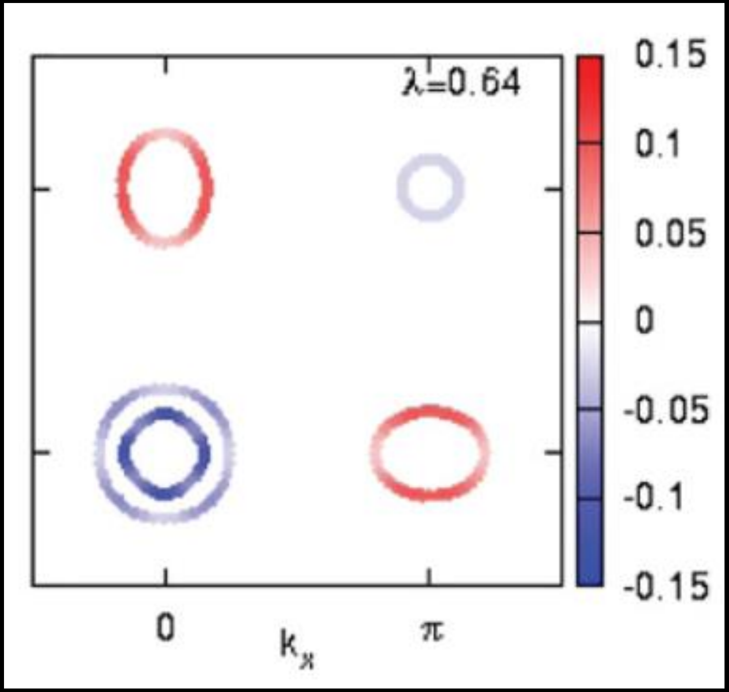

P J Hirschfeld *et al.*, Rep.Prog.Phys.74, 124508 (2011)

Anisotropic SC Energy Gaps in LiFeAs by ARPES

STM and ARPES are consistent around Γ.

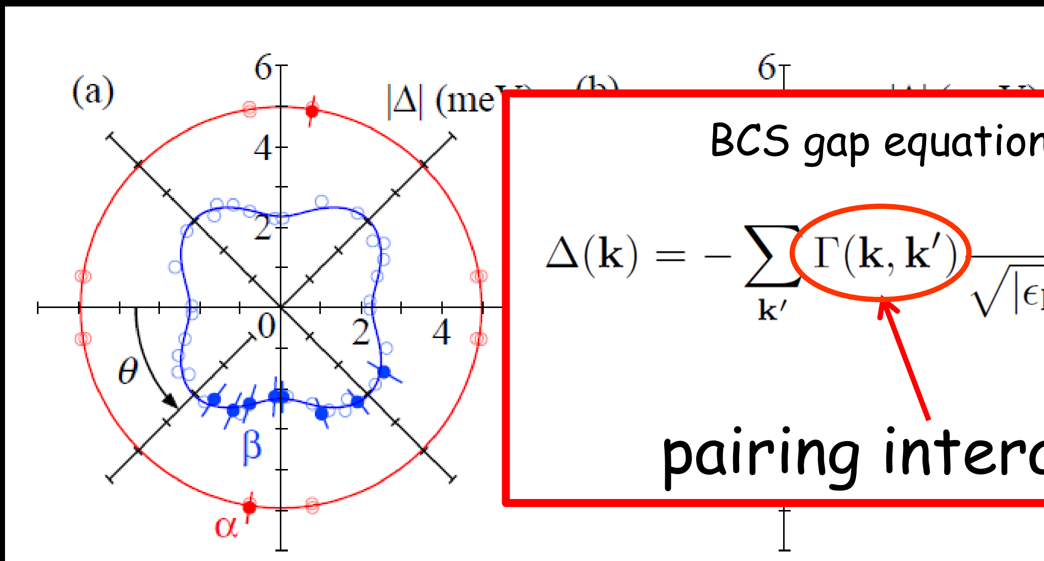

S.V. Borisenko *et al.*, Symmetry 4, 251 (2012)
K. Umezawa *et al.* PRL 108, 037002 (2012)

BCS gap equation at T=0

$$\Delta(\mathbf{k}) = -\sum_{\mathbf{k}'} \Gamma(\mathbf{k},\mathbf{k}') \frac{\Delta(\mathbf{k}')}{\sqrt{|\epsilon_{\mathbf{k}'}|^2 + |\Delta(\mathbf{k}')|^2}},$$

pairing interaction?

Consistent with AFSF theory.

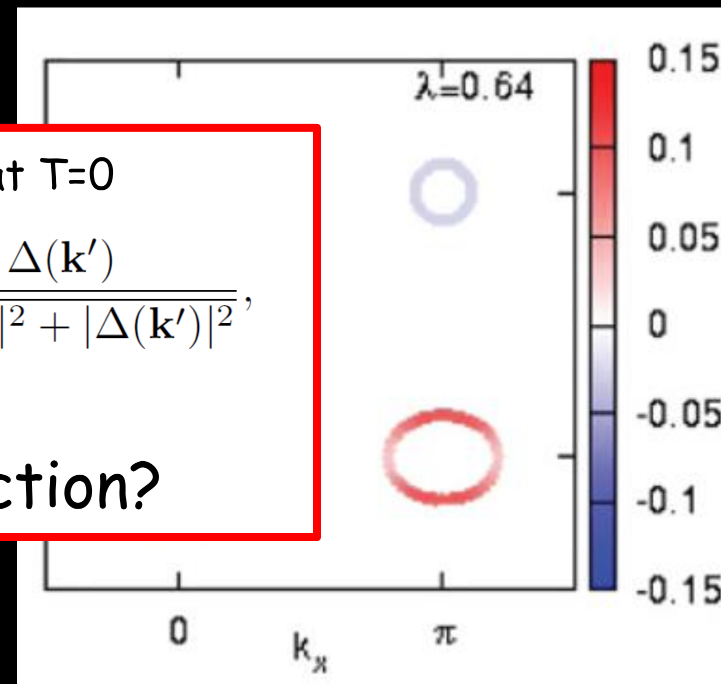

P J Hirschfeld *et al.*, Rep.Prog.Phys.74, 124508 (2011)

Electron-Boson Interaction

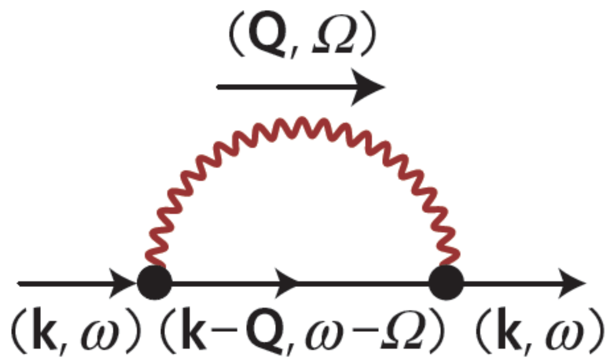

$$[\hat{G}(\mathbf{k},\omega)]^{-1} = [\hat{G}^0(\mathbf{k},\omega)]^{-1} - \hat{\Sigma}(\mathbf{k},\omega)$$

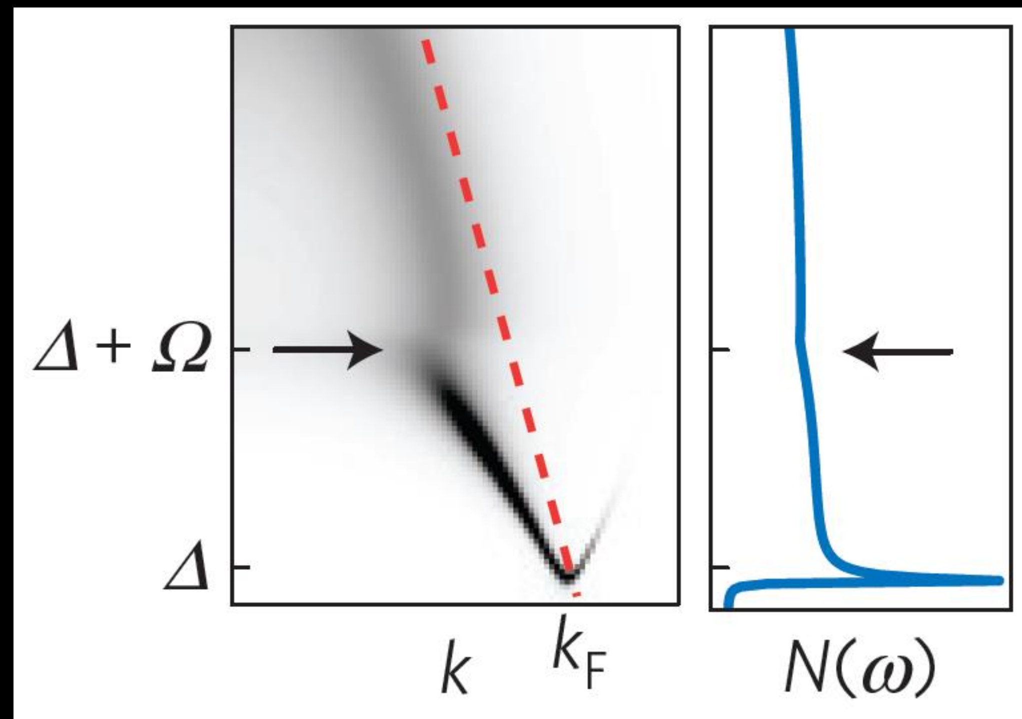

$$Re\hat{\Sigma}(\vec{k},\omega) \rightarrow \vec{k}(\omega)$$

$$Im\hat{\Sigma}(\vec{k},\omega) \rightarrow \tau^{-1}(\vec{k},\omega)$$

Superconductivity by Tunneling Spectroscopy

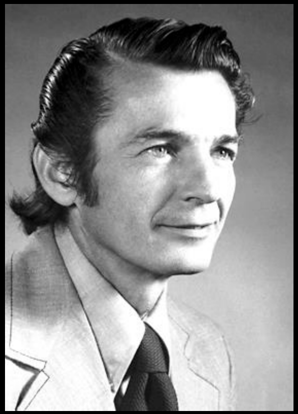

Ivar Giaever
Nobel Prize 1973

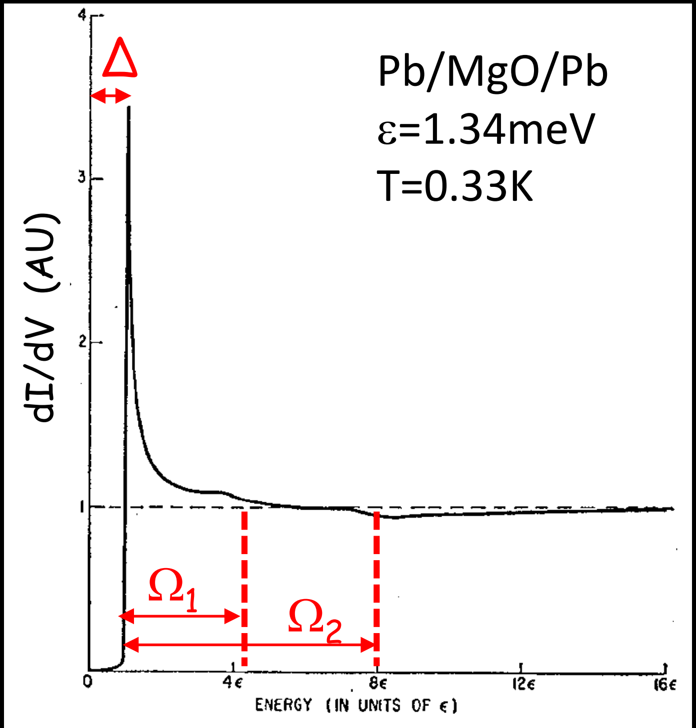

I. Giaever, Phys. Rev. 126, 941 (1962)

Electron-Phonon Interaction by Tunneling Spectroscopy

William McMillan

John Rowell

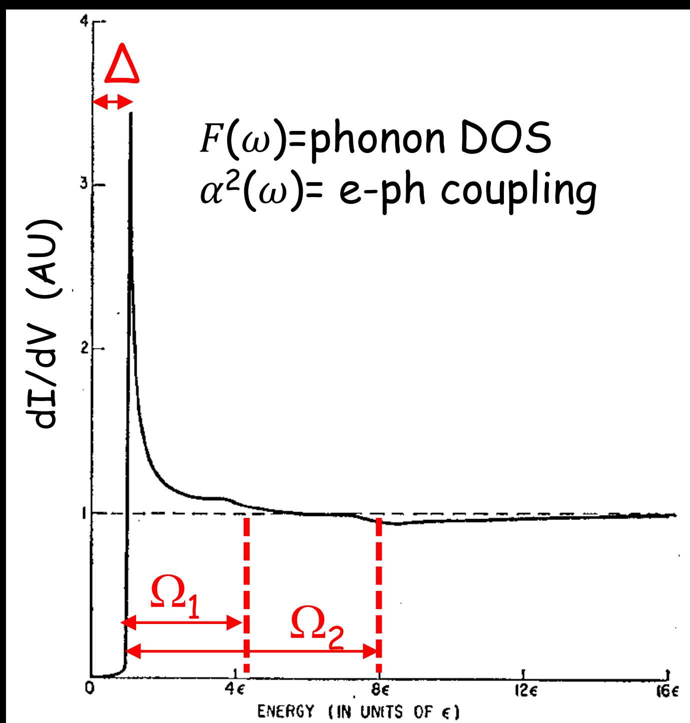

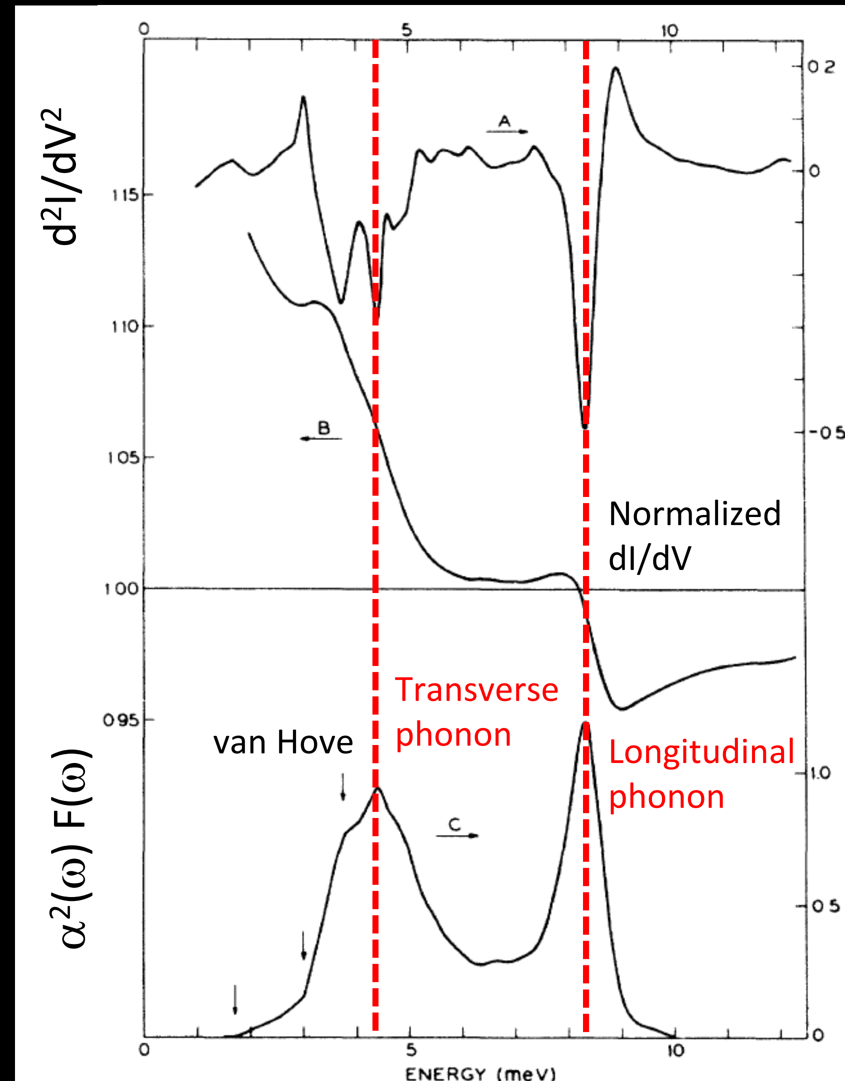

W.L. McMillan & J.W. Rowell, PRL 14, 108 (1965)

Atomic Visualization of Electron-Boson Coupling in FeSC

Milan Allan

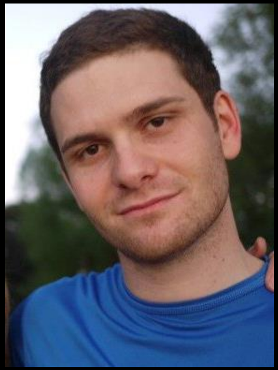

Andreas Rost

"Dip-hump" in spectrum of FeSC

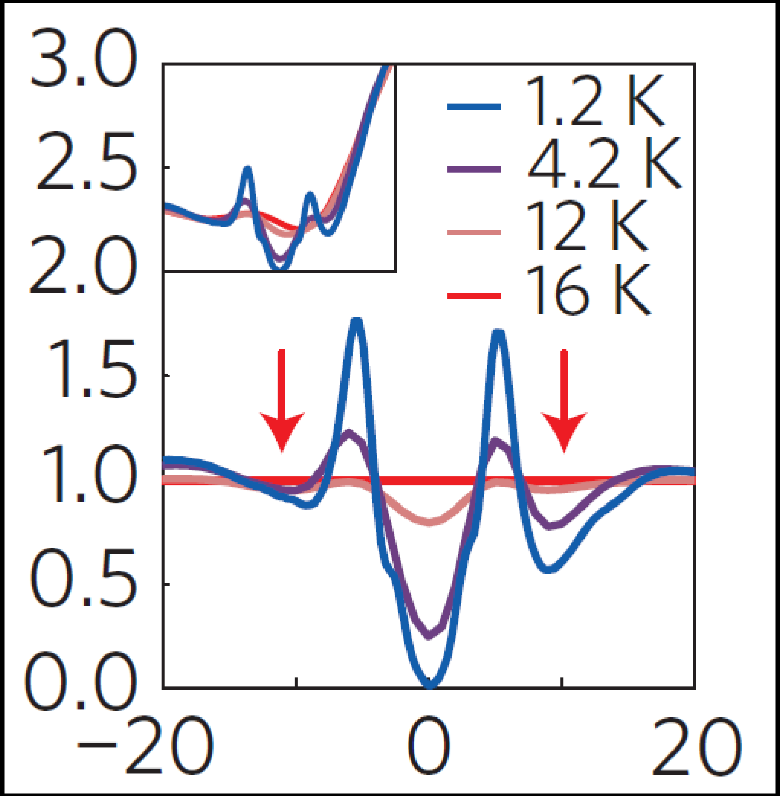

Momentum info?

M. P. Allan & A.W. Rost *et al.*, Science **336**, 563 (2012)
M. P. Allan, Kyungmin Lee & A. W. Rost *et al.*, Nature Physics 11, 177 (2015)

QPI in LiFeAs

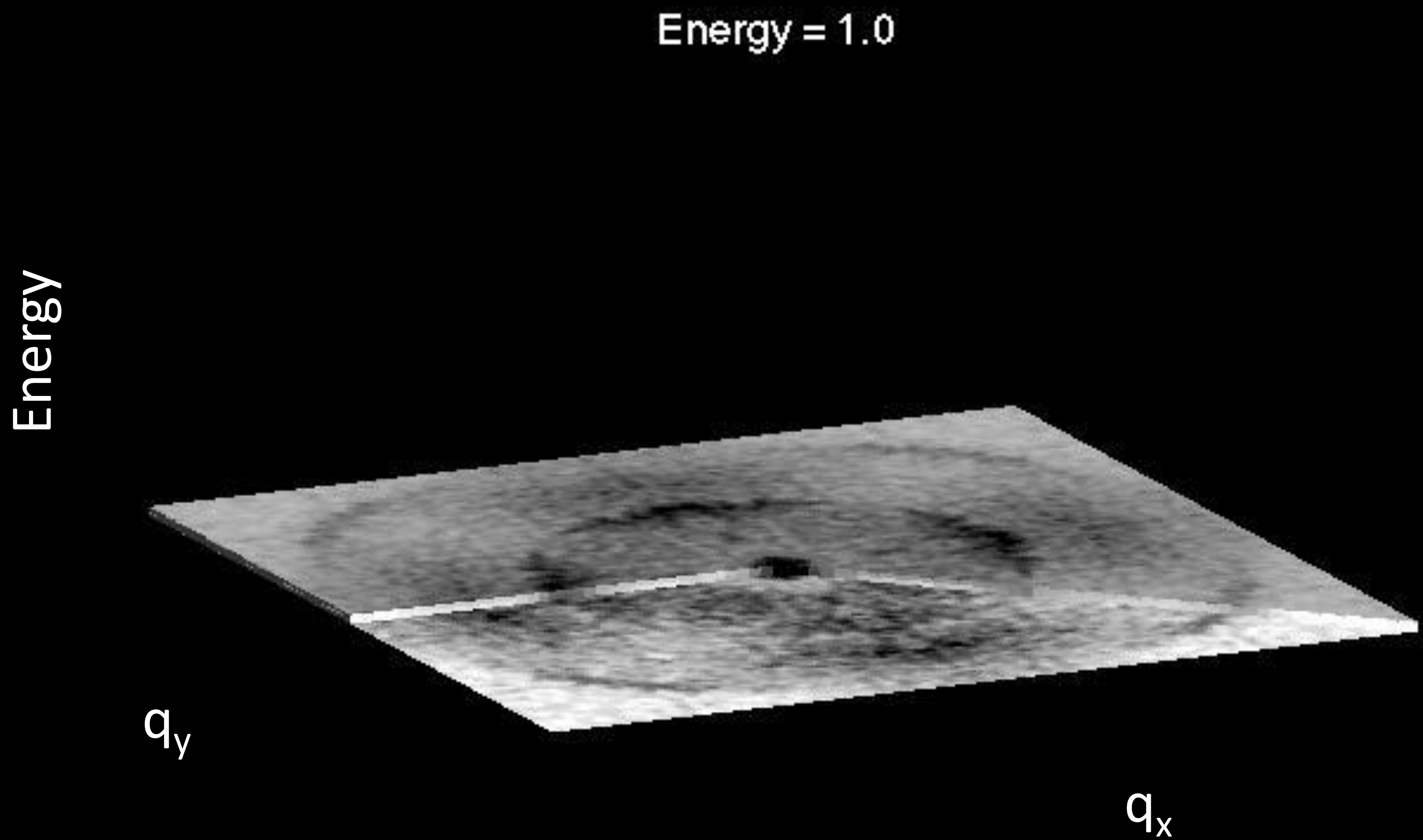

M. P. Allan, Kyungmin Lee & A. W. Rost *et al.*, Nature Physics 11, 177 (2015)

Atomic Visualization of Electron-Boson Coupling in FeSC

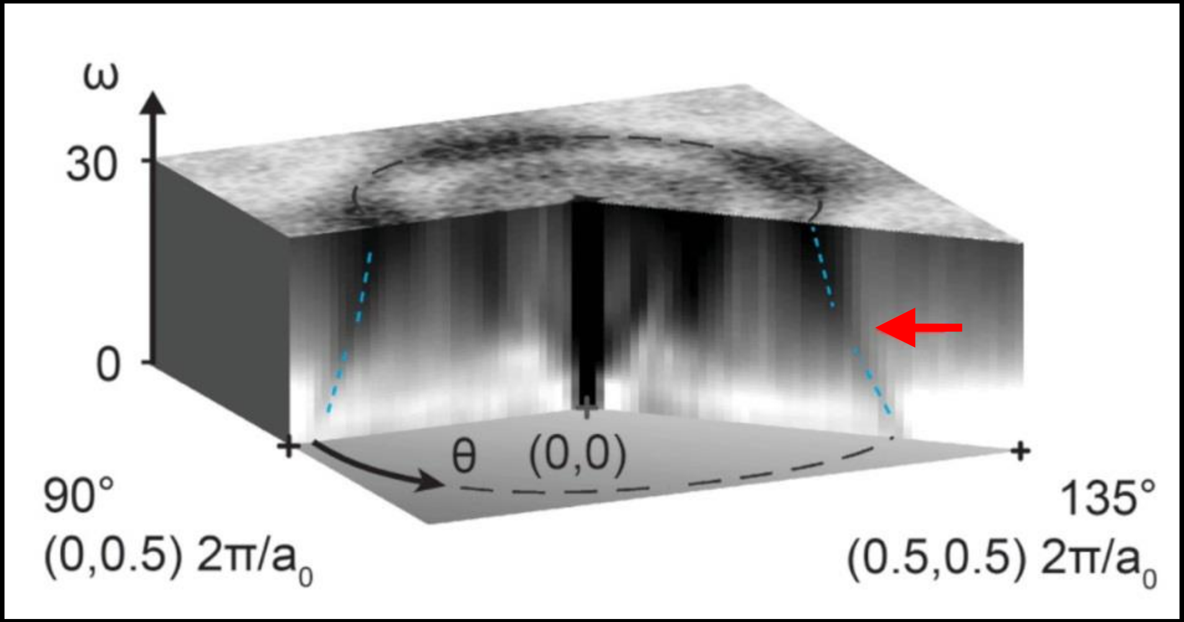

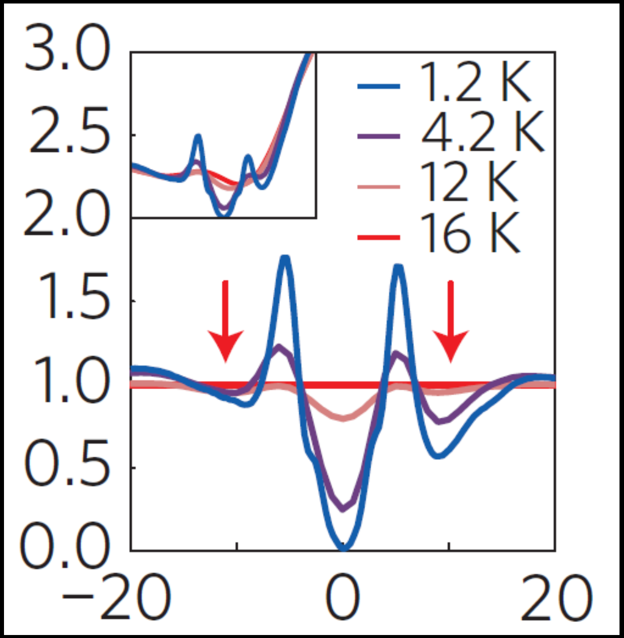

The change in dispersion occurs at the same energy as the 'traditional' Electron-Boson coupling signature in the spectrum.

M. P. Allan, Kyungmin Lee & A. W. Rost *et al.*, Nature Physics 11, 177 (2015)

Atomic Visualization of Electron-Boson Coupling in FeSC

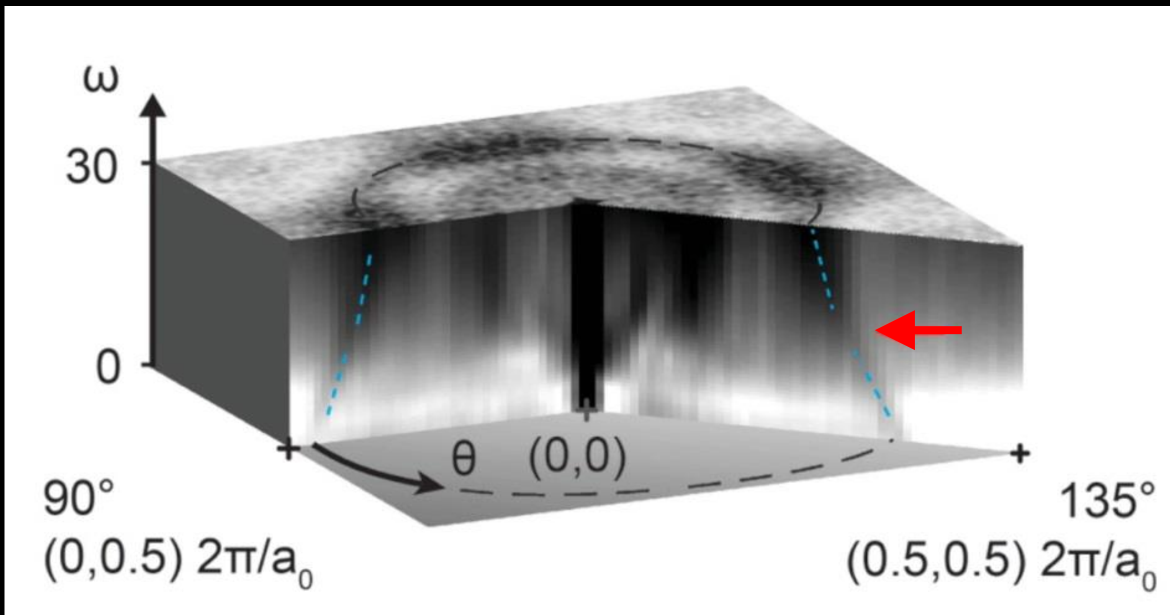

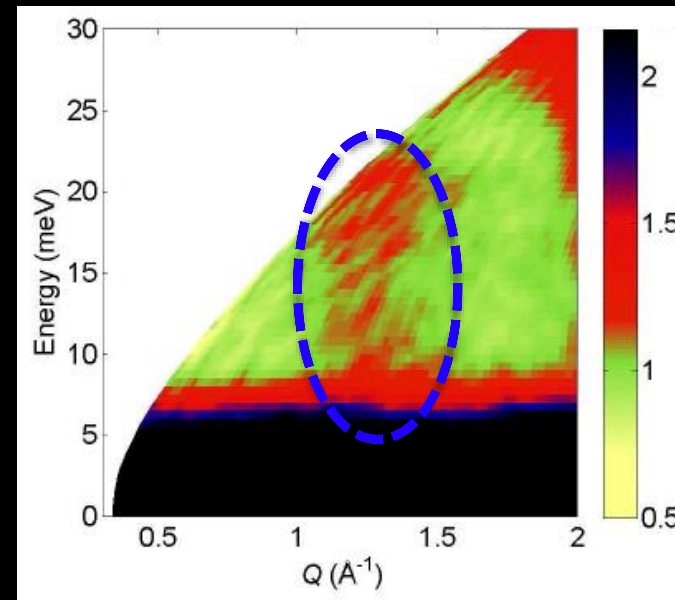

A.E. Taylor *et al.*, PRB 83, 220514 (2011)

The change in dispersion occurs at the same energy as the 'traditional' Electron-Boson coupling signature in the spectrum.

M. P. Allan, Kyungmin Lee & A. W. Rost *et al.*, Nature Physics 11, 177 (2015)

Atomic Visualization of Electron-Boson Coupling in FeSC

The self energy due to e-b coupling is strongly anisotropic

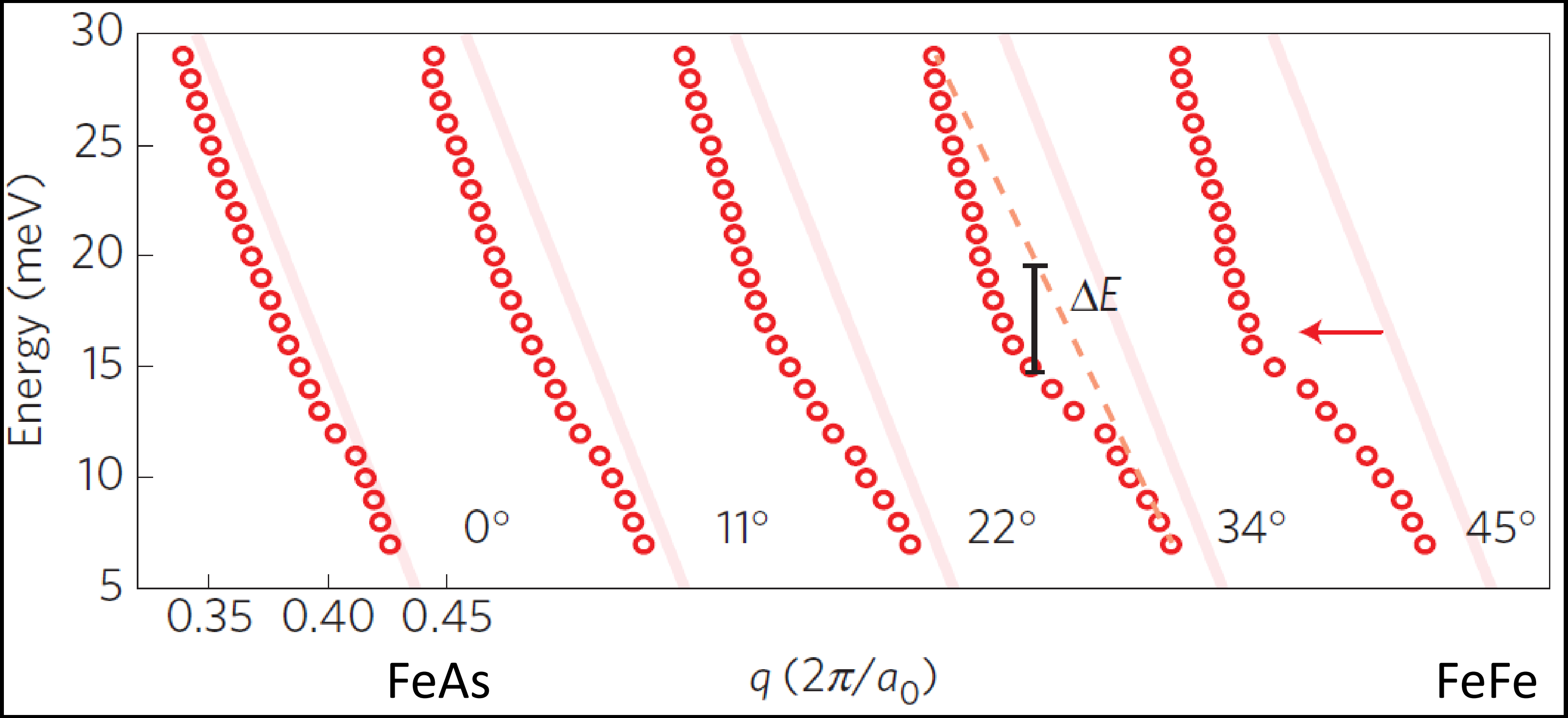

M. P. Allan, Kyungmin Lee & A. W. Rost *et al.*, Nature Physics 11, 177 (2015)

Theoretical Calculation of E-B Couplings

d-orbital fluctuations by Fe Eg-phonon

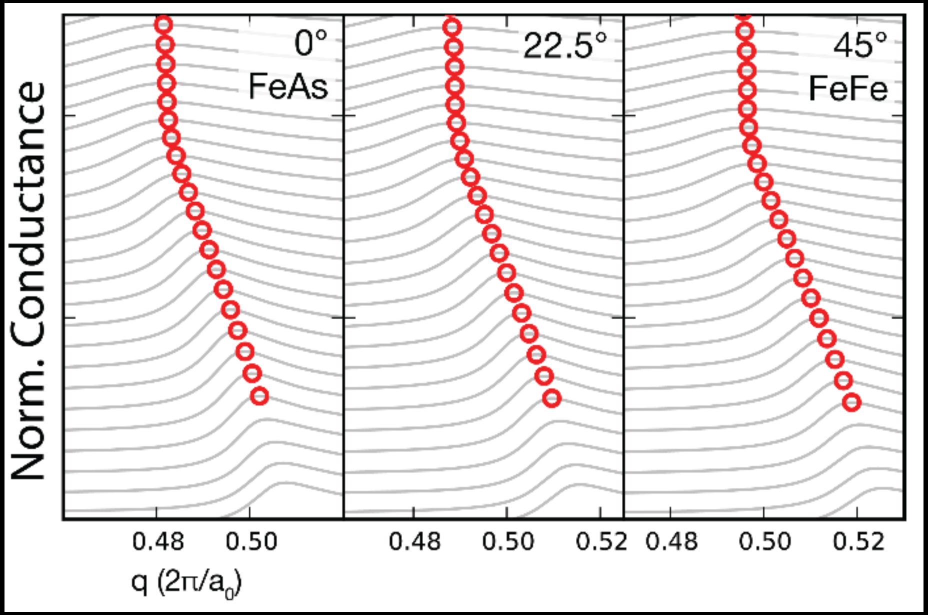

Kyungmin Lee

Mark Fischer

Eun-Ah Kim

M. P. Allan, Kyungmin Lee & A. W. Rost *et al.*, Nature Physics 11, 177 (2015)

Theoretical Calculation of E-B Couplings

d-orbital fluctuations by Fe Eg-phonon

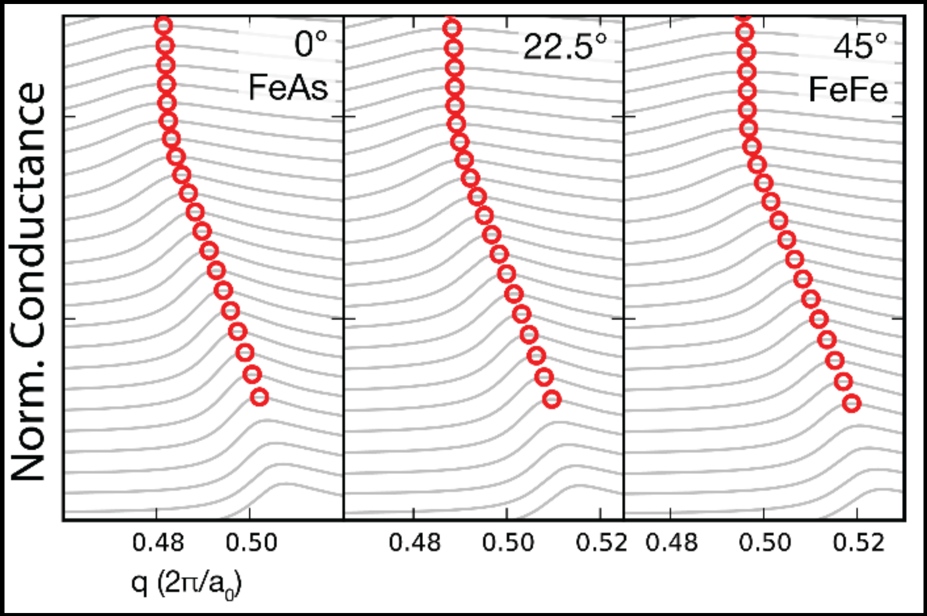

AF spin fluctuation

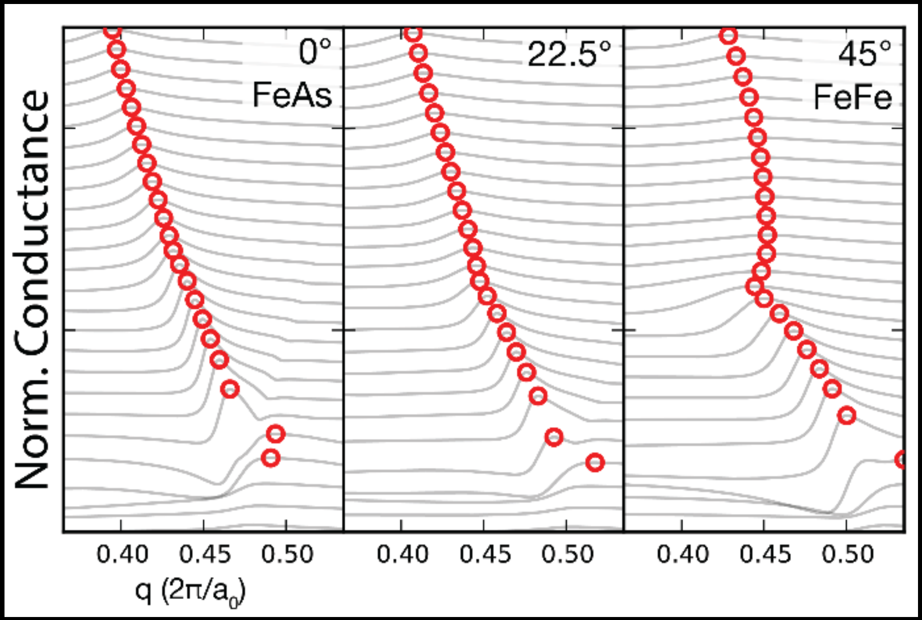

M. P. Allan, Kyungmin Lee & A. W. Rost *et al.*, Nature Physics 11, 177 (2015)

Theoretical Calculation of E-B Couplings

d-orbital fluctuations by Fe Eg-phonon

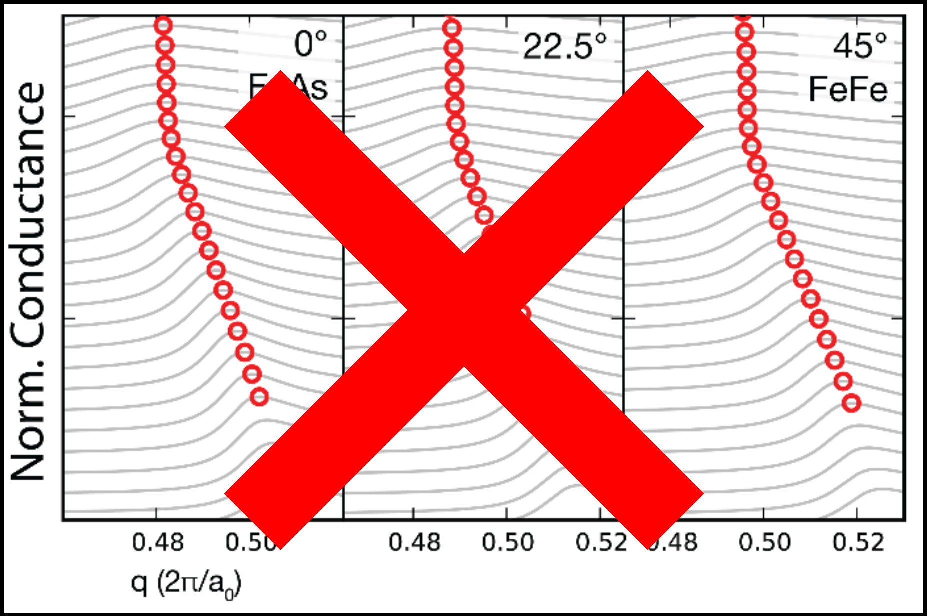

AF spin fluctuation

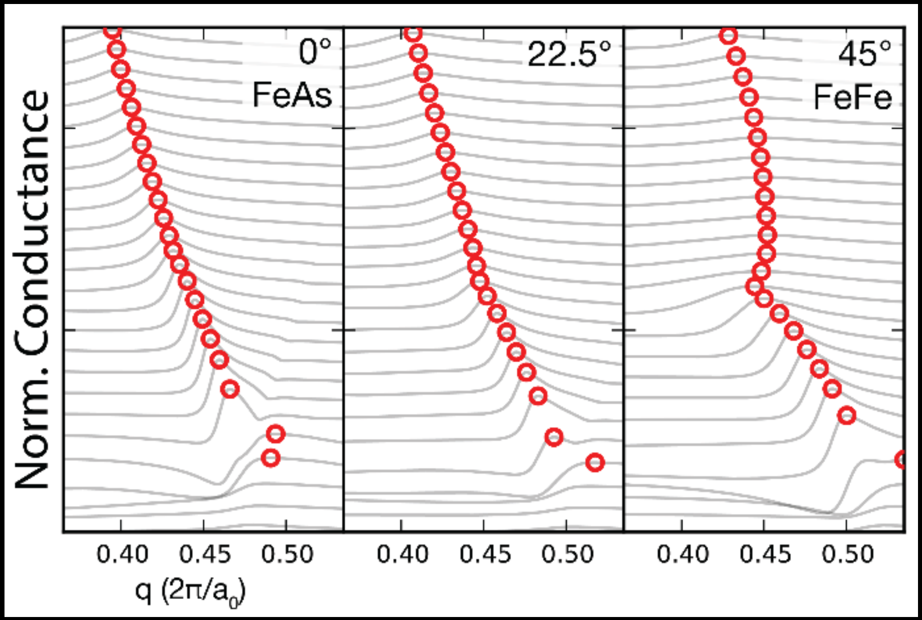

M. P. Allan, Kyungmin Lee & A. W. Rost *et al.*, Nature Physics 11, 177 (2015)

"Fingerprint" of Pairing Mechanism in FeSC

Our experimental results support AF spin fluctuation pairing!

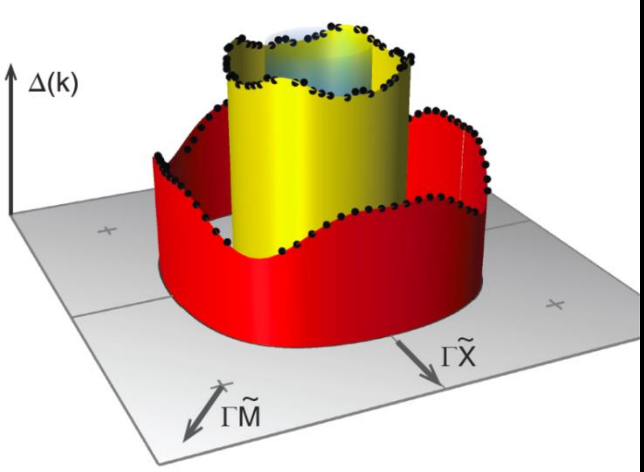

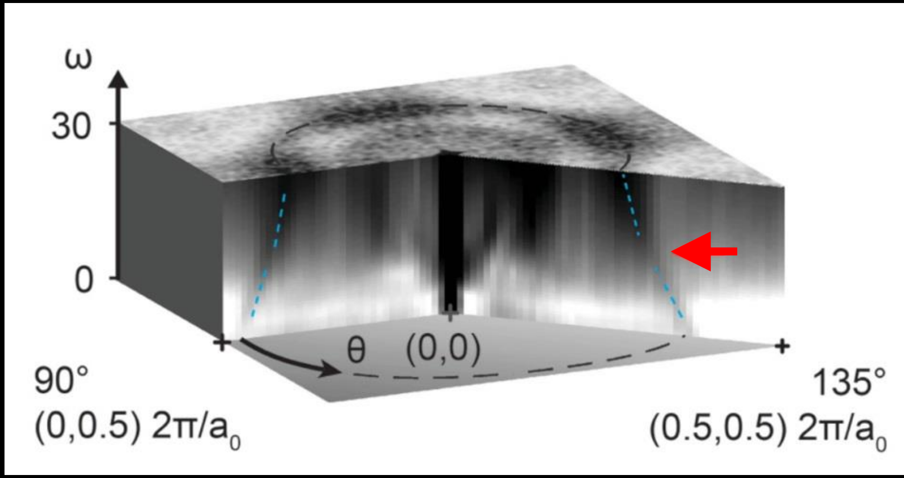

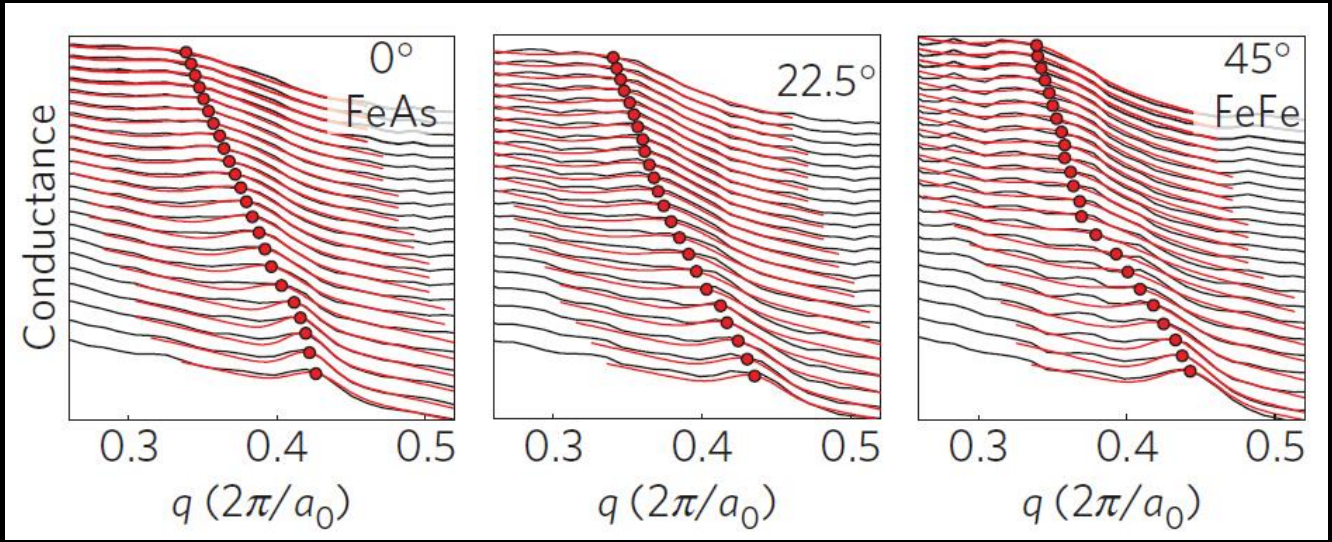

M. P. Allan, Kyungmin Lee & A. W. Rost *et al.*, Nature Physics 11, 177 (2015)

M. P. Allan & A.W. Rost *et al.*, Science **336**, 563 (2012)

Single Unit-Cell FeSe Films on SrTiO3

Qikun Xue
薛其坤

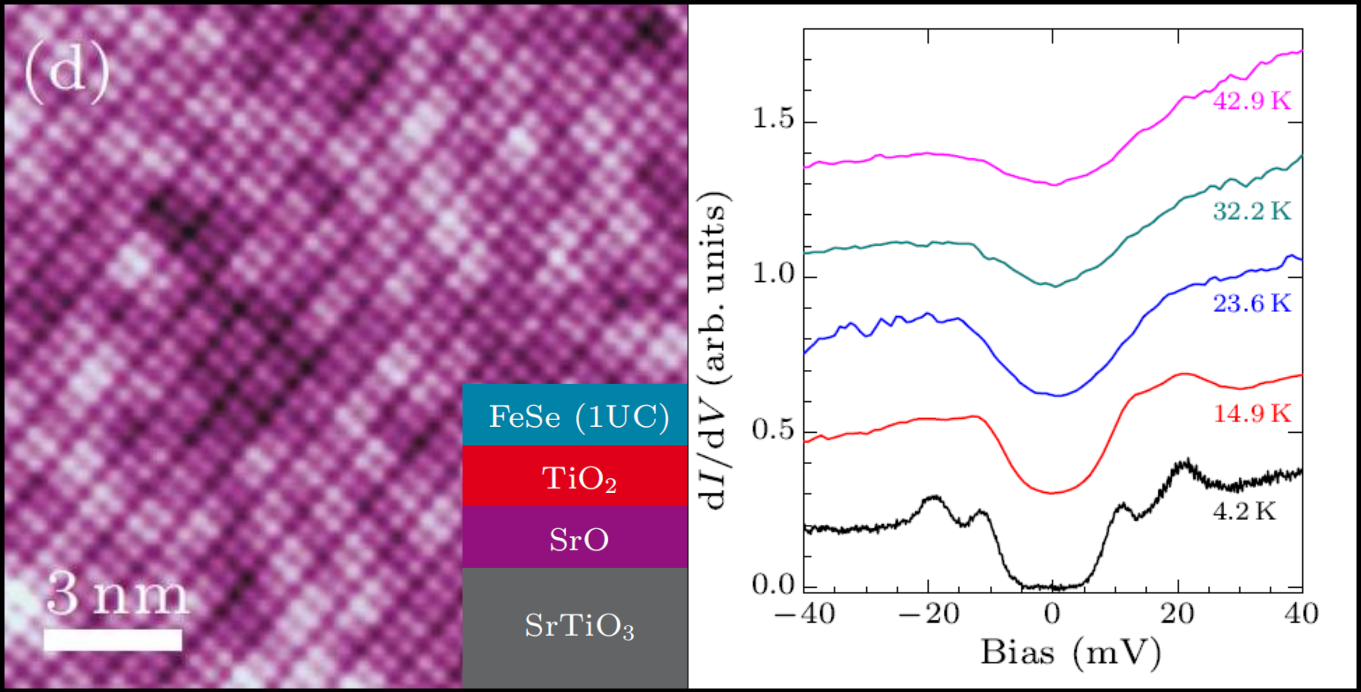

Q.Y. Wang *et al.*, CHIN. PHYS. LETT. 29.037402(2012)

Single Unit-Cell FeSe Films on SrTiO3

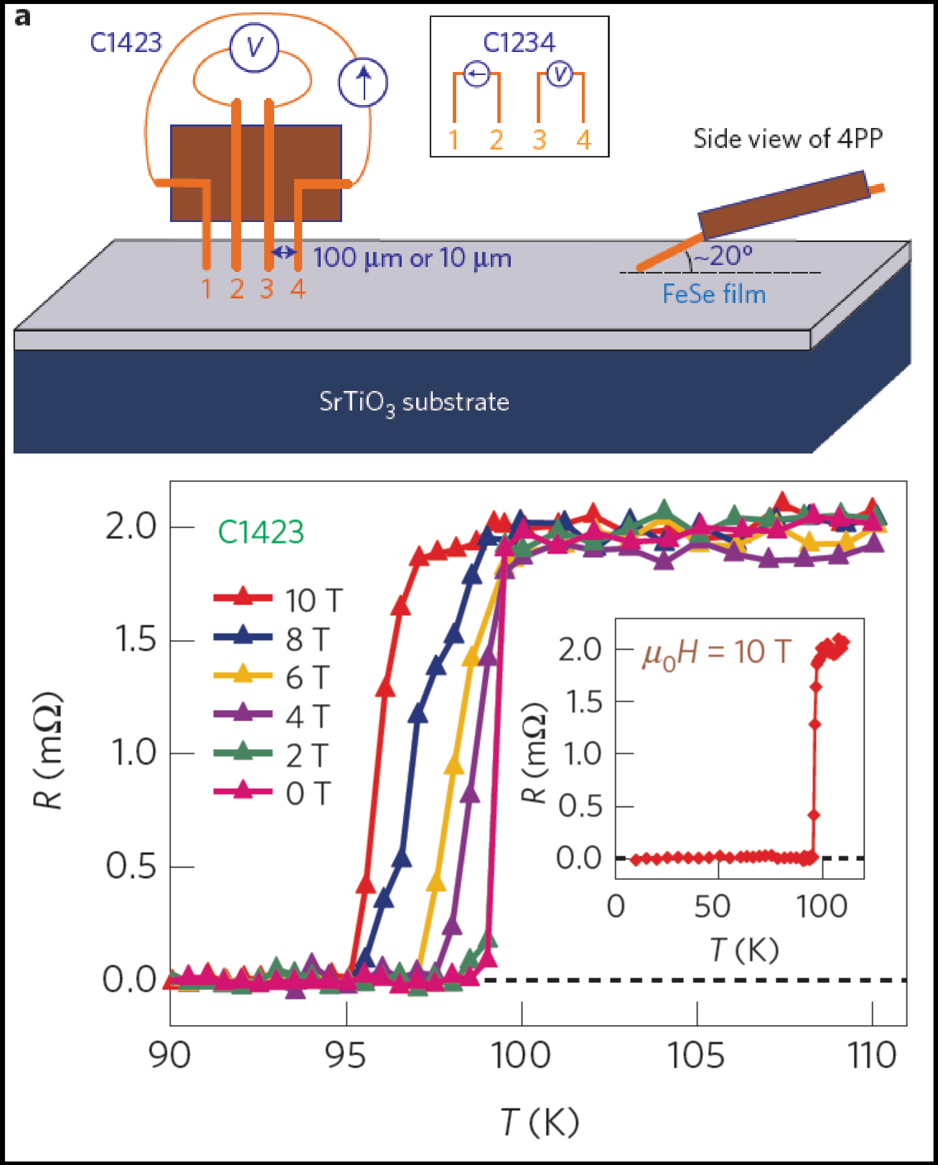

Jian-Feng Ge *et al.*, Nature Materials 14,285 (2015)